A CELL-BASED SENSOR OF FLUID SHEAR STRESS FOR MICROFLUIDICS

Sarvesh Varma

B.A.Sc., Nanotechnology Engineering, University of Waterloo, 2010

SUBMITTED TO THE DEPARTMENT OF ELECTRICAL ENGINEERING AND COMPUTER SCIENCE IN PARTIAL FULFILLMENT OF THE REQUIREMENTS FOR THE DEGREE OF

MASTER OF SCIENCE

AT THE

MASSACHUSETTS INSTITUTE OF TECHNOLOGY

June 2013

Signature of Author_____

Sarvesh Varma
Department of Electrical Engineering and Computer Science
May 23, 2013

Certified by_____

Joel Voldman
Associate Professor of Electrical Engineering and Computer Science
Thesis Supervisor

Accepted by_____

Leslie A. Kolodziejski
Professor of Electrical Engineering and Computer Sciences
Chairman, Department Committee on Graduate Committee

A CELL-BASED SENSOR OF FLUID SHEAR STRESS FOR MICROFLUIDICS

by

Sarvesh Varma

Submitted to the Department of Electrical Engineering and Computer Science

May 23, 2013

in Partial Fulfillment of the Requirements for the Degree of Master of Science

ABSTRACT

Fluid flow is an essential feature of every microsystem involving cell handling, culture or sorting. The particular application determines the relevant flow rates used in a device. Flows inevitably generate fluid shear stress (FSS) that may cause undesirable physiological cell stress. Simple assays of cell viability, morphology or growth are typically reported to indicate any gross disturbances to cell physiology. However, no straightforward metric exists to specifically evaluate physiological implications of FSS within microfluidic devices, or among competing microfluidic technologies).This thesis presents the first genetically encoded cell sensors that fluoresce in a quantitative fashion upon FSS pathway activation. A transcriptional sensor was chosen, meaning that fluorescence would be turned on when transcription of a relevant protein was initiated. Creating an effective transcriptional sensor requires identifying an appropriate inducible promoter to drive fluorescence expression upon FSS. To this end, the native mechanotransduction of a widely used and easy-to-culture cell line (NIH3T3s) was elucidated by culturing them in a microfluidic device and applying logarithmic FSS via microfluidic perfusion. A panel of shear-responsive genes was analyzed using qRT-PCR, which resulted in the choice of EGR-1 upregulation as the node for FSS detection. A reporter plasmid with a minimal EGR-1 promoter driving the expression of Turbo-RFP fluorescence was chosen and the cell sensor was created by stable transfection and clonal selection. Inducing the pathway with Phorbol-myristate-acetate resulted in fluorescence induction by both microscopy and flow cytometry, verifying the sensor functionality. The fluorescence activation was then characterized across PMA doses and durations. Next, the sensors were tested using multiple duration microfluidic perfusions, where it was noted that the mean induced fluorescence intensity correlated to applied FSS intensity, as desired. It is anticipated that these cell sensors will have wide application in the microsystems community, allowing the device designer to engineer systems with acceptable FSS, and allowing the end-user to evaluate impact of FSS upon their assay of interest.

Thesis Supervisor: Joel Voldman
Title: Associate Professor of Electrical Engineering and Computer Science

Acknowledgements

This thesis would have not been possible without the valuable supervision of Prof. Joel Voldman. I am enormously grateful to him and all his kind considerations and assistance in getting this thesis done. Additionally, I am very grateful to have the opportunity to work in his lab and learn so much within this environment.

As a student, I have an immense amount of debt to the knowledge, inspiration and teachings provided by all my teachers from high-school, to undergrad, to grad school. I am indebted to all my mentors and everyone who has provided me advice on my academic choices as well as provided perspectives on how to lead a better life. I am thankful to all the professors for teaching me valuable lessons either in a classroom environment or in a lab environment.

The support of all my friends has been tremendously appreciated and valued. Without all of them, I would have not maintained any sanity or happiness throughout my education and growth.

I am extremely grateful to everyone in the Voldman lab- past and present members for their help and kind encouragement. The same goes to all of my previous colleagues in various environments and locations.

If you know me, you would know relative to the deadline, at which point I would chose to write this acknowledgement section. The amount of gratitude I have towards all of you is overwhelming and cannot be described in short. I owe you all.

Finally, I dedicate this thesis to my family, ever-loving my parents and my precious sister. I would have never been able to do anything in my life without your support, love and blessings.

Table of Contents

Table of Figures

Chapter 1: Introduction

1.1. Cell-based microsystems that impose fluid shear stress on cells

In the context of cell-based microsystems and technologies, the past few decades provide a plethora of platforms where cells have been cultured and processed for various applications. Large efforts have been made towards developing cell-type-specific systems where the chosen phenotype significantly impacts device design and cell culture techniques. For instance, in-vitro toxicity models and devices have been designed for primary hepatocytes [1], whereas an on-chip lung model was designed for primary alveolar epithelial cells [2]. Similarly, there has been substantial development of devices designed independently of cell types chosen to be used with them. Some examples include devices meant to manipulate or sort cells with light [3], electric fields [4], magnetic fields [5] or by hydrodynamic trapping [6].

Fluid flow is an essential feature of every microsystem involving cell handling, culture or sorting. The particular application determines the relevant flow rates used in a device [7]. Microfluidic platforms and technologies can generally be categorized by virtue of their operational flow rate and experimental duration. There is a whole gamut of devices which operate at high flow fluid rates for short durations, such as high-throughput cell sorters [5], inertial-force devices [8] and droplet-based microsystems [9, 10] to name a few. Such devices commonly use non-adherent cells, or adherent cells maintained in suspension, because cells are meant to have short residence durations within the device. In another flow regime, many devices are meant to apply very low flow rates for long durations. Typical examples of such microfluidic devices are those used for long term cell static culture [11] or perfusion culture [12, 13].

Flows inevitably generate fluid shear stress (FSS) that may cause undesirable physiological cell stress. In the 'short-but-intense' flow category of devices, cells experience large FSS (~100s-1000s dynes/cm^2) for a short duration (milliseconds-seconds). For the other category of 'prolonged-and-gentle' flow based devices, cells experience lower FSS (0.001-10 dynes/cm^2) for long durations (~hours-days). Several other microfluidic technologies fall in between these two extremes, where cells could experience moderate shear stresses (~10s-100s dynes/cm^2) for moderate durations (~minutes-hours). An illustration mapping the range of shear exposures and durations of various microfluidic systems is shown in **Figure 1-1**.

It is important to realize that such categorization of fluid shear stress in microenvironments implies a level of subjectivity. To illustrate, in one study, a microsystem platform was used to apply shear of 0.2-5 dynes/cm^2 shear stress on rat kidney cells for 12 hours[14]. In another study, a microfluidic device was used to study stem cell self-renewal, which required 0.007 dynes/cm^2 for 3-7 days [13]. The first study in comparison with the second could be categorized

as one with 'short-but-intense' shear stress. To contrast, in a third study osteoblast cells were differentiated for 10 days using a microfluidic platform with a fluid shear stress of 0.07 dynes/cm^2[15]. When comparing this third study to the second, the third could be categorized as one with 'long-and-intense' shear. These examples essentially highlight an underlying fact that the device operation and design differ because of the chosen cell-type. This fact makes categorization of fluid shear stress intensity and duration within microsystems somewhat subjective. Therefore, the choice of fluid flow conditions (FSS intensity and duration) may not only depend on the device application, but also on the chosen cell phenotype, as shown in **Figure 1-2** [7]. Fluid shear stress may not always be detrimental to cell health because in some cases it is required for beneficial outcomes such as endothelial cell maintenance [16]. Nevertheless, in the context of cell-based microsystems and technologies, shear stress is generally viewed as a stress stimulus.

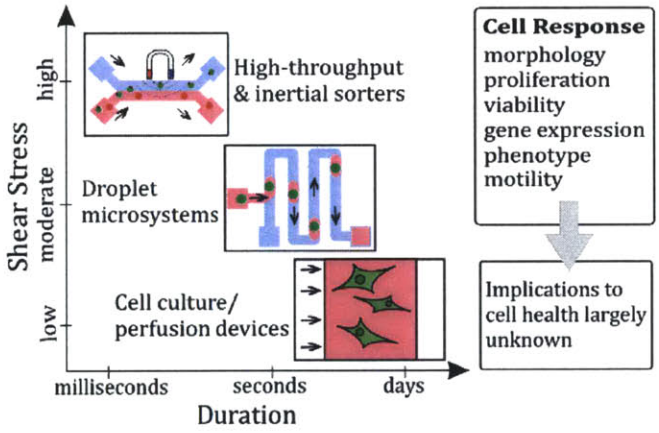

Figure 1-1 Fluid shear stress is ubiquitous in microsystems with a large range of imparted shear intensities and durations. Resulting cell responses are complex and largely uncorrelated with cell health in microsystems.

It is conceivable that in the context of many cell-based microsystems, the implementation of protocols itself may influence cell physiology and therefore may cause undesirable stress conditions. For example, fluid shear stress can cause physiological changes to migrating leukocytes and their activation profiles within the vasculature [17]. When handling or sorting such cells, a system generating fluid shear stress could presumably alter the physiology and therefore the functionality of such cells. Knowing the effect of microsystems upon cell health is therefore important to the designer as it would be desirable to minimize any adverse impact on cells simply due to the device environment. Likewise, the same knowledge is useful for the end-user of the technology for evaluate the extent to which the cell physiology may be biased due to the experimental setup and operations.

CELL TYPE	Culture Chamber height	Media residence time	Estimated Shear Stress
	microns	*min*	*dyn-cm^{-2}*
Primary rat Hepatocytes	100	0.0026	0.7
	85-500	0.042-15.63	0.01-21
HepG2 human hepatocytes	100	0.4	1.4-1.6
	50	0.033-4.17	0.001-4
Primary bovine endothelial cells	50	0.033-4.17	0.001-4
Bovine aortic endothelial cells	100	0.009	20
HeLa cells	50	0.033-4.17	0.001-4
Human Neural stem cells	100	24	0.0005
Human SY5Y neuroblastoma	50	0.033-4.17	0.001-4
3T3 fibroblasts	50	0.033-4.17	0.001-4
MC3T3-El osteoblasts	100-200	8	0.05-0.7

Figure 1-2 Microfluidic perfusion conditions for various cells types, showing large diversity of applied shear stress intensities. Information adapted from [7] .

Unfortunately, it is challenging to quantify how an intentionally or unintentionally imparted fluid shear stress may affect the cell physiology. Cells demonstrate a complex combination of responses towards external stress stimuli. The exact set of cellular decisions depends on the bio-chemical and bio-physical cellular environment, the cell type, as well as on the type, intensity, and duration of the applied fluid shear stress [18]. Stress causes cells to either promote self-protection, repair and therefore survival, or to proceed towards a destructive fate by programmed cell death. Initial cell responses are geared towards recovery and defense against the insult. However, if unbearable, the cell activates death signaling pathways such apoptosis, pyroptosis, or necrosis [19, 20].

In order to gain insight into cell physiology, microscopy is used to characterize morphology, proliferation and motility; MTT assay for studying metabolism; staining and flow cytometry to analyze cellular viability or phenotype, RT-PCR for revealing changes in gene expression; and ELISA for analysis of antigen production. An assortment of these measures paints a picture of cellular responses towards a stressful stimulus at a given time. A large number of micro-analytical systems focus on the extraction of intracellular contents for analysis of metabolities and genetic material [7]. In a more specific context of gene expression, several off-chip assays can be used to analyze mRNA/Protein levels, protein-protein interactions, phosphorylation and translocation of relevant regulatory biomolecules (**Figure 1-3**).

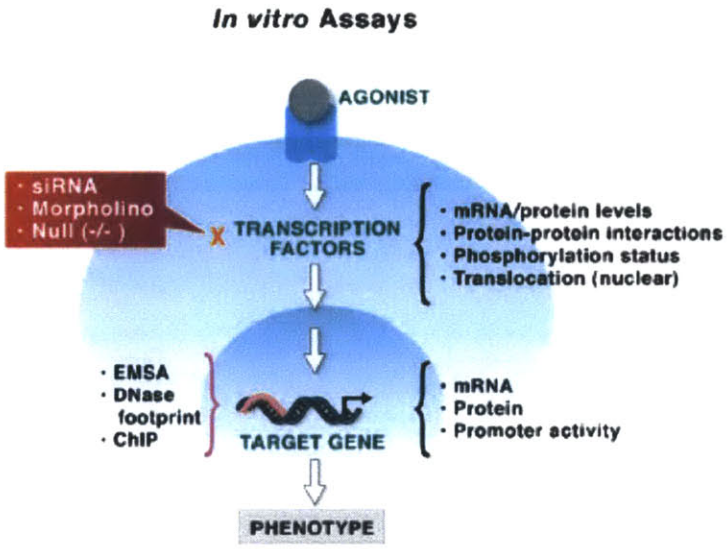

Figure 1-3 Schematic of a variety of in-vitro techniques used for analysis of cell physiology in the context of genetics. Obtained with permission from [21].

However, microsystems engineered for cell biology may not necessarily be able to utilize all of these methods to evaluate their impact on cell physiology. Part of the reason lies in the fact that many of the traditional assays for cell physiology require large cell numbers or complicated protocols which may not be feasible with all device platforms. Nevertheless, studies of cell morphology, viability and growth rate are performed by microscopy itself- a tool available for most experimentalists and device designers. It is therefore typical to observe microsystems engineers presenting viability, morphology and growth rate data as gross indicators of cell health in the context of their devices. For example, an on-chip cell culture platform meant for long term cell culture used cell-viability staining and morphology information as an indicator of favorable cell culture conditions [22]. In another example, cell morphology was used to infer cell physiology in a microfluidic single-cell culture array [6]. Lecault, and others cultured hematopoietic stem cells in a microfluidic device and compared growth rates of their on-chip and off-chip cultures as a metric of evaluating stem cell physiology [23]. As there is no current 'standard' or metric for quantifying physiological shear stress in microsystems, it is currently not straightforward to compare platforms to each other for evaluating cell physiology. This thesis will address this concern by providing a unique cell-based sensor approach that could be useful in the microsystems community for evaluation of fluid shear stress.

1.2. Motivation and approach for a cell-based sensor for fluid shear stress

In this thesis a cell-based fluid shear stress sensor will be developed by correlating applied stress exposure to resulting stress pathway activation and subsequent gene expression.

Primarily this will be advantageous because changes in gene expression are up-stream to the later chronic changes in cell physiology that dictate morphology, proliferation and viability. Conveniently, gene expression is quantifiable (by RT-PCR, protein immunoblotting, etc.) as compared to other observable metrics such as morphology. The caveat of using RT-PCR or blotting is that these methods are end-step processes which require cell processing and are eventually detrimental to the cells. Therefore, a cell health sensor that allows for a visual and non-destructive assessment of gene expression through quantitative fluorescence will be beneficial and desirable.

A genetically encoded live-cell sensor that provides information regarding chosen stress pathway activation via expression of fluorescence is a relevant solution to this concern. This ability will eliminate the need for disruptive cellular processing and does not require any additional reagents for fluorescence visualization. Furthermore, this sensor would be able to provide an extra dimension of information about cell heath alongside morphology, growth rate and viability available through microscopy alone. Such a sensor could be used for real time monitoring of cell health at a single-cell level by recording fluorescence with microscopy and live-cell imaging. The presented sensor will be a reporter cell-line, whose expression of a fluorescent protein is driven by a promoter of a stress responsive gene. This approach is shown in **Figure 1-4**.

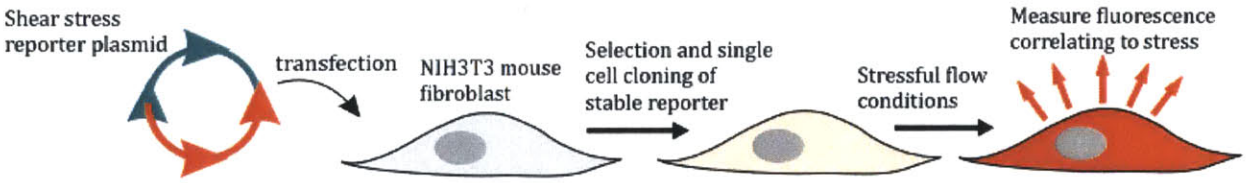

Figure 1-4: Schematic showing the approach to create a fluid shear stress sensor in NIH3T3 cells

A clonal population of such a sensor will be selected based on high sensitivity and selectivity towards a given stress stimulus. Mapping fluorescence expression dynamics towards a sub-lethal range of stress intensity would be extremely useful in characterizing the sensor response. Subsequently, these cells could be provided to the cell-based microsystems community to evaluate device designs and operations with more comprehensive insight towards its impact on cell health.

In order to develop the proposed sensor, the primary goal is to choose a cell line which is representative of a 'model' cell line that most laboratories would be comfortable using and culturing. Also, the cell line needs to be relatively straight forward to engineer with an ability to elicit a response to shear stress with moderate sensitivity. In this thesis, the shear stress sensor is embedded within NIH-3T3 cells, which are mesenchymal cells and are known to show a shear

stress response [24]. The underlying functionality of this shear sensor is modeled after mechanosensitive biology of endothelial cells. These cells reside at the lumen wall, and can sense flow induced shear stresses in order to adapt towards a homeostatic state. In accordance to a range of vascular fluid shear stresses, these cells exhibit shear induced genetic responses, in a manner that makes them natural shear stress sensors (**Figure 1-5**)[21].

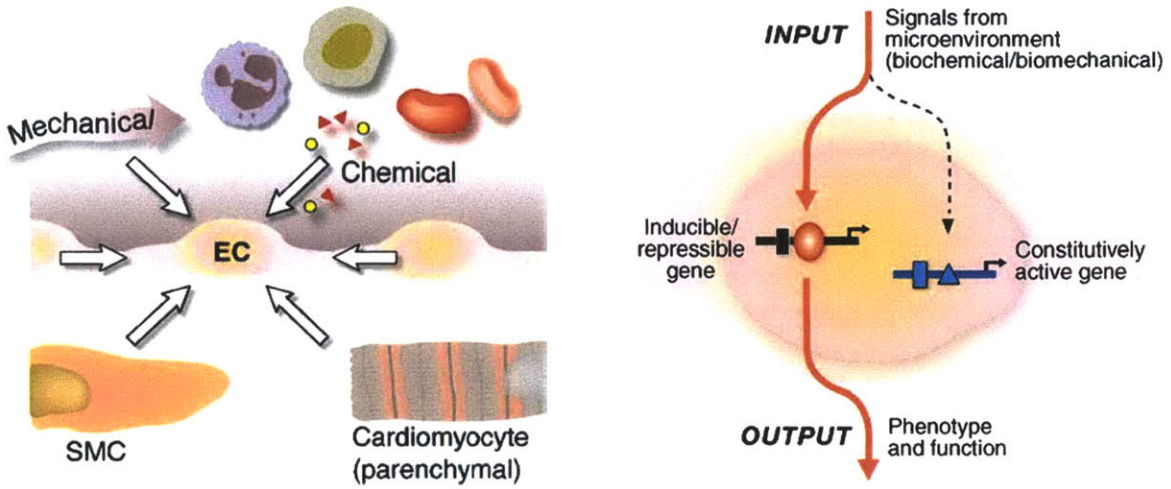

Figure 1-5: Schematic showing various stimuli induced endothelial cell gene expression. Obtained with permission from [21].

1.3. Fluid shear-stress mechanobiology

Similar to cells flowing in a microsystem, blood flow in vasculature also experiences fluid shear stress of various ranges. In contrast to laminar flow characteristics found in microfluidics, blood flow is relatively complex and can follow both laminar-like and turbulent regimes (**Figure 1-6**) [25]. While physiological shear stresses range from 1-20 dyne/cm^2, it is possible to observe high ranges of shear stresses in disease states. Interestingly the range of physiological and disease-state shear stress intensities is also found in many microsystems, which is why vascular mechanotransduction mechanisms are relevant for creating a shear stress sensor for microsystems.

In order to assess the implications of fluid shear stress on cell physiology it is important to understand the mechanisms by which endothelial cells experience and adapt to an applied shear force. Fluid shear stress is transmitted through luminal trans-membrane proteins, via tension of the cytoskeleton, to the nuclear membrane. This phenomenon is called mechanotransmission, and can influence morphological changes by cytoskeleton rearrangements. At the same time, shear stress also affects the cell physiology through membrane signaling, second messengers, and activation of transcription factors. This type of response to shear stress is categorized as mechanotransduction, and is fundamentally tied to

stress pathway activation and gene expression modulation [18]. A schematic overview of these effects are shown in **Figure 1-7** [26].

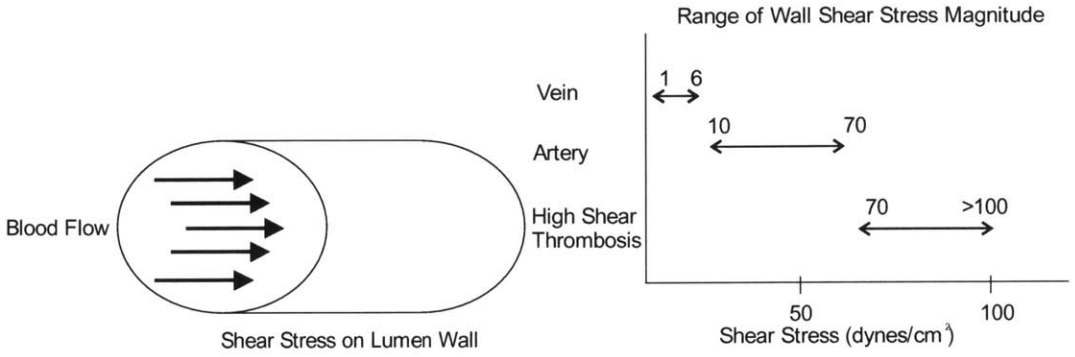

Figure 1-6: Schematic showing the cross-sectional illustration of blood vessel with hemodynamic shear stress, along with ranges of shear stress magnitudes encountered in arteries, veins, and in high shear stress conditions. Adapted with permission from [25].

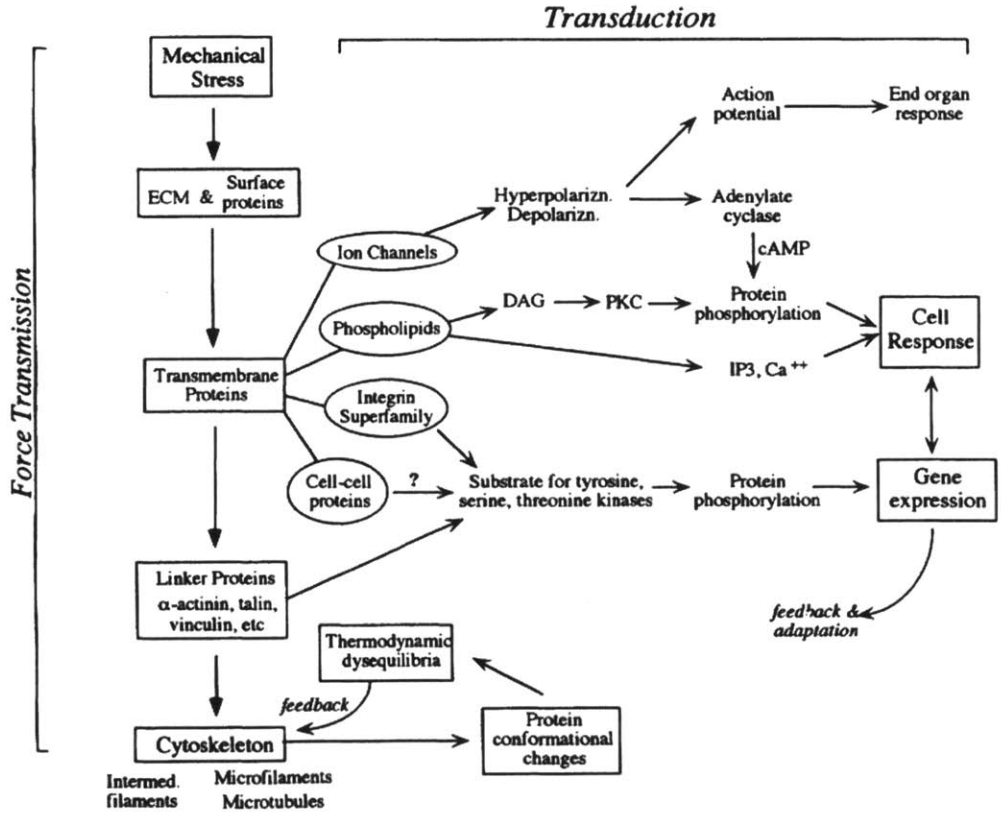

Figure 1-7 Overview of mechanotransmission and mechanotransduction due to fluid shear stress. Obtained with permission from [26].

In terms of designing a shear stress sensor for microsystems, it will useful to know if cells are sensitive to only a particular kind of flow profile. For example, if a shear stress sensor is based

on cells which are naturally only sensitive to pulsatile (blood) flow, then they may not be as responsive to continuous laminar flow observed in many microfluidic systems. Fortunately, in terms of gene expression, many flow profiles are found to elicit a biological response (**Figure 1-8**) [27]. Therefore, designing a shear stress sensor will require investigation of shear sensitive genes with sensitivity to relevant flow patterns (steady and laminar) more commonly found in microsystems. Furthermore, it is interesting to note that even within the regime of uniform laminar shear stress, cells can be sensitive either acute exposure or chronic exposure to shear stress and therefore illicit differential gene expression patterns (**Figure 1-9**) [28].

This makes it possible to investigate a subset of shear inducible genes for a particular microsystem flow profile. The 'gentle-but-prolonged' category of microfluidic devices may impart shear stress intensities which may possibly be below the detection limit of cells within their natural environment. While such stresses may still affect cellular physiology, it is possible these effects may be smaller than that from the category of 'short-but-intense' shears. In this thesis, genes sensitive to acute and uniform laminar shear stress will be explored, in order to investigate physiological stress from 'short-but-intense' category of microfluidic devices.

Most of the seminal work in analyzing the effects of shear stress on cell physiology and gene expression has been performed using primary endothelial cells such as bovine aortic endothelial cells (BAECs) or human umbilical vascular endothelial cells (HUVECs) due to their relevance to vascular diseases and blood pathology. Various shear sensitive genes have been identified in literature using these cells and others [29] and with various expression dynamics.

Endothelial Cell Responses to Different Types of Unsteady Laminar Shear Stress

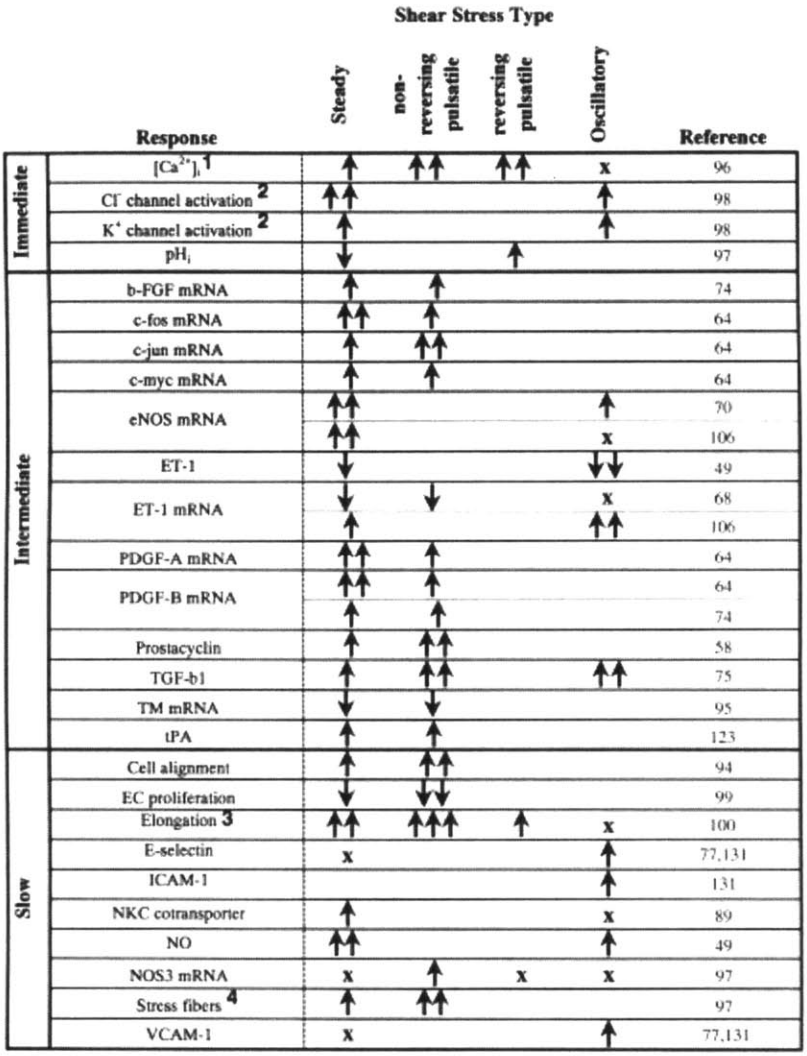

Figure 1-8 Shear inducible gene expression dynamics with sensitivity towards different flow patterns. Obtained with permission from [27].

	Uniform laminar shear stress
Induction: Acute:	PGI synthase, connexin43, c-myc, c-fos, c-jun, egr1 PDGF-A, tissue factor, smad 6, 7.
Chronic:	PDGF-B, TGF-β, *b*-FGF, HB-EG CNP, COX-2, Thrombomdulin, HO-1, thrombospondin laminin B1, myosin light chain kinase, Mn SOD ICAM-1, GRO, IL-1, IL-6, IL-8 receptor, tPA, lysyl oxidase, Cu/Zn SOD.
Repression:	PAI-1, Endothelin converting enzyme, NADH dehydrogenase. VCAM-1 (lymphatic EC)
Acute induction prolonged repression:	Endothelin-1, ACE, thrombomodulin.

Figure 1-9 Genes sensitive to various exposure profiles of uniform laminar shear stress. Obtained with permission from [28]

Figure 1-10 illustrates an overview of biochemical events that are activated by shear stress, including gene expression [30].

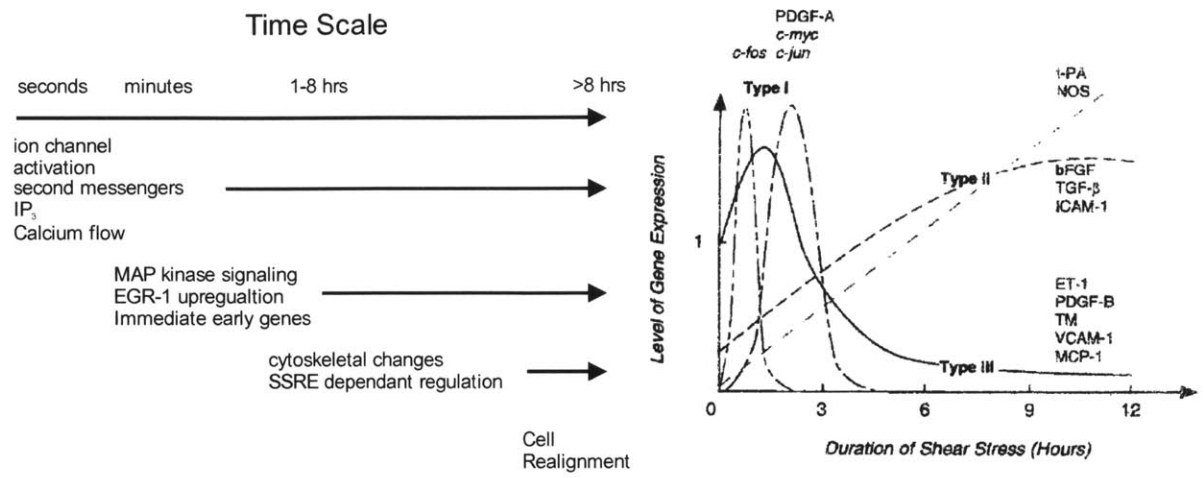

Figure 1-10: Sequence of biochemical activation events upon shear stress (*left*). Gene expression dynamics with respect to shear stress duration with genes categorized by the expression profile types *Iright*). Figure adapted from [30, 31] with permission.

In order to specifically focus on shear gene induction due to acute exposures, it is imperative to focus on genes that are upregulated within minutes of exposure. It will also be interesting to focus on genes with regulation that returns to basal levels following maximal induction. Such feature would allow the sensor to 'reset' after some time and could potentially be usable for another shear stress measurement. Therefore in this thesis, genes following the Type and Type IIII category (**Figure 1-10**) will be investigated.

Taken together, it can be seen that shear responsiveness of endothelial cells can be highly specific towards many fluid shear stress characteristics. In this thesis a gene panel of relevant shear sensitive genes will be explored given the stated sensitivity preferences towards shear intensity, flow profiles, and exposure duration. The main idea would be to identify the ideal shear sensitive gene in NIH3T3 cells, with consistent and high level of inductions. It would also be important to choose a gene that is conserved and explored within many cell phenotypes, for the cell sensor to represent a generalized shear-induced physiological stress among the many cell types used in microsystems. In this thesis, the chosen shear responsive genes will be PDGF-α, PDGF-β, MCP-1, EGR-1, c-Fos, ICAM-1, VCAM-1 and TF. To check cross-sensitivity to other stress pathways such as DNA damage and heat shock pathway, p53 and HSF-1 will be chosen as representative genes respectively.

In this thesis, the shear-induced gene expression in NIH3T3 cells is studying by using a logarithmic shear-stress device that can multiplex 6 shear conditions at once [12]. Gene expression profiles will be specifically evaluated upon cells following various perfusion conditions using qRT-PCR.

In order to elucidate the relevant shear pathway in NIH3T3s, it is important to understand the cause of shear sensitivity of the chosen gene by understanding regulatory domains in its promoter sequence. In literature, several shear response elements are correlated to the chosen gene panel [30]. These response elements are essentially short sequences in the promoter that are essential to elicit induction of that gene upon shear stress. Specifically, the PDGF-α, PDGF-β, MCP-1, and TF response elements were identified and named as Sp1/Egr-1, SSRE, TRE and Sp1 [28]. In many cases, these sequences are the binding sites to known transcription factors which are inferred to be activated upon shear stress. A general characteristic of the shear stress physiology is that there is no-consensus transcription factor that is activated upon shear stress across a range of genes, let alone cellular phenotypes. One possible shear induced pathway relevant to the chosen gene panel is shown in **Figure 1-11**.

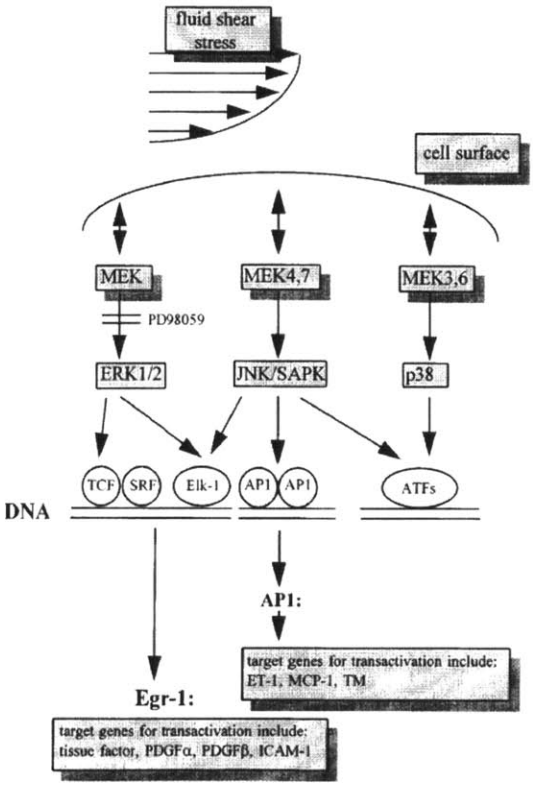

Figure 1-11: Possible shear induced MEK-ERK 1/2 pathway relevant to regulation of chosen gene panel. Obtained with permission from [30].

As the native promoters of the shear responsive genes contain multiple response elements, it is possible that desirable shear sensitivity may not necessarily guarantee desired induction selectivity towards shear stress. To investigate this further, the chosen approach in this thesis will be to clone three tandem response elements in the multiple cloning site of a promoter-less vector (pTurboRFP-PRL). This is a typical approach mentioned in the research literature [32] as well as in commercially available reporter plasmids. Following this approach will allow

construction and also comparison of reporter cell lines that will be induced by chemicals known to trigger the inferred shear pathway from initial genetic analysis. The induced expression will be evaluated in terms of induced fluorescence expression as well as the by quantifying the fraction of induced population.

Following the investigation of shear induced genetic expression profiles as well as chemical induction profiles of reporter cell lines, a suitable promoter for shear stress induction will be identified, and used to construct the final shear stress reporter cell line. This cell line will be first characterized in its response to chemicals stimulating pathways similar to that of the inferred shear pathway. Subsequently, the reporter cell line will be cloned and used for characterization of devices imparting fluid shear stress.

In summary, this proposed cell-based sensor will provide a more convenient approach to quantify cell health in microsystems. With its application, it will be possible to be to eliminate the need for having large cell numbers for obtaining information regarding cell physiology. Similarly, system characterization will be convenient due to minimal steps and processing required characterizing the proposed cells sensor response. Finally, the future distribution and propagation of this cell-sensor in the microsystems community could allow it to become one of the 'standard' metrics in evaluating microsystem design.

1.4. Thesis overview

In order to pursue creating a shear stress sensor with the considerations described as above, the main objectives of this these are:

1. Analyzing changes in gene expression of cells using microfluidic perfusion platform that imparts a range of fluid shear stress (**Chapter 2**:).

2. Development and characterization of a set of reporter cell lines to choose an appropriate promoter for shear stress **(Chapter 3:).**

3. Development and characterization of the shear stress sensor **(Chapter 4:).**

The main conclusions, contributions and future prospects of this thesis work will be provided in **Chapter 5**: .

Chapter 2: Microfluidic Shear-Induced Gene Expression

2.1. Introduction

This chapter discusses fluid shear stress-induced gene expression in NIH3T3 cells. First, immediate-early gene expression profile of shear inducible genes was characterized by serum treatment. Microfluidic devices were developed and used to apply logarithmic shear stresses on these cells. Induced gene expression was analyzed by qRT-PCR to characterize shear stress pathways in NIH3T3s, which could be later utilized to identify suitable shear-inducible promoter candidates.

2.1.1. Immediate-early pathway induction

Each inducible promoter can have multiple response elements (binding sites) of different regulatory transcription factors, which could synergistically orchestrate transcription in a complex fashion. In fact, certain transcription factors can increase mRNA levels of one gene and decrease that of another through the same shear stress response element. For example, fluid shear stress induced AP-1 transcription factor can increase levels of MCP-1 as well as decrease VCAM-1 levels in HUVEC cells through the same AP-1 response element [30]. Both of these genes have NF-κB binding sites as well, which have been reported to regulate shear stress induced PDGFB expression. It is not clear if that transcription factor NF-κB could also affect shear induced regulation by AP-1. Such transcription aspects add complexity to elucidating a unique shear mechanism.

One method of thoroughly characterizing shear induced pathways could be to study gene expression dynamics due to large range of shear stimulus exposure doses. Such screening is a cumbersome process and has not yet been reported for NIH3T3 cells. One report however, has reported a genome-wide study of these cells experiencing mechanical stretching in-vitro [33]. Two prominent genes reported to be upregulated due to this stress were EGR-1 and c-Fos. While the stimulus is not the same as fluid shear stress, it induced these two genes which are interestingly also upregulated due to fluid shear stress.

Specifically, EGR-1 and c-Fos were deduced to be responsible for the downstream shear induced expression of PDGFA and MCP-1 respectively. EGR-1 and c-Fos encode for transcription factors which share many similar characteristics. In fact, these two genes have been categorized as immediate-early response genes whose transcription transiently rises to very high levels following growth factor or mitogen stimulation and subsequently decays to basal levels [34, 35]. Such induction kinetics have been linked to these genes having serum

response factor (SRF) REs in their promoters, as show in **Figure 2-1** Primary response genes c-Fos and EGR-1 sharing common regulatory elements such as serum response element (S) and the cAMP response element (C). Information adapted from [37].

[34, 36, 37].

Figure 2-1 Primary response genes c-Fos and EGR-1 sharing common regulatory elements such as serum response element (S) and the cAMP response element (C). Information adapted from [37].

Interestingly, PKC and MEK/ERK dependent expression of EGR-1 and c-Fos due to wound induction or applied fluid shear stress involves the activation of this serum response element (SRE), shown in Figure 2-2 **Figure 2-1 Primary response genes c-Fos and EGR-1 sharing common regulatory elements such as serum response element (S) and the cAMP response element (C). Information adapted from [37].**

[38-42]. Therefore, it was of interest to first verify if such a mechanism existed in NIH3T3 cells, and could be triggered by chemical stimulus, such as by serum treatment.

2.1.2. Shear induced gene panel

In order to directly evaluate shear stress driven regulation of inducible genes, a panel of genes was chosen from literature as: PDGFA, MCP-1, c-Fos, EGR-1, PDGFB and TF [30]. These genes have known shear stress response elements within their promoters, suggesting ability to be upregulated by fluid shear stress [28]. VCAM-1 was added to this panel of genes because it has been reported to be down-regulated due to shear stress [43]. Representative genes from other stress pathways such as DNA damage and heat shock pathways were chosen as p53 and HSF1, in order to cross-talk between stress pathways due to fluid shear stress.

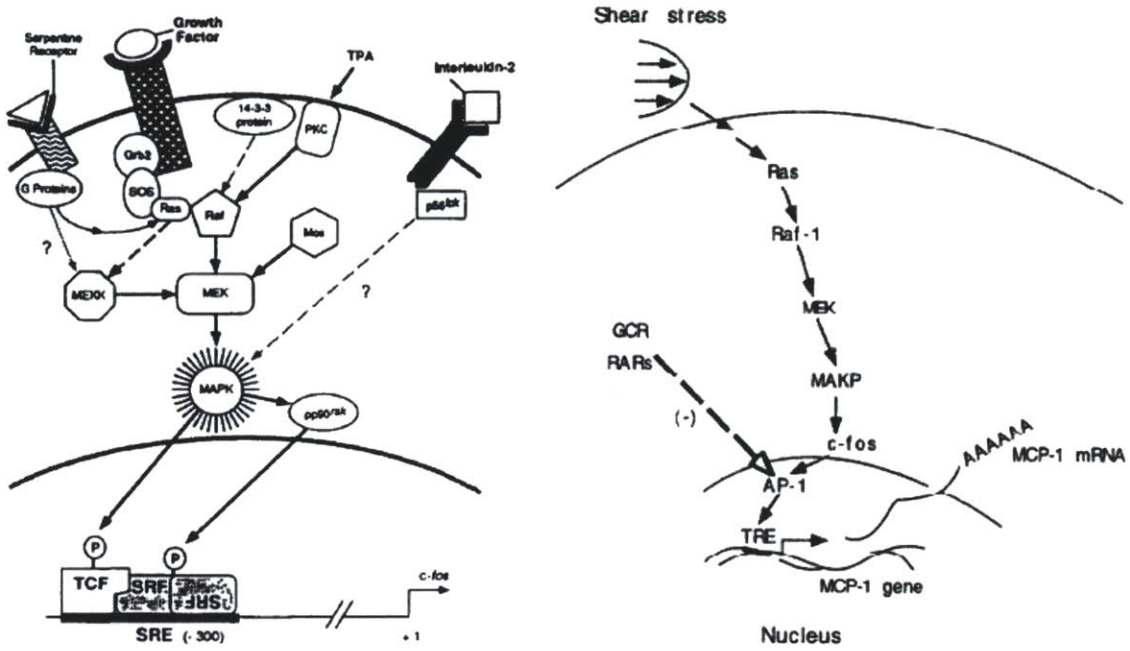

Figure 2-2 Similarity of SRE driven c-Fos induction by various stimuli and shear stress induced c-Fos pathway. Obtained with permission from [41] [44].

2.2. Materials and Methods

2.2.1. Cell culture

NIH3T3 cells were expanded from a continuing cell stock in the laboratory, with the parental cell line originating from ATCC cell bank (ATCC® CRL-1658™). The culture conditions were maintained according to the proposed ATCC protocol. The cell culture media ATCC-formulated Dulbecco's Modified Eagle's Medium, with high glucose content (Catalog No. 30-2002) was supplemented with bovine calf serum (10% v/v), L-glutamine (2% v/v) and penicillin-streptomycin (1% v/v).

2.2.2. Serum inductions

Cells were seeded in 6-well plates to reach 80% confluence. Serum free media (0.15% serum) was introduced to cell cultures for 24 hours in order to serum-starve cells prior to induction. The serum starved cells were then incubated with regular cell culture media with 3, 10 and 20% (v/v) serum concentrations for 30 minutes, 1 hour and 2 hour durations. The reference controls were cell cultures with no serum inductions. Cells were lysed for RNA extraction immediately after the serum exposure. Induced expression was normalized to basal expression of serum starved cells.

2.2.3. Device fabrication and perfusion setup

The general perfusion operation is outlined in **Figure 2-3**. Cells were seeded in a microfluidic device overnight, perfused with media, collected and used for qRT-PCR analysis of induced gene expression. In this chapter, two different microfluidic devices were used for this purpose.

For long term (3 hour) perfusions, a microfluidic device that can impart logarithmic shear stress on adherent cells was used to evaluate shear induced gene expression **Figure 2-3**D [12]. Toh and others previously characterized this device operations and fabrication protocols, which were followed identically for this chapter. **Figure 2-3**B shows the perfusion setup with the closed loop perfusion network and peristaltic pump. **Figure 2-3**C shows the clamping procedure used to assemble a leak-proof device setup.

Following perfusions, microfluidic devices were disassembled from their clamped configuration and aligned to a vacuum-sealed membrane manifold. This manifold allowed for accessing of individual cell chambers for cell lysis buffer needed for subsequent RNA collection process. Procedure of disassembling the microfluidic device and assembling the vacuum-based network for cell lysate collection is shown in **Figure 2-4**.

For short term (1-2 hour) perfusions, a new device was designed and used for gene expression studies. These devices were casted from a designed mold, ordered from Fineline Inc. Each device consisted of 8 chambers (20 mm length x 2.5 mm width x 0.15 mm height). Wall shear stress and flow profiles were modelled according to previous work [12]. These chambers were four times larger in surface area than the device descibed above, allowing for larger cell numbers to be analyzed after perfusion. The device mold and individual chamber design are shown in Figure 2-5. After punching holes for inlets and outlets, the device was plasma bonded to a borosilicate glass slide (76.2 mm length x 25.4 mm width). Within half an hour of bonding and baking the device, ethanol (80% purity and 0.2 µm filtered) solution was manually added to all chambers for 5 minutes to sterilize the chambers and to wet the surfaces with an aqeous solution. This ethanol solution was rinsed with deionized water 5 times to remove any residue (ethanol, PDMS, or otherwise) potentially toxic to cell culture. A 0.1% aqeous gelatin solution was then introduced for 30 minutes to make the surface favorable for cell adhesion and proliferation. Subseuqently, regular cell culture media (0.2 µm filtered) was manually introduced into each chamber to prime the device. The entire device, without any fluidic connections, was stored in a cell culture incubator for 16-24 hours to equilibrate the device with media constituents and cell culture environment.

On the day after device priming, cells of interest were brought to suspension at 5 x 10^6 cells/ml concentration in media that was previously equilibrated to the incubator environment. The

cells were strained to remove any large cell clusters. Inside a sterile environment, the media in each chamber was rinsed and replaced with 100 µL of fresh and pre-equilibrated cell culture media. Subsequently, 30 µL of cell suspension was manually dispensed into each chamber sequentially. With a chamber volume of 7.5 µL, approximately 37,500 cells were introduced into each chamber. This condition provided cells at 80-90% confluency the next day, prior to perfusion. Furthermore, this cell number accounted for any marignal error in cell attachment during seeding or perfusion processes. The device with cells was placed inside a sterile dish and then inside a sterile incubator for 24 hours.

On the day proceeding seeding, cells in each chamber were imaged using microscopy. For perfusion studies, each experiment consisted of running parallel perfusions at a given flow rate (divided into logarthmic flows according to external tubing diamter ratios) for a given duration. The static condition consisted of cells in culture dish experiencing no flow. Chambers experiencing flow were connected to 20-30 mL reservoirs of cell culture media. All chambers were connected by external closed loop fluidic connections and the entire device was placed in a cell culture incubator for the perfusion duration **Figure 2-4**B. The pump was used to first prime the tubing connections at the experimental flow rate through a device bypass in order to remove any potential bubbles in the systems and to ensure a leak-free connectivity. The bypass was then routed to the device to begin the perfusion.

Following perfusion, this device was disconnected from the perfusion setup and the cells were imaged again with microscopy. The cell media within each chamber was manually replaced with Trypsin (0.25% v/v with no EDTA) (at 37°C) for 5-10 minutes. The suspended cells were collected, centrifuged and resuspended in lysis buffer prior to RNA extraction.

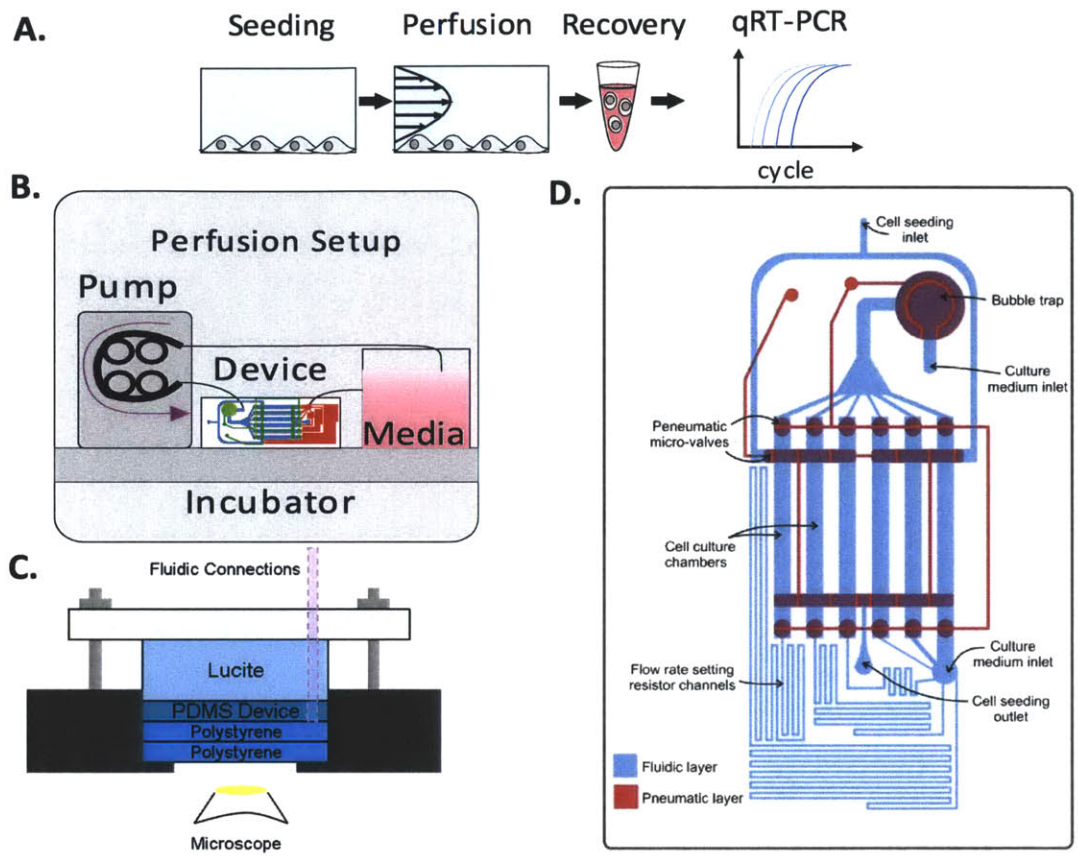

Figure 2-3 Perfusion experimental A: approach, B: setup , C: assembly and D: chip layout (unpublished figure from [12]).

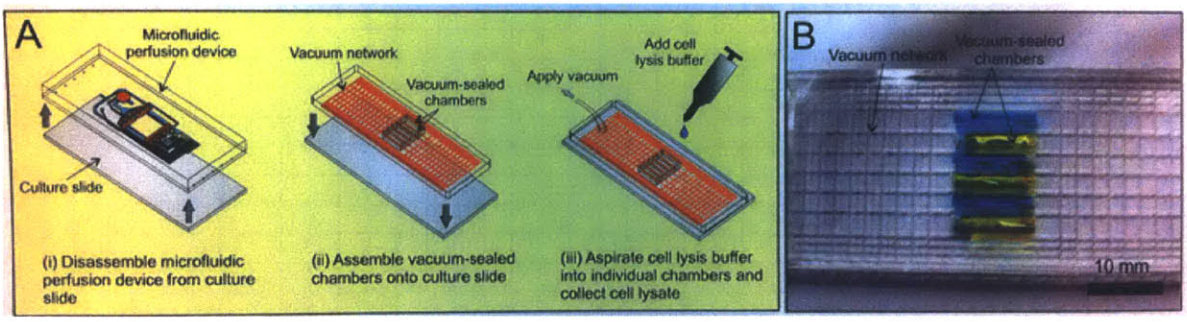

Figure 2-4 Device disassembly procedure for collecting cell lysate (A) using PDMS vacuum network manifold (B) (unpublished figure from [12]).

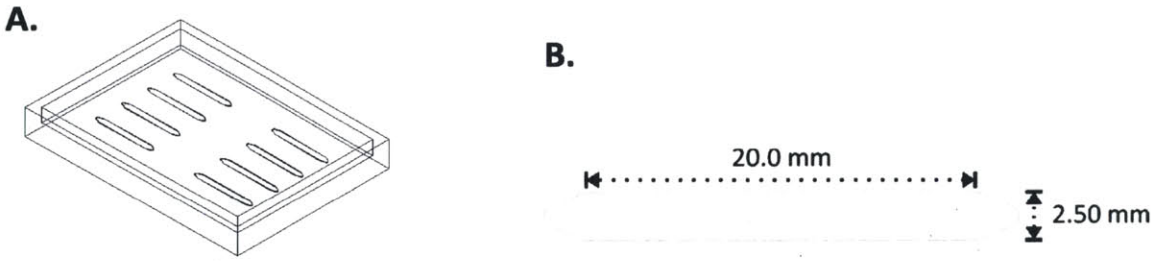

Figure 2-5 Mold for perfusion device of 8 microfluidic chambers (A), with individual dimensions (B).

2.2.4. Quantitative RT-PCR

Cellular mRNA was extracted from the collected lysate using Qiagen RNeasy Micro kit (catalog #:74004) using its reccomended protocol. The collected mRNA quality and concentration was evaluated using NanoDrop 1000 Spectrophotometer. The amount of mRNA used for reversre transcription was taken as 1 µg from all sample conditions and convered to cDNA using random hexamer primers. Specifically, the PCR mixture composition and thermocycling protocol was taken from DyNAmo cDNA synthesis kit (Thermo Scientific, catalog # F-470L). The qPCR reaction setup utilized the Bio-Rad iQ SYBR Green Supermix (Bio Rad, catalog # 170-8882) The PCR reaction was conducted and analyzed with Bio Rad CFX96 Touch™ Real-Time PCR Detection System, according to its recommended protocol. Gene expression profiles were quantified and normalized as relative expression to GAPDH, using its standard curve.

PCR primers used for qRT-PCR are listed in the following page. These primers, spanning exon junctions, were designed using NCBI Primer-BLAST tool, to all have no non-specific products as verified by NCBI BLAST results. Each primer length was kept around 20 base pairs, with product lengths (in this case, 100 base pairs). Likewise, the primer sets were checked for any primer-dimer possibilities, both *in-silico*, and with each experiment. The GC content was also kept comparable among primers (around 60%). Such considerations were taken in order to achieve similar priming and amplification efficiencies from each gene primer set.

PCR Primers

Gene	GeneBank ID/Source	Primer	Sequence (5'-->3')	Product Size	Exon junction	Start-Stop	Melting Temp	GC %
p53	NM_001127233.1	Fwd	AGGGCTCACTCC AGCCTCCAG	113	1248-1249	1147-1167	63.5	66.7
		Rev	AGGGGAGGGAT GAAGTGATGGG			1259-1238	60.7	59.1
HSF1	NM_008296.2	Fwd	TGCTGGAGCCCG AGTGGGAA	110	273-274	262-281	63.8	65
		Rev	TGCCGCACGAAG CTAGCCAT			371-352	62.2	60
PDGFB	NM_011057.3	Fwd	ATCCAGGGAGCA GCGAGCCAA	116	1411-1412	1395-1415	63.7	61.9
		Rev	CCGCCTTGTCAT GGGTGTGCT			1510-1490	62.7	61.9
MCP-1	NM_011333	Fwd	CAGCCAGATGCA GTTAACGCCC	106	161-162	155-176	60.9	59.1
		Rev	ACCTGCTGCTGG TGATCCTCTTGT			260-237	62.4	54.2
PDGFA	NM_008808	Fwd	ACTCCGTAGGGG CTGAGGATGC	97	342-343	334-355	63	63.6
		Rev	CGAATGGGCACA GGCCGCTT			430-411	63.6	65
TF	NM_010171	Fwd	GCGGGTGCAGG CATTCCAGAG	95	266-267	257-277	63.5	66.7
		Rev	TAGTTGGTGGGT TTGGGTTGCCA			351-329	61.4	52.2
c-Fos	NM_010234.2	Fwd	GGCTTACGCCAG AGCGGGAA	90	532-533	451-470	62.5	65
		Rev	GGAGATAGCTGC TCTACTTTGCCCC			540-516	60.9	56
EGR-1	NM_007913.5	Fwd	GCACCTGACCAC AGAGTCCTTTTC	103	580-581	567-590	59.8	54.2
		Rev	GGTGATGGGAG GCAACCGAG			669-650	60.6	65
pTurbo RFP	pTurboRFP-C (Evrogen)	Fwd	CAGAACGGCTGC ATCATCTA	116		346-366	54.8	50
		Rev	GGGTACAGCATC TCGGTGTT			461-481	57.1	55

2.3. Results and Discussion

2.3.1. Serum pathway induction

The primary goal of serum induction was to mimic an immediate-early pathway in NIH3T3 cells, similar to what may be the case for fluid shear stress imparted pathway induction. It is seen from **Figure 2-6** that these cells can indeed express immediate-early genes c-Fos and EGR-1 upon serum treatment of 30 minutes. Both transcripts are expressed at the highest level compared to any other gene or downstream targets, with sensitivity towards serum concentration. Observing this anticipated behavior suggested that an immediate-early serum-induced pathway could occur in NIH3T3 cells involving c-Fos and EGR-1. While serum induction may not necessarily be the true mechanism of shear induction in NIH3T3s, it shares similar pathway nodes and expression dynamics for both shear induced c-Fos and EGR-1, as described in literature [38-42].

It was further noticed that at 1 hour of induction, PDGFA, MCP1 and TF start to increase expression, with lowered expression of c-Fos and EGR-1. PDGFA and TF are downstream targets of EGR-1 and their shear induced expression is initiated after EGR-1 upregulation itself [45]. Similarly, MCP1 is a downstream target of shear induced AP-1 (consisting of c-Fos and c-Jun) that follows immediate high but transient expression of c-Fos [32]. Upon 2 hours of serum induction, there is more prominent serum concentration dependent expression of PDGFA, MCP1 and TF. EGR-1 and c-Fos levels return to basal levels for 3% serum concentration exposure and were comparable to each other for 10% and 20% concentrations at 2 hours. It was not clear why there was higher c-Fos and EGR-1 expression for the latter two serum dosages at 2 hours from 1 hour exposure. It is possible that other delayed regulatory pathways may be involved to control the expression of c-Fos and EGR-1 at 2 hour time point.

Interestingly, other downstream targets of other shear inducible genes, as well as representative genes from DNA damage (p53) and heat shock pathway (HSF) were not stimulated by serum. PDGFB and ICAM1 are reported to be downstream targets of shear induced NF-κB transcription factor, which did not show serum sensitivity in this experiment. Shear induction mechanism of NF-κB has not been clearly elucidated in literature and it is possible that its pathway may not be analogous to serum induced pathways or shear induced pathway of c-Fos and EGR-1.

Taken together, this experiment demonstrated ability of NIH3T3 to trigger an immediate-early induction pathway. In this case the cells show sensitivity to serum concentrations and durations of exposure. The induction dynamics and profiles are similar to that observed for shear induction; however no further studies were performed to definitely support this assertion for NIH3T3s. These results provided some confidence in using NIH3T3 cells as a model cell line to

sense an immediate-early pathway triggered by fluid shear stress that happens to be share similar profiles to a serum induced immediate-early pathway.

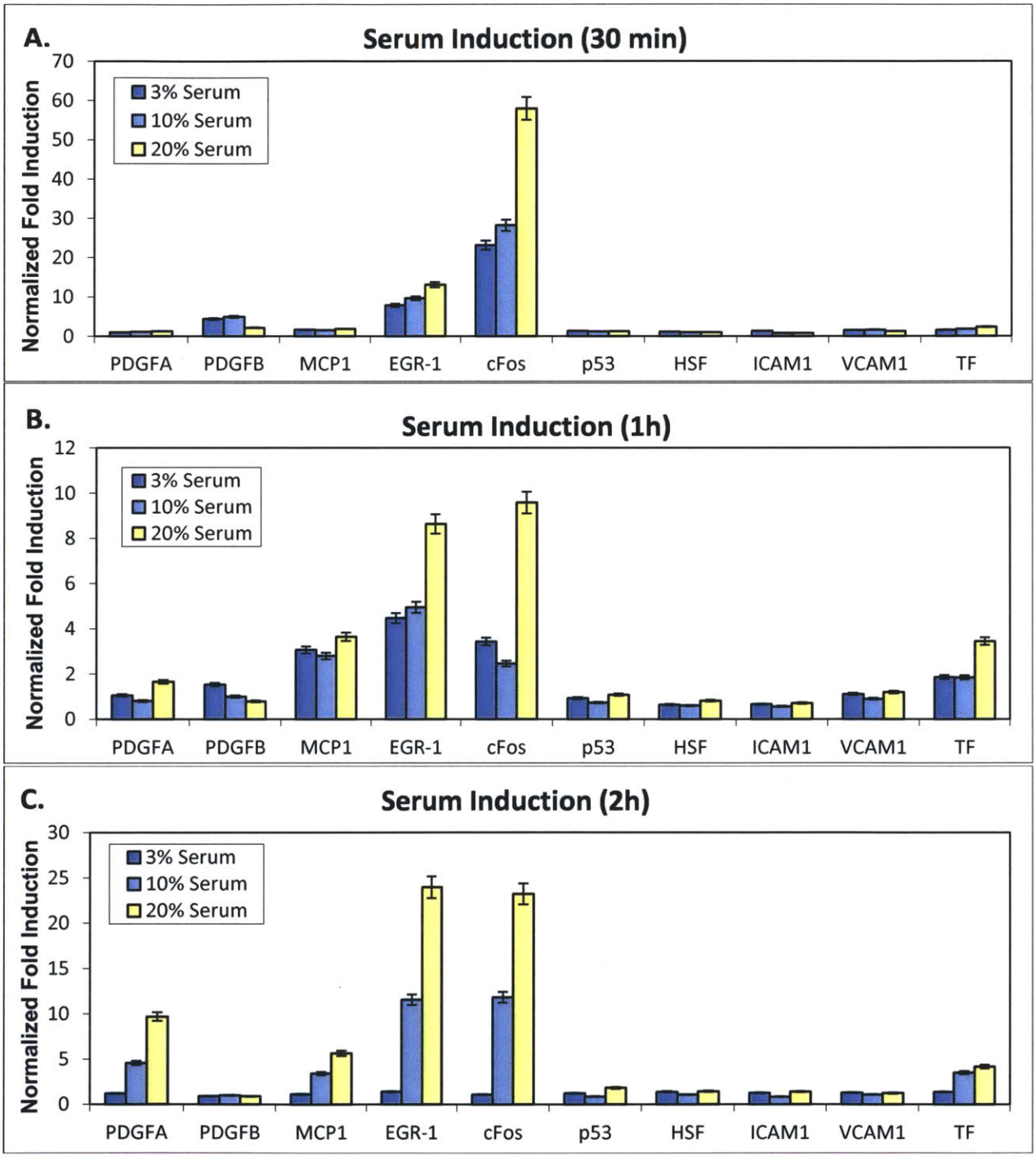

Figure 2-6 GAPDH normalized gene expression of serum induced cells at 30 min (A), 1 hour (B) and 2 hour (C) exposure duration. N = 2 experiments, error bar: standard error of mean.

2.3.2. Perfusions

Cell morphology was used to qualitatively assess any potential gross physiological changes due to the cell seeding process within microfluidic devices. As desired, it was observed that cell morphology within the device was similar to that observed from cells cultured in a dish (**Figure 2-7**). Cell growth rate was indirectly inferred by qualitative assessment of cell confluence over two days of cell culture in a dish and in cell chambers. The observed cell growth rate (not quantified) within the device was however, slightly lower than that seen in the native environment. However, as growth rate is an indicator of cell health relevant for prolonged culturing, it was not within the scope of these perfusion studies to optimize such long term cell culture conditions within the device.

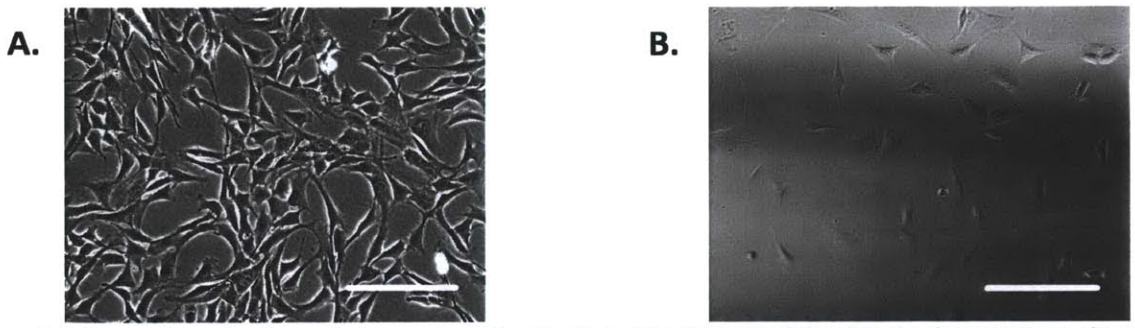

Figure 2-7 Comparison of cell morphology and proliferation in a cell culture dish (A) and in the device prior to shear exposure (B). Scale bar: 150 μm.

Cells in each chamber of the microfluidic device (**Figure 2-3**) were imaged using microscopy during the seeding process (**Figure 2-8**A). Adherent cells were imaged the following day (**Figure 2-8**B), where comparable cell confluence was observed, suggesting identical cell culture conditions among chambers of the device. These cells were also imaged immediately after applied shear stress, (**Figure 2-8**C) where it was observed that cells indeed maintained similar morphology and confluence before and after perfusion. In some experiments, there was cell loss observed for the highest shear conditions. This effect was compensated by a higher cell seeding density in order to have adequate cell number for gene expression analysis.

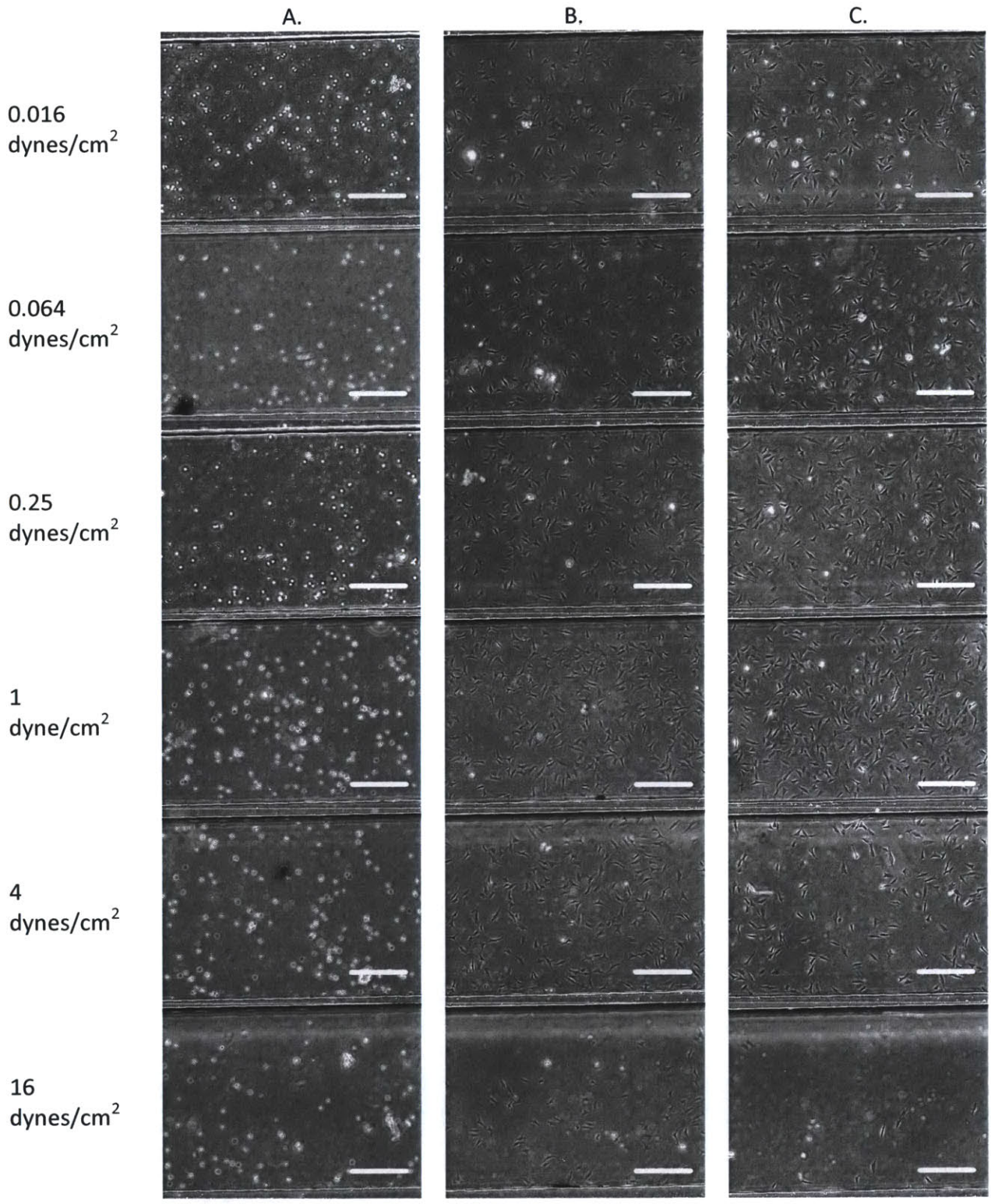

Figure 2-8 Cell seeding process across shear condition chambers (A), resulting adherent cells after 24 hours (B) and the same immediately following perfusions (C). Scale bar: 150 μm.

Using this device, 3 hour perfusions were performed on NIH3T3 cells and their resulting gene expression for shear induced genes is shown in **Figure 2-9**. Here, it was observed that EGR-1 had the highest sensitivity to shear stress, according to its expression correlating with stress levels. A similar, but more moderate trend was observed for c-Fos and its downstream MCP1 gene. PDGFA demonstrated elevated levels as well however it was not clear if the expression truly correlated with applied shear stress intensity. PDGFB had the highest elevated levels among all genes however this gene also had the highest variance in expression among experimental conditions. Based on analysis of PCR product melt curves, it was realized that PDGFB product always created non-specific products, or could not be amplified at all using the same primers and starting cDNA template quantity as that from reference static cultures and reference standard murine cDNA. Despite primer and PCR procedure optimization, this issue could not be solved and therefore due to consistent unreliability in PDGFB PCR data, this gene was removed from the analyzed gene panel of subsequent data sets. These results collectively demonstrated that it was indeed possible to analyze shear stress induced gene expression in NIH3T3 cells.

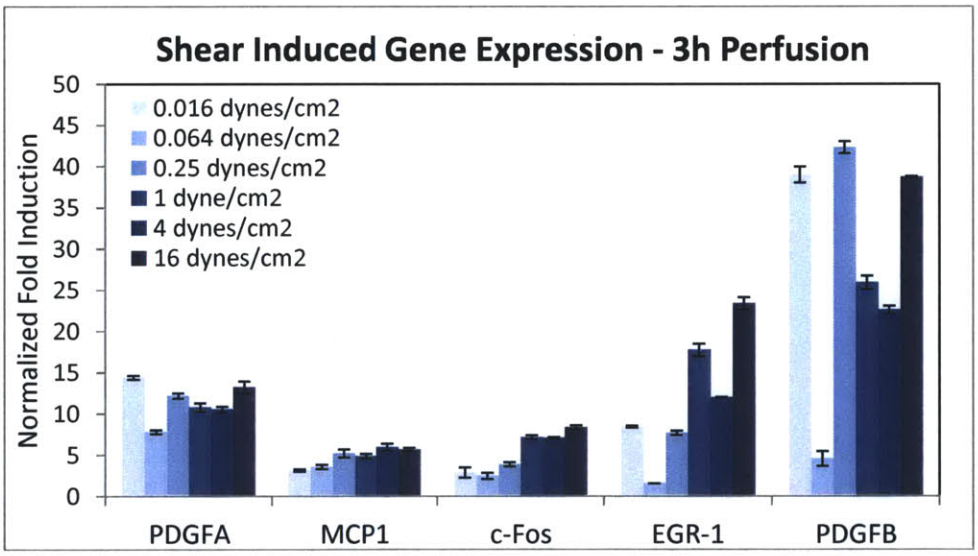

Figure 2-9 Shear induced gene expression from 3 hour perfusion. N = 2 experiments, error bar: standard error of mean.

There were two main drawbacks of assessing such gene expressions with the device used initially [12]. The first major concern was regarding the usage of vacuum manifold to collect RNA. This process was very sensitive to vacuum line pressure and pipetting technique. Quite frequently the lysate was accidentally lost to the vacuum line maintaining the seal between the manifold and the polystyrene slide containing cells. This process was tricky because the slide could not be dried as that process could presumably kill cells as well as denature/destroy genetic material undesirably. A 'wet' slide consequently hindered proper sealing of the vacuum manifold to the surface, thereby leading to frequent loss of lysate.

The second drawback of using this device was that it could only culture at most a couple thousand cells with reasonable confluence (~5 x10^4 cells/cm^2). While traditional column-based RNA extraction kits advertise ability of RNA collection from less than a 1000 cells, they were not as effective in collecting high quality RNA in these experiments. Given any cell loss from perfusion or collection process, the amount and quality of RNA collected was frequently sub-optimal for subsequent PCR steps. Specifically, typical RNA amount collected from a chamber ranged from 40-100 ng. Typically, the ratio of RNA absorbance at 260 nm to 230 nm is used as measured sample quality where two-fold absorbance at 260/230 nm is considered good quality RNA. In most cases, due to low amount of collected RNA, the relative signal from contaminants was higher, which lowered this ratio to around 1.1-1.6. Even though it was possible to proceed with PCR and gene analysis from these experiments, it was not clear if RNA degradation or impurity could have biased the results. Furthermore, the low amount of RNA collected from the lysate also limited the amount reverse transcription, and therefore the number of genes used in PCR. Taken together, the process of RNA collection as well the quality of RNA collected were both limiting effective and reliable gene expression studies through this approach.

With this motivation a second device was designed and fabricated that utilized a different approach to collect cells (**Figure 2-5**B). First of all, as the device was plasma bonded to glass, it was irrelevant to use a vacuum manifold for cell recovery. Cell lysate was collected directly from each chamber from the media perfusion inlet and outlet, which guaranteed minimal loss of collected genetic material. Also, the surface area for cell coverage in each chamber was four times larger than that from the previous device. This increase in area correspondingly provided four times as many cells used for gene analysis. The amount of RNA collected was significantly higher with much better quality. RNA absorbance measured by spectrophotometer at 260:230 nm was around two fold, as desired. The increase in RNA amount directly corresponded to the ability to screen though a larger set of shear inducible genes through PCR, thereby providing more information per perfusion experiment than before. Motivated by such improvements, the second device was used for subsequent perfusion analysis.

However, different challenges were identified in the usability of the second device. Due to lack of on-chip fluid control such as the lack of de-bubbler, bubbles were frequently found in the device chambers after overnight cell incubations (**Figure 2-10**A). In the previous device, the pneumatic valves controlling fluidics were vacuum operated, and were left actuated during the overnight cell incubation. As PDMS is gas permeable, the vacuum applied through the open valves helped prevent bubble formation in chambers. Similarly, the lack of on chip fluid rerouting led to introduction of cellular debris and clumps from within the cell loading tubing to the chambers (**Figure 2-10**B). These clumps prevented proper perfusion of seeded cells and sometimes caused leaks due pressure build up in fluidic connections. Lastly, the glass substrate

used for plasma bonding the PDMS was sub-optimal in cell adhesion at high shear rates. Occasional cell detachment and losses were observed after perfusions (Figure 2-10C).

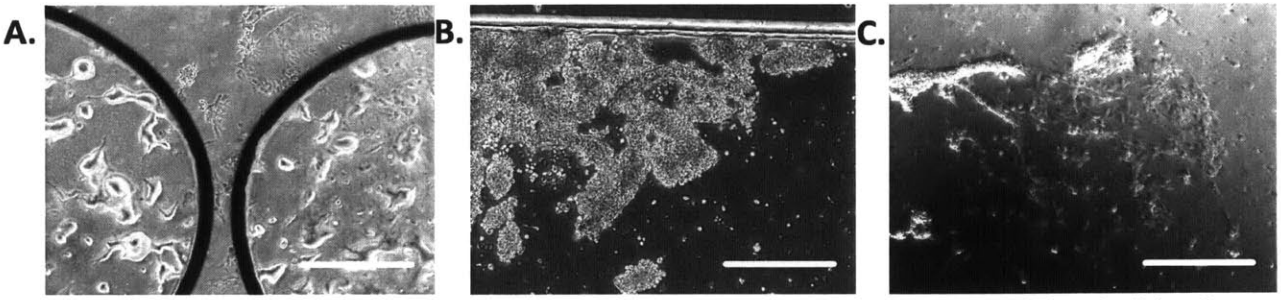

Figure 2-10 Operational challenges with the designed device: chambers with bubbles (A), cell debris (B), and cell detachment issues (C). Scale bar: 300 μm.

These challenges were successfully overcome by modifications to operational procedures. Cells were seeded manually by pipetting into the channel inlets, instead of using a fluidic network. This drastically minimized the dead volume containing cell debris and therefore the chances of that entering device chambers. Furthermore, the device was incubated for overnight cell seeding, without any fluidic connectivity. This helped the device environment directly equilibrate with incubator environment and therefore prevented any change in pressures inside the device chambers that would have resulted in bubble formation. Lastly, in order to assist in better cell adhesion, the chambers were incubated with 0.1 % gelatin solution. This approach marginally improved cell adhesion during high shear. However, despite any loss, there were adequate cells in the chambers useful for subsequent recovery and analysis. In the future, more rigorous surface treatment with adhesion promoting molecules could be investigated. Regardless, these improvements made it possible to proceed with this device more effectively.

In this device, cell seeding was compared to that from cells in seeded in a dish (**Figure 2-11**A, B). Cell morphology and confluence was indeed comparable between the two conditions.

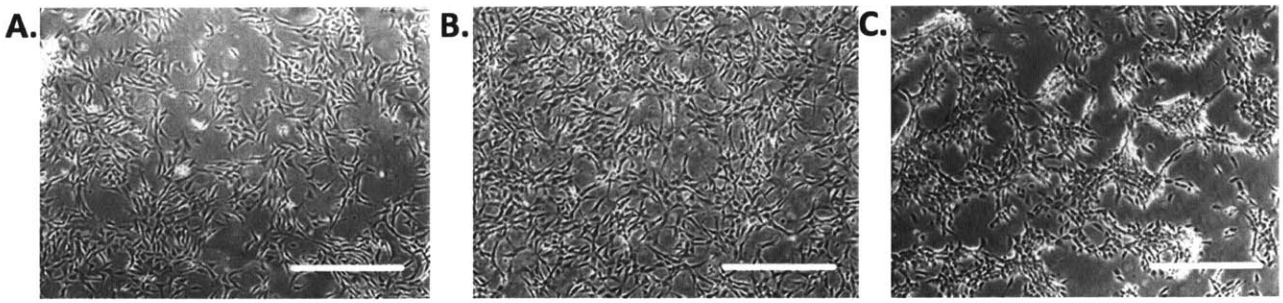

Figure 2-11 Comparison of cell morphology after 24h of seeding in a culture dish (A) and in a chamber device before perfusion (B). Cell morphology and adhesion in a typical chamber following high shear perfusion (C). Scale bar: 300 μm.

Cells were also imaged before and after perfusion (**Figure 2-11**B, C). Despite some cell loss due to detachment, there were adequate cells recoverable for subsequent genetic analysis.

Shear induced gene expression from 1 and 2 hour perfusions, with the use of this device, are shown in **Figure 2-12**A and **Figure 2-12**B respectively.

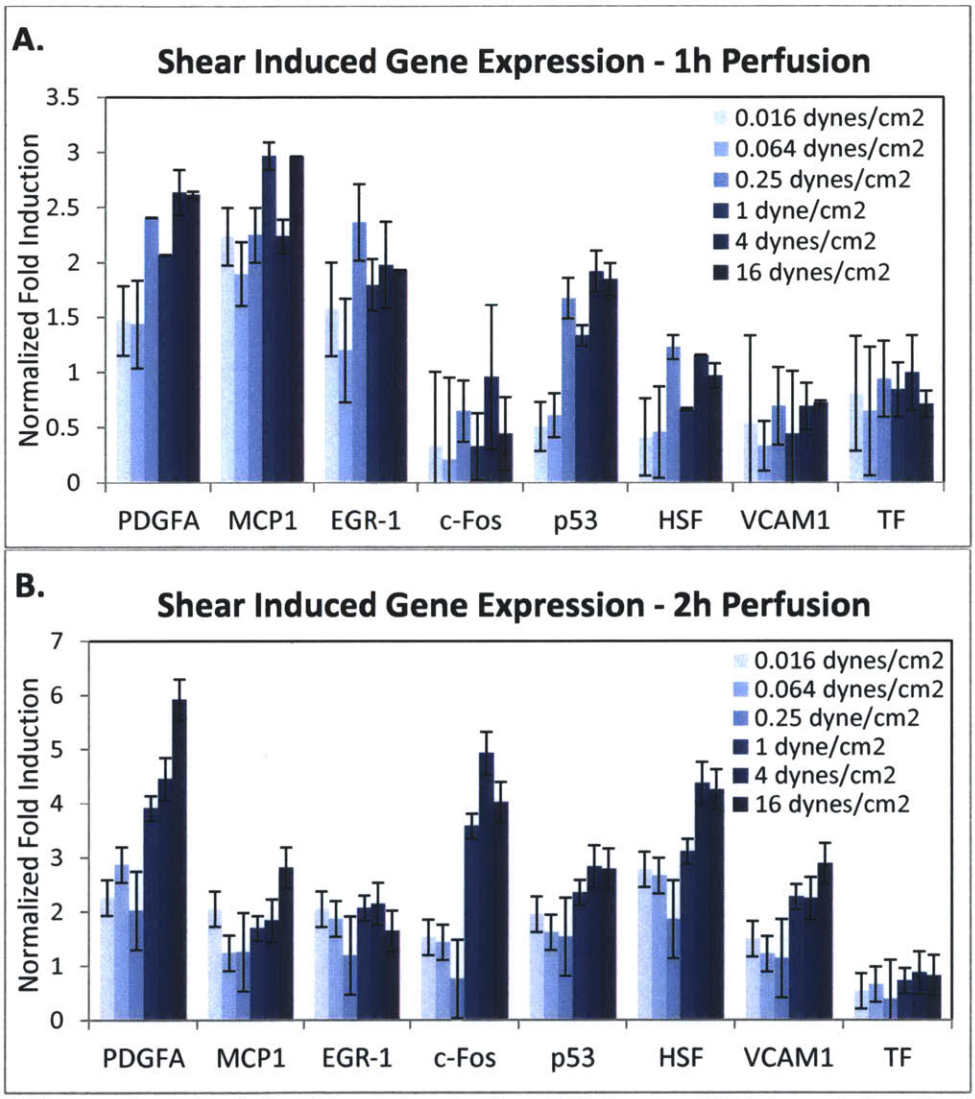

Figure 2-12 GAPDH normalized shear induced gene expression from (A) 1 hour and (B) 2 hour perfusions. N = 2 experiments, error bar: standard error of mean.

Shear sensitive gene TF remained within basal levels for both 1 and 2 hour durations. The shear induction of this gene has been correlated to phosphorylation of SP1 transcription factor, which upregulates its expression [46]. Interestingly, c-Fos demonstrated lower-than-basal levels of expression with respect to static controls for the one hour perfusion, but with increased expression for 2 hour perfusion. Additionally, VCAM1, which is reported to be downregulated

upon shear stress remained at basal levels for 2 hour perfusion but showed some increased expression at 1 hour perfusion. It is not clear from these experiments if this unexpected expression behavior is truly reproducible and representative of shear induction in NIH3T3 cells.

P53 was upregulated at higher shear rates for both 1 hour and 2 hour perfusions, implying possible cross talk between shear pathway and DNA damage pathways. Similarly, while HSF was below basal levels for 1 hour perfusions, it demonstrated increased expression at 2 hours of perfusion with correlation to stress intensity. Such expression also is suggestive of possible cross-talk of shear pathway and heat shock pathway.

Of more interest were the expression profiles of EGR-1, PDGFA and MCP1, which were most significantly upregulated upon shear stress in both 1 and 2 hour perfusions. Among the conducted experiments, PDGFA demonstrated the highest range of expression level sensitivity to shear intensity. MCP1 also suggested an expression profile correlating to shear intensity, but it was not as pronounced as PDGFA. In fact, the results from the previous device (3 hour perfusion) also showed elevated levels of these genes. Interestingly, elevated levels of PDGFA were always observed next to elevated levels of EGR-1 expression in **Figure 2-9** and **Figure 2-12**. While MCP1 levels were also increased and seemingly correlated to shear intensity, c-Fos expression profiles were not always observed to have similar characteristics. As mentioned earlier, EGR-1 upregulation and activation is responsible for downstream shear induction of PDGFA, and AP-1 (c-Fos /c-Jun) transcription factor upregulation and activation is responsible for downstream shear induction of MCP1. The similar correlation observed of PDGFA and EGR-1 towards each other, as well as to applied shear, was suggestive of EGR-1 driven PDGFA to be a prominent shear induction mechanism inferred from the conducted experiments.

As mentioned earlier, one of the main motivations for the pathway elucidation studies was to gain insight about mechanotransduction in NIH3T3 cells, as well as to identify genes with shear intensity sensitivity. In this case, from the qRT-PCR studies, the out of the shear sensitive genes tested, two preferred genes were identified as PDGFA and EGR-1. This created the motivation to investigate the EGR-1 binding site in the PDGFA promoter as one of the options for designing the shear stress inducible promoter.

2.4. Conclusions

This chapter discussed initial investigation of an immediate-early pathway induction in NIH3T3s. Serum induction was used to trigger such a pathway, as it shared similarities to shear induced transcription mechanisms related to c-Fos and EGR-1 genes. The results demonstrated that such a pathway could successfully be triggered in NIH3T3 cells, which provided some confidence to use them as a sensor for fluid shear stress that relied on immediate-early transcription mechanism.

Two device platforms were used to evaluate shear induced gene expression of these cells explicitly, through qRT-PCR of a panel of shear inducible genes. The first device was used to characterize 3-hour perfusion inductions while a second device was used to characterizing 1 and 2 hour perfusions. The second device was designed to specifically overcome drawbacks of the first device and its operations, which hindered efficient genetic analysis. Although there were some challenges in operation of the second device itself, they were successfully solved in order to proceed with subsequent perfusions.

Finally, the perfusion results were useful in providing insightful information about shear induced gene expression profiles. Some unexpected expression profiles of genes such as TF, c-Fos and VCAM were observed, however not further investigated. Representative genes of DNA damage and heat shock pathways (p53 and HSF) showed increased levels at 2 hours of perfusion, possibly due to cross-talk between those pathways and the shear stress pathway. Most importantly, PDGFA, MCP-1 and EGR-1 demonstrated consistent upregulation among all experiments and shear durations. PDGFA and MCP1 expression was seemingly correlated with applied shear intensity, however further experimentation may be needed to statistically verify these claims. As EGR-1 and PDGFA expression was increased consistently upon shear stress. In particular EGR-1 was inferred to be an important node of shear-induction in NIH3T3s and therefore it was proposed to investigate its promoter for development of a shear stress sensor.

Chapter 3: Induction Promoters

3.1. Introduction

With the goal of eventually realizing a fluid shear stress inducible promoter, this chapter discusses the motivation and development of a multiple reporter cell lines based on unique inducible response elements. Each response element was chosen due to known relation to known shear stress inductions. The methods used to construct these cell lines are explained. Chemical stimulus induced pathway functionality was first confirmed in each reporter cell line using qRT-PCR. Fluorescent microscopy and flow cytometry techniques were used to characterize reporter fluorescence due to chemical treatments for inducing the relevant pathway. The inductions are evaluated in terms of the expression of RFP, as well as the fraction of the population responding to an applied stimulus. All reporter cell lines were compared with these parameters in order to gain insight about promoter design for creating a shear stress reporter cell line.

3.1.1. Shear stress response elements

Promoters of stimulus inducible genes contain binding sites (response elements) of transcription factors which regulate their expression profiles. In the case of fluid shear stress, several regulatory transcription factors have been identified to regulate shear inducible genes through their shear stress response elements. The role of transcription factors could be to either up-regulate or down-regulate the transcription of a certain shear inducible gene. A panel of fluid shear stress inducible genes is shown in **Figure 3-1**[30].

Gene	Cell Type	mRNA Response	Transcription Factor Binding Sites
Endothelin-1	HUVEC/BAEC	Decrease	AP-1
VCAM-1	HUVEC	Decrease	AP-1, NF-κB
ACE	RAEC	Decrease	SSRE, AP-1, Egr-1
Tissue factor	BAEC	Increase	Sp1
Tissue factor	HAEC/HUVEC	Increase	Egr-1
TM	HUVEC	Increase	AP-1
PDGF-α	BAEC	Increase	SSRE, Egr-1
PDGF-β	BAEC	Increase	SSRE
ICAM-1	HUVEC	Increase	SSRE, AP-1, NF-κB
TGF-β	BAEC	Increase	SSRE, AP-1, NF-κB
Egr-1	HeLa/BAEC	Increase	SREs
c-*fos*	HUVEC	Increase	SSRE
c-*jun*	HUVEC	Increase	SSRE, AP-1
e-NOS	HUVEC	Increase	SSRE, AP-1, NF-κB
MCP-1	HUVEC	Increase	SSRE, AP-1, NF-κB

Figure 3-1 Panel of shear sensitive genes in different endothelial cells with their regulatory transcription factor. Obtained with permission from [30].

Based on a subset of these genes, certain shear sensitive response element (RE) sequences have been identified within their promoters and are listed in **Figure 3-2**.

Element	*Defined in*	*Sequence*	*Protein(s)*
PDGF-B/SSRE (positive)	PDGF-B chain	-GAGACC-	NFκB, NFAT
PDGF-A/SSRE (positive)	PDGF-A chain	-GGGGGCGGGG GCGGGGGCGGG GG-	Sp1/Egr1
TRE (positive)	MCP-1	-TGACTCC-	c-fos/c-jun
SP1 (positive)	Tissue Factor	-GGGGCGGGGC GG-	Phosphorylated Sp1
AP-1 (negative)	VCAM-1	-TGACTCA-	c-Jun dimers (?)

Figure 3-2 Positive and negative shear stress response elements within the promoters of shear inducible genes, and their regulatory transcription factors. Obtained with permission from [28].

In order to proceed towards creating a shear stress reporter, it was important to identify an ideal promoter that drives shear induced fluorescence expression. In the previous chapter, PDGFA was identified to be upregulated most prominently due to shear stress. This gene expression implied the activation of upstream transcription factor EGR-1 [28, 30, 50-53]. Both human and murine PDGFA genes have multiple response elements from different regulatory transcription factors which mediate transcription through positive and negative regulatory regions [54-57]. While SP1/EGR-1 RE has been associated with PDGFA upregulation in some cell phenotypes, it has not been directly correlated for shear induced PDGFA in NIH3T3s cells. Consequently, the overlapping response elements of SP1/EGR-1 and EGR-1 RE itself were chosen to be investigated within promoters of reporter cell lines. SP1 RE cell line was also created as SP1 was described as a shear stress response element in the Tissue Factor gene [46].

Additionally, due to shear sensitivity of MCP-1 seen in the previous chapter, it was decided to investigate the role of its AP-1 driven expression [32]. AP-1 is a transcription factor consisting of c-Fos and c-Jun protein complex that binds to a TRE RE sequence [58]. Within this transcription factor, c-Fos has been reported to demonstrate relatively higher shear sensitivity than c-Jun [59]. To investigate c-Fos meditated AP-1 regulation of TRE sequence upon shear [32], a cell line with TRE RE driven expression was constructed as well. Finally a cell line containing a shear sensitive response element identified in PDGFB, termed SSRE, was also used to construct a reporter cell line for comparison [60].

3.1.2. Promoter constructs

One of the main considerations in creating a fluorescence reporter cell line is the choice of the fluorescence protein (RFP). In this case, red fluorescence protein was chosen as the protein of interest. There are several known and commercially available versions of RFP. These have been compared in terms of fluorescence properties in literature [61-64] and are summarized in **Table 3-1** Table 3-1. It was important to choose a variant of RFP which was the brightest and had the quickest maturation time in cells, such that the reporter cells could express a bright fluorescent signal quickly. Being a monomer, mCherry had the quickest maturation time but was not as bright as other proteins. Among the two brightest RFP proteins compared, DsRed and TurboRFP, TurboRFP had a much quicker maturation time, possibly because of its dimer structure. With this motivation, TurboRFP was chosen as the inducible red fluorescent protein.

All promoters were cloned within the multiple cloning sites (MCS) of pTurboPRL-RFP backbone vector, shown in **Figure 3-3** (Evrogen catalog #: FP715). Three tandem repeats of response elements corresponding to its correlated gene were placed between the XhoI and BamHI restriction enzyme cutting sites in the MCS, as illustrated in **Figure 3-4**. A minimal promoter sequence (minP) containing a TATA box was taken from a commercially available minimal promoter plasmid (Promega catalog #: pGL4.23). As this promoter lacked any inducible response element, it was constructed to act as a negative control reference. A plasmid containing CMV promoter was used as a positive control, and was purchased from Evrogen (catalog #: FP231).

Table 3-1: Comparison of Red Fluorescent Proteins

Red Fluorescent protein	Structure	Excitation/ Emmision Maximum (nm)	Molar Extinction Coefficient: E (M^{-1} cm^{-1})	Fluorescence Quantum Yield: Q	Brightness (E*Q/1000)	Maturation time at 37°C
mCherry	Monomer	587/610	72000	0.22	16	15 min
Tag-RFP	Monomer	555/584	98000	0.41	40	100 min
Tag-RFP-T	Monomer	555/584	81000	0.41	33	100 min
TurboRFP	Dimer	553/574	92000	0.67	62	1.5 h
DsRed	Tetramer	558/583	75000	0.79	59	10 h
DsRed2	Tetramer	563/582	65000	0.55	36	100 min
DsRed-Express	Tetramer	557/579	30000	0.4	12	36 min
DsRed-Express2	Tetramer	554/591	35600	0.42	15	42 min
DsRed-Max	Tetramer	560/589	48000	0.41	20	1.2 h

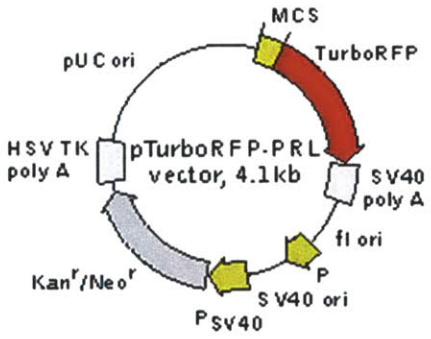

Figure 3-3 Plasmid map of pTurboPRL-RFP (Evrogen catalog #FP715). All inducible promoters were placed within its MCS.

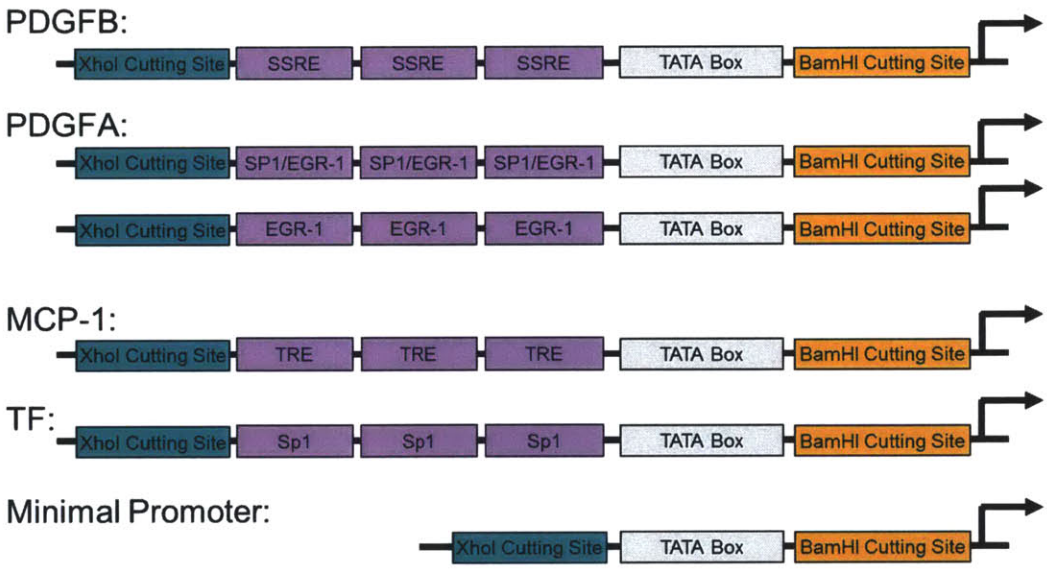

Figure 3-4 Promoter design containing tandem shear stress response elements, along with a minimal promoter as a reference

The sequences of each of the RE constructs is given below:

SP1 [65]:

CTCGAGATTCGATCGGGGCGGGGCGAGATTCGATCGGGGCGGGGCGAGATTCGATCGGGGCGGGGCG
AGTAGAGGG**TATATAA**TGGAAGCTCGACTTCCAGGGATCC

EGR-1 [65]:

CTCGAGGGGGCGGGGGCGCTACCTCTTCTTGGGGCGGGGGCGCTACCTCTTCTTGGGGCGGGGGCGCT
ACCTCTTCTTTAGAGGG**TATATAA**TGGAAGCTCGACTTCCAGGGATCC

SP1/EGR-1 [45, 65, 66]:

CTCGAGGGGGGGGCGGGGGCGGGGGCGGGGGAGGGGGGGGGGCGGGGGCGGGGGCGGGGGA
GGGGGGGGGGCGGGGGCGGGGGCGGGGGAGGGTAGAGGG**TATATAA**TGGAAGCTCGACTTCCAG
GATCC

TRE [32, 67-72]:

CTCGAGCGCTTGATGACTCCGCTTGAACGCTTGATGACTCCGCTTGAACGCTTGATGACTCCGCTTGAAT
AGAGGG**TATATAA**TGGAAGCTCGACTTCCAGGGATCC

SSRE [73-75]:

CTCGAGTCGGCTCTCAGAGACCCCCTTCGGCTCTCAGAGACCCCCTTCGGCTCTCAGAGACCCCCTTAGA
GGG**TATATAA**TGGAAGCTCGACTTCCAGGGATCC

Minimal Promoter:

CTCGAGATACTGTCAGTGCTACATAGAGGG**TATATAA**TGGAAGCTCGACTTCCAGCTGCAATGGATCC

Here, XhoI cutting site is depicted in green, BamHI cutting site is in yellow and the tandem response element sites are highlighted in blue. The TATA box in all sequences is highlighted in bold. All sequences are listed in 5-3' direction and do not contain any other transcription factor binding sites based on BLAST results from TransFac and NCBI databases.

3.2. Methods

3.2.1. Cell line construction: materials and methods

Each synthesized plasmid from Genewiz was created an endotoxin-free process and hence was safe to use for direct transfection in NIH3T3 cells. The lyophilized DNA was suspended in TE buffer to a concentration of 500 ng/µL, and then stored in an aliquot at -20 degrees Celsius. In this case all plasmids were transfected in to NIH3T3 cells with stable constitutive expression of Ypet protein under a CMV promoter, and hygromycin selection marker based on a plasmid obtained from Addgene (pCEP4Ypet-mamm). Prior to transfection, these cells (approximately 2 x 10^6 in number) were seeded in regular culture media in a 10 cm diameter Nunc cell culture petri dish and were grown for 1-2 days until the confluence was around 80%. In this manner, triplicate dishes were prepared for each plasmid transfection.

Each set of the triplicate dishes were transfected with the each plasmid. One dish was used for transfection with a constitutively expressing RFP plasmid (Evrogen, catalog #: FP231) as a positive control, while another was not transfected at all and saved for a selection control dish. On the day of transfection, the DNA solution was thawed to 4 degrees Celsius on ice. Superfect transfection reagent from Qiagen (catalog #: 301305) was used for the transfections. This solution was also brought to room temperature prior to transfection. In a DNAse and RNAse free eppendorf tube, a pre-mixed transfection was prepared using 10 µg of plasmid DNA with 60 µL of Superfect reagent and diluting the solution with cell growth medium – DMEM without L-glutamine, serum or any antibiotics (Gibco catalog#: 11960-044) to a volume of 300 µL. The solution was mixed by pipetting and incubated at room temperature for ten minutes for the transfection-complex to form. In the same manner, the control transfection solution was prepared by omitting the plasmid DNA and replacing its volume by that of cell media mentioned above. In the meanwhile, the cell dishes were removed from the incubator, and the media was aspirated and replaced with PBS buffer solution. After the transfection-complex incubation was completed, each 300 µL solution was added 3 mL of cell culture media with serum and antibiotics and mixed by pipetting twice. PBS buffer solution was aspirated from all dishes and the new DNA solution was added to all dishes immediately.

All the dishes were stored in the incubator for 3 hours and then the DNA solutions were replaced with 10 mL of regular cell culture media. All dishes were incubated overnight for transient transfection prior to introduction of G-418 selection antibiotic at 1 µg/mL concentration for a week. This chemical selection provided cells with stable transfection and integration of the plasmid. The end time of selection was decided when there were no remaining live cells in the negative control (non-transfected) dish.

3.2.2. Chemical inductions

All stable transfected cells with an inducible plasmid were divided into two categories based on the culture media conditions used prior to induction. In all cases, cells were serum starved prior to chemical induction, as mentioned earlier. Specifically, one set of cells was exposed to media containing serum at 0.15%, used as serum free media (SFM) for 48 hours [76-78]. The second set was exposed to SFM for 24 hours and then SFM + PMA, or SFM + Serum, or SFM + TNFα (various doses). In some cases increased serum media (20% v/v) was used for PMA inductions to investigate induction enhancement. The last set was kept as a reference with the regular cell culture media (10% serum, 1% penicyllin/streptomycin, 2% L-glutamine). For the second set, PMA exposure doses were 10 ng/ml and 100 ng/ml, or the same with media containing 20% serum. TNFα was used for certain inductions at 10 ng/ml in regular media or with media containing 20% serum. All inductions were kept at 2 hour exposure, after which the cell solutions were replaced with regular culture media. For qRT-PCR, the cells were lysed immediately for studying gene expression changes. In the case of quantitative fluorescence analysis, the induced cells were incubated for 24 post exposure. Subsequently, these cells as well as the reference control cells were imaged using fluorescence microscopy for relative qualitative comparision, prior to flow cytometry analysis.

3.2.3. Quantitative RT-PCR

Cellular mRNA was collected using Qiagen RNeasy Micro kit (catalog #:74004) using its reccomended protocol. The collected mRNA quality and concentration was evaluated using NanoDrop 1000 Spectrophotomete. The amount of mRNA used for reversre transcription was taken as 1 μg from all sample conditions and convered to cDNA using random hexamer primers. Specifically, the PCR mixture composition and thermocycling protocol was taken from DyNAmo cDNA synthesis kit (Thermo Scientific, catalog # F-470L). The qPCR reaction setup utilized the Bio-Rad iQ SYBR Green Supermix (Bio Rad, catalog # 170-8882) and primer sets mentioned in the previous chapter. The PCR reaction was conducted and analyzed with Bio Rad CFX96 Touch™ Real-Time PCR Detection System, according to its recommended protocol. Gene expression profiles were quanitified and normalized as relative expression to GAPDH, using its standard curve.

3.2.4. Flow cytometry setup

All cells were analyzed using BD LSR II HTS flow cyometer. For the detection channels, PE-TexasRed-YG-A (Red channel) filter was used with an excitation wavelength of 561 nm and emission detector centered at 610 nm with a 20 nm bandwidth. The reference channel was chosen to be FITC with an excitation wavelength of 488 nm and its emission detector centered at 530 nm with a 30 nm bandwidth. The flow cytometry experimental template was setup using untransfected cells, stable RFP expressing cells (positive control) and stable YPet expressing cells (secondary reference positive control).

Flow cytometry instrument gains and settings were set in order to capture the dynamic range of expression based on these controls and were used consistently among all flow cytometry experiments. The primary gates first were set to select the majority of cell populations from the forward and side scatter information. The subset of all the events analyzed that qualified as cells were set by the intersection gates named P1, P2, and P3 within the forward and side scatter channels as as shown in

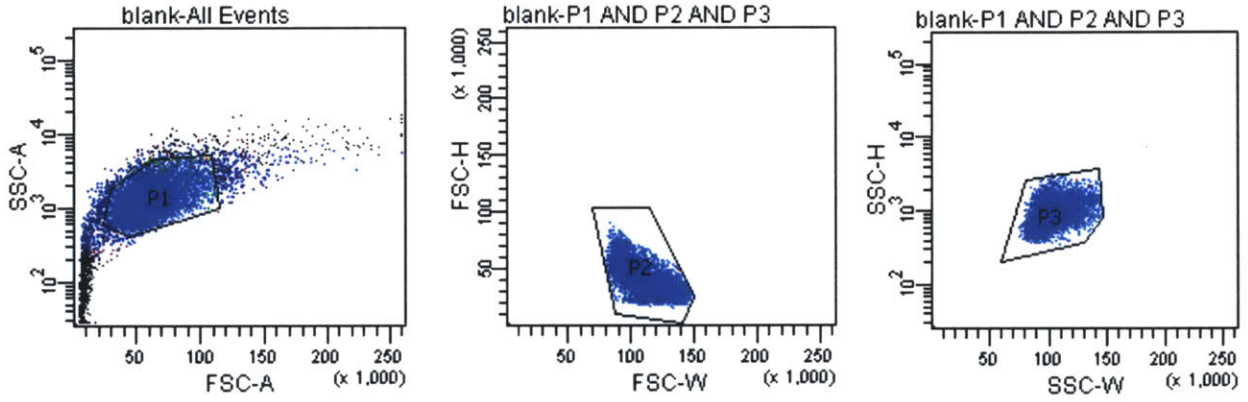

Figure 3-5 . The combined population from the intersection of P1, P2 and P3 gates was analyzed for expression of red fluorescence against FITC reference channel.

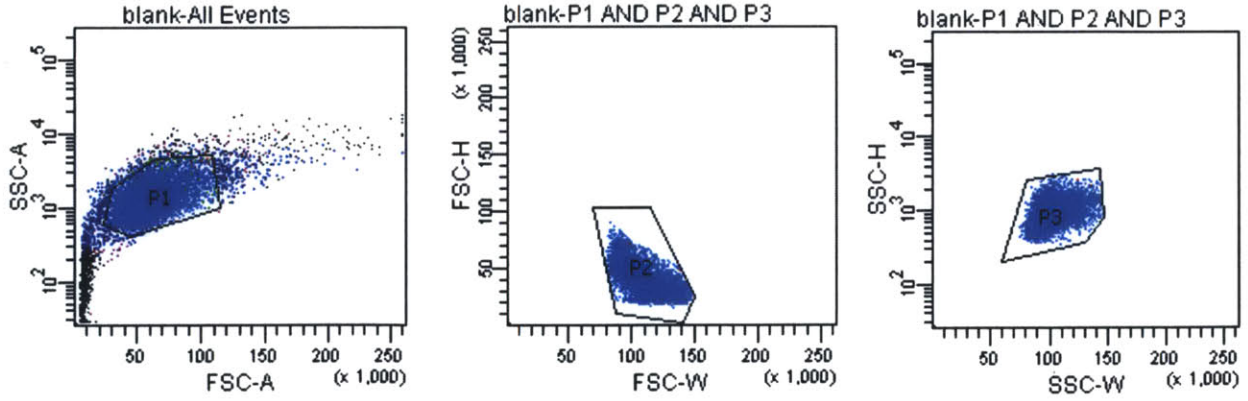

Figure 3-5 Forward and side scatter gates chosen in flow cytometry to highlight regions of live cells.

The fluorescence cluster of the untransfected (blank) cell population was centered with an approximate zero mean fluorescence in all channels. A horizontal gate was set above to threshold the maximum background fluorescence from the control population to create a sub-population called P5. The distribution fluoresecence intensity was analyzed by a histogram of the red channel. An example of P5 within P1, P2 and P3 gates, as well as the RFP intensity distribution histrogram for a non-fluorescent cell population is shown in **Figure 3-6**.

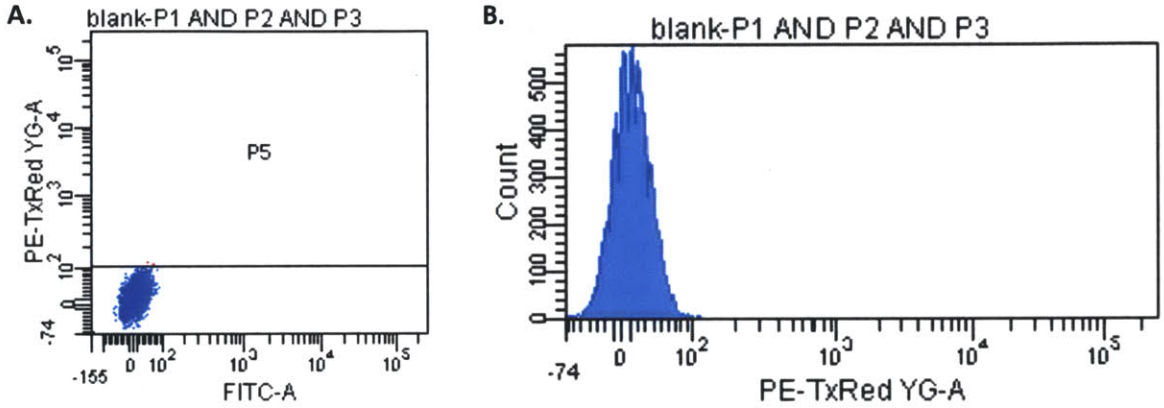

Figure 3-6 A Gating the auto-fluorescence of blank cells to create P5 region. B. RFP intensity distribution plotted for the entire cell population within the side and forward gates (P1, P2, and P3) in the PE-TexasRed (RFP) channel.

The percentage of cells in the P5 gate was termed '% activated cells' for all the experimental conditions. When comparing the fold induction of percent activated population, or in other words, the shift in the flourescence distribution histogram, the % activated cells in P5 of the induced population was normalized by that in non-induced population. To analyze the change in the fluorescence upon induction, the mean red intensity of the combined P1, P2 and P3 population was compared from before and after induction. The mean RFP fluorescence of this poulation after induction was divided by that of the uninduced population and was termed as the normalized fold RFP induction.

3.3. Results and Discussion

In order to obtain a facile handle on shear stress driven transcription, it is important to investigate chemical stimuli that could mimic the shear driven pathway of a particular inducible gene. This would provide a simplistic method to screen through a variety of pathway induction conditions in order to characterize and evaluate reporter response.

Small molecule PMA is known to trigger EGR-1 replacement of SP1 from its binding site in the PDGFA promoter, in a manner similar to the mechanism proposed for shear-dependent up-regulation for that gene [45]. Additionally, PMA can trigger upregulation of both c-Fos and EGR-1 genes through their common upstream PKC-ERK pathway [38, 41]. Interestingly, the cytokine TNFα has also been reported to phosphorylate and activate ERK 1/2 pathway which leads to EGR-1 and c-Fos upregulation in vascular smooth muscle cell lesions [79]. Furthermore, serum treatments can upregulate c-Fos and EGR-1 levels and activity, by virtue of similar of serum response elements in their promoters. [36]. Due to multiple chemical agonists possibly able to mimic injury or shear stress driven transcription pathways, PMA, TNFα and serum were all used to investigate RE reporter cell line inductions. Specifically, chemical inductions of cell lines containing REs of SP1, SP1/EGR-1, EGR-1 and TRE were performed with PMA treatment. In the case of PDGFB, NF-κB has been associated with its shear induced gene expression in the sense that it was found to bind to its promoter through the SSRE even though it was not the consensus NF-κB binding site. The exact mechanism or underlying pathway has not been identified [73]. As SSRE is proposed to be a putative binding site for this transcription factor, it was decided to induce this cell line expression primarily with TNFα, a known inducer of NF-κB [73, 80].

3.3.1. Fluorescence microscopy

PMA inductions of SP1/EGR-1, EGR-1 and TRE cell lines, and TNFα inductions of SSRE cell lines were observed with qualitative fluorescent microscopy (**Figure 3-7**). For cell lines of EGR-1, TRE and SSRE REs, there was no fluorescence observed for either the control or induced conditions. Further visual inspection of these cell lines across many regions in the culture dishes, as well as over many passages revealed minimal cell fluorescence. As these cell lines survived through the antibiotic selection process, the low fluorescence before and after induction suggested possible poor binding of regulatory transcription factors on those REs. SP1/EGR1 cell line demonstrated fluorescence before and after induction which was later quantified by flow cytometry. Additionally, the cell line created with the minimal promoter sequence, also shown in **Figure 3-7**, had no observable fluorescence. This cell line was also induced and no fluorescence was observed as well (data not shown). This behavior was expected as there is no regulatory

transcription factor binding site in the minimal promoter and therefore there was no non-specific upregulation of fluorescence.

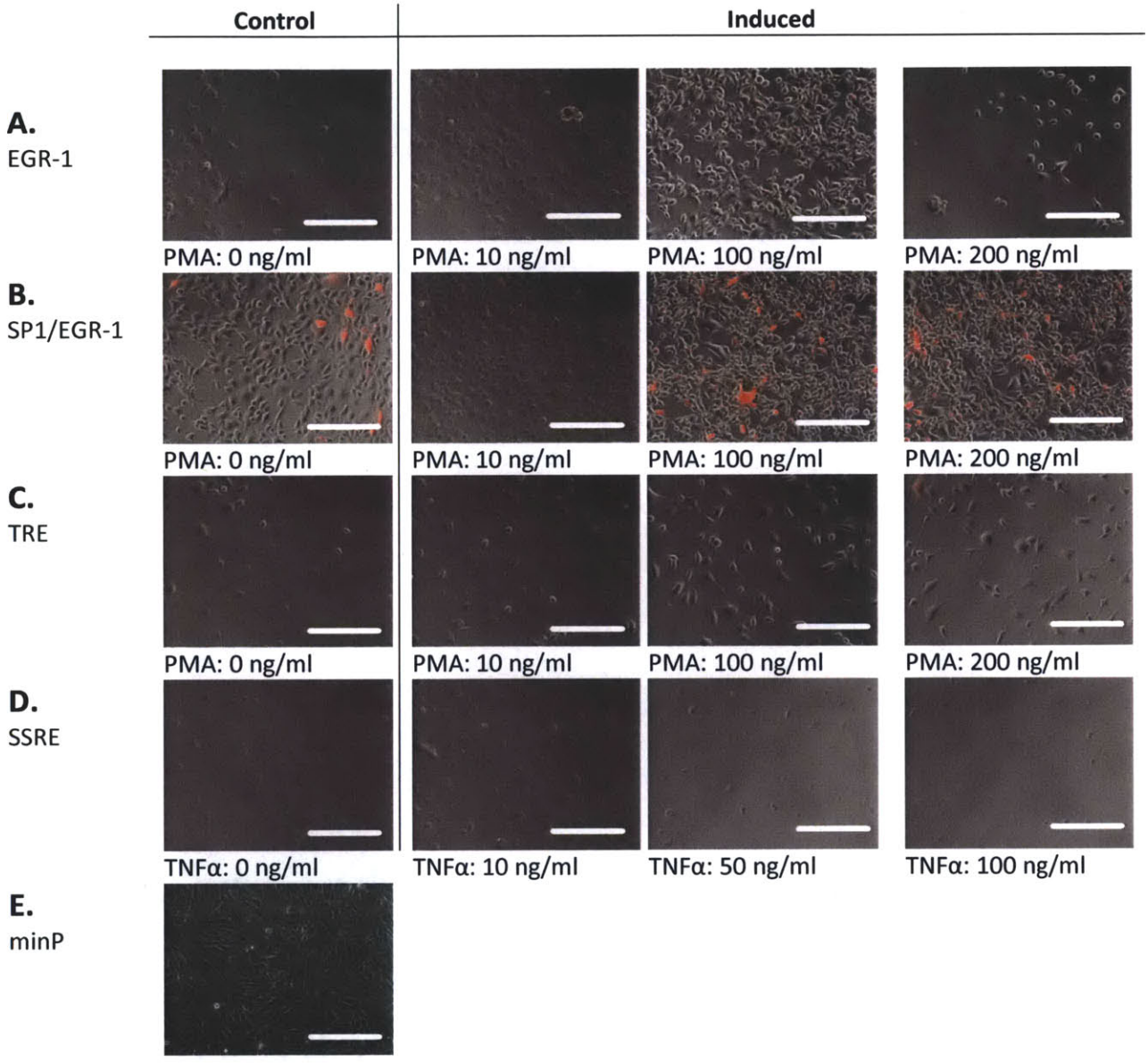

Figure 3-7 Merged phase and fluorescence images (2 sec exposure) of reference control cells and 2-hour induced cells after 24 hours of post-treatment incubation. Cells with response elements of A. EGR-1 B. SP1/EGR-1 C. TRE and D. SSRE. E. Reference negative control from the minimal promoter. Scale bar: 150 μm.

3.3.2. Induced gene expression – qRT-PCR analysis

Figure 3-8 shows the inductions of the SSRE RE cell line. TNFα induced gene expression profile showed the most prominent upregulation of MCP-1, with elevated levels of c-Fos and EGR-1. It is possible that these two transcription factors may have been upregulated due to the stimulus, to then induce unintentional MCP-1 inductions. Nevertheless, the main gene targeted through this stimulus was PDGFB through NF-κB activation of SSRE within its promoter. PDGFB was indeed at elevated expression with comparison to other genes in the panel and in fact, was at the most pronounced induction when compared to all other reporter RE cell lines by their respective chemical inductions (**Figure 3-8, Figure 3-9, Figure 3-10, Figure 3-11**).

Figure 3-9, Figure 3-10 and **Figure 3-11** illustrate PMA induced gene expression profiles of EGR-1, SP1/EGR-1 and TRE RE cell lines respectively. As both EGR-1 and c-Fos are PMA inducible genes, it was not surprising to see that these genes were most prominently expressed by a 2-hour exposure to PMA in all three RE cell lines. EGR-1 expression (normalized fold induction) are typically much higher than that of c-Fos levels [35], which was seen to be the case for SP1/EGR-1 and TRE cell lines. Due to reasons unknown, this was however the case for the EGR-1 RE cell line gene induction as c-Fos expression was slightly higher than EGR-1. Regardless, from all these three cell lines, it was seen that PMA could indeed induce high expression levels of EGR-1 and c-Fos. Within these three cell lines, the downstream targets of EGR-1 (PDGFA) and c-Fos (MCP-1) were not found to be upregulated significantly. It is possible that such downstream regulation may have different transcription sensitivity towards the chosen dosage and duration of PMA exposure.

Interestingly, there was no significant induction of RFP at the transcription level for any of the RE cell lines upon this stimulus. This suggests that either the upregulation of RFP expression was not correlated to the stimulus at the transcriptional level, or that the dynamics of RFP gene induction were different than that of the target genes, and was not captured in the 2-hour window. This uncertainty was further explored by evaluating florescence expression of RFP by flow cytometry, the translation of which would have resulted from any induced RFP mRNA.

3.3.3. Induced RFP expression – flow cytometry analysis

Many combinations of chemical inductions using PMA, serum and TNFα were analyzed by flow cytometry. For SSRE induction shown in **Figure 3-8**, PMA had no effect on changes in population mean RFP intensity. Serum with PMA demonstrated minor elevated expression, with most prominent expression by TNFα. If NF-κB was indeed induced by TNFα as postulated by PCR results, it is possible that it could have regulated RFP expression changes through the SSRE response element driving RFP expression. However, when observing the changes in the percentage of cells expressing RFP, the induction seemed to be ineffective. The entire

population mean fluorescence was similar to the mean auto-fluorescence of non-fluorescent cells used as a negative control. Only a few percent of cells were induced by the stimulus, suggesting ineffective induction of the entire population. A similar case was observed for EGR-1 RE and TRE RE cell lines **(Figure 3-9** and **Figure 3-11** respectively). One possible explanation could be an ineffective binding at the RE promoter or because of a plasmid integration issue that prevents functional regulation.

Furthermore, PMA induced RFP levels were not significantly upregulated for TRE and EGR-1 RE cell lines, even though these contained known RE of transcription factors AP-1 (consisting of c-Fos and c-Jun) and EGR-1. SP-1 transcript and protein levels have been reported to be insensitive to PMA exposure, as it regulates basal levels of PDGFA and PDGFB genes [45, 81, 82], however in one case its phosphorylation has been linked to upregulate Tissue factor gene upon shear through its RE [46]. As seen from **Figure 3-12**, RFP levels and cell activation levels of the SP1 RE are unchanged by PMA exposure. A relatively high fraction of cells with activation (RFP expression) even prior to induction suggests that SP1 may have indeed been regulating basal transcription of RFP which was not inducible by PMA. The correlation of serum induction, or TNFα induction towards SP1 transcription regulation was not explored. Additionally, SP1/EGR-1 RE cell line showed similar characteristics in cell activation levels and PMA induction profile (**Figure 3-10**). While not entirely conclusive, it is possible that SP1 may be regulating the basal transcriptional activity of this RE reporter cell line as well. If EGR-1 elevated mRNA transcripts are assumed to be correlated to increased EGR-1 translation and transcriptional activation, then it may be possible that the EGR-1-SP1 displacement model may not be applicable for upregualtion of SP1/EGR-1. Similarly, if elevated expression c-Fos transcripts correlated to increased AP-1 formation and activation, then it is possible that regulation of RFP through the TRE RE may be non-functional.

RFP is a protein not naturally occurring in NIH3T3 cells and therefore it is improbable that there was a post-transcriptional regulation of RFP mRNA. It is true however, that these populations could potentially be sorted (via FACS) to create a population of responding cells based on the fraction of induced cells. This would reveal if the population heterogeneity was masking a small subset of properly inducible cells.

Taken together, the lack of correlation of gene upregulation of c-Fos and EGR-1 transcripts to their transcriptional regulation of RFP hinted towards sub-optimal promoter design. Previous work on generating synthetic hybrid promoters containing a combination of shear stress response elements was also not entirely successful in demonstrating shear induced upregulation [83]. Silberman and others explained that the organization of shear stress response elements within the promoter, (relative location of the response element to the

transcription start site) as well as the promoter sequence itself may play a critical role in determining shear dependent induction [83].

The results from **Section 2.3** indicated EGR-1 and PDGFA to be to two possible options for the shear stress inducible promoter. There, the results of perfusion induced gene inductions indicated upregulation of PDGFA gene in an intensity dependent manner because of shear stress. This implied the prior activation and upregulation of EGR-1 in NIH3T3 cells. In light of the result from this chapter, it was inferred that tandem SP1/EGR-1 binding sites found in the native PDGFA promoter, used to design the RE promoter were not effective in significantly inducing RFP by chemical induction of the shear pathway. Also, EGR-1 upregulation seen in the PCR results from this chapter showed prominent upregulation by chemical inductions, at least at the transcript levels. These facts together suggested towards picking EGR-1 promoter, as opposed to the three tandem SP1/EGR1 RE sites from PDGFA, for driving induced fluorescence expression of the shear reporter.

In fact, fluorescence expression driven by a promoter of downstream gene target of EGR-1 (such as by the PDGFA promoter) promoter might require longer pathway induction time [47]. This may not be relevant if one wants to measure the effects of acutely applied shear stress. Additionally, downstream gene products may have more specificity towards a particular phenotype and functionality and therefore those products may necessarily be representative of general shear induced physiological stresses found in most cell phenotypes. EGR-1 induction can occur within minutes [34, 35] and is reported in a variety of cell types experiencing shear stress [48, 49], thereby making its promoter a suitable candidate to sense and report shear stress.

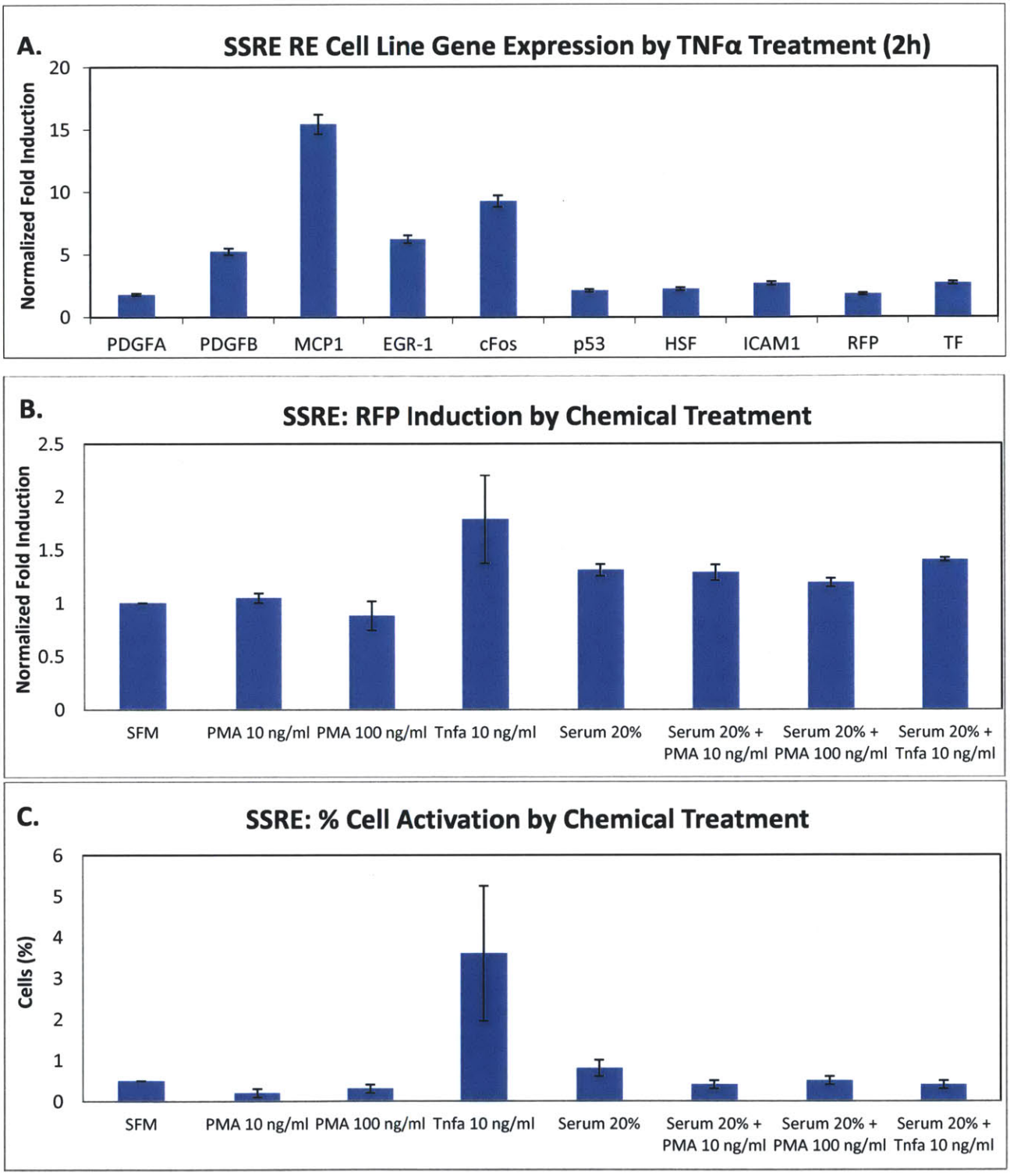

Figure 3-8 SSRE RE cell line chemical induction: Gene expression due to 2h of TNFα exposure (A) normalized induced RFP expression (B) and fractional cell activation (C), due to a variety of chemical stimuli. N = 2, error bar: standard error of mean.

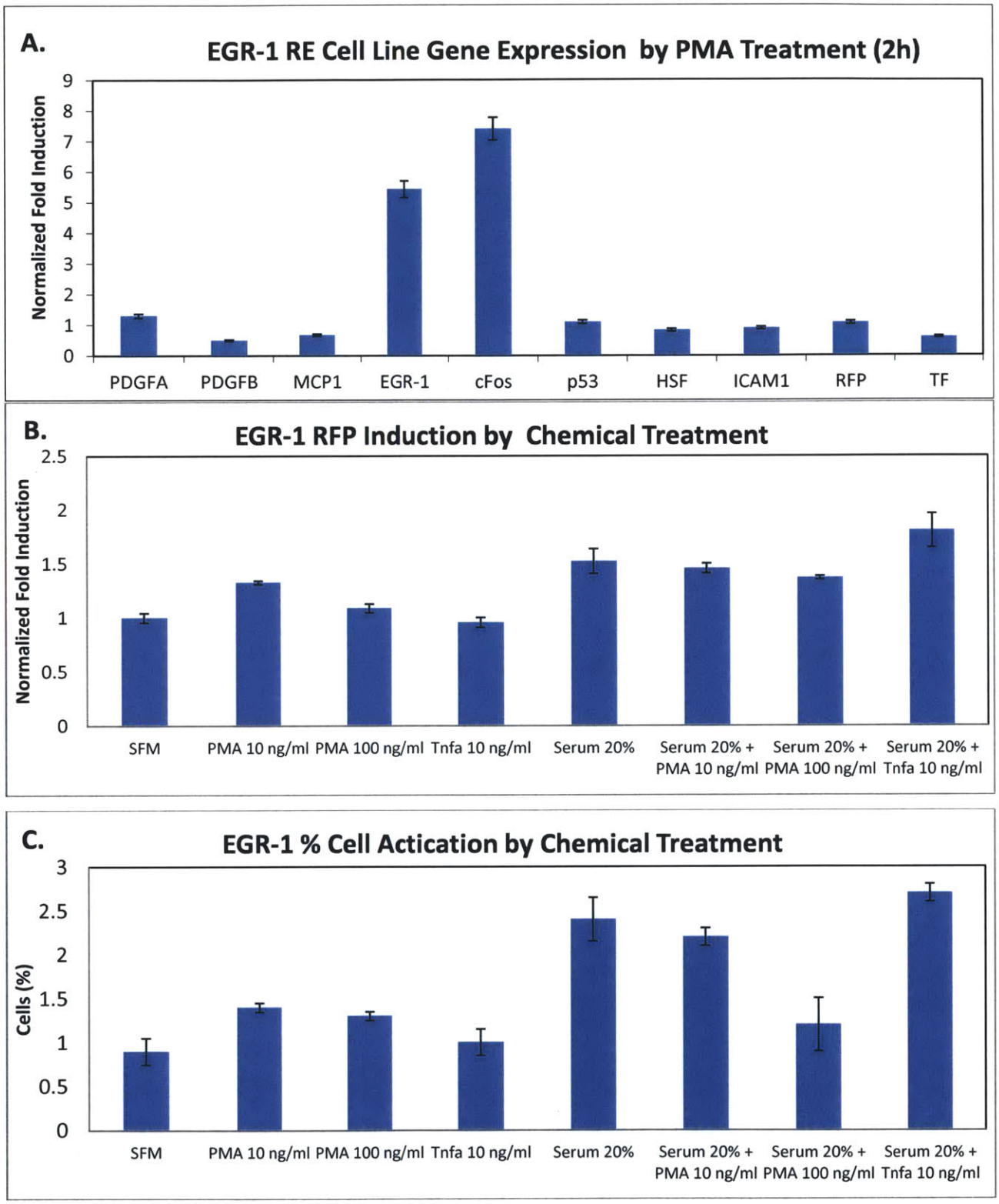

Figure 3-9 EGR-1 RE cell line chemical induction: Gene expression due to 2h of PMA exposure (A) normalized induced RFP expression (B) and fractional cell activation (C), due to a variety of chemical stimuli. N = 2, error bar: standard error of mean.

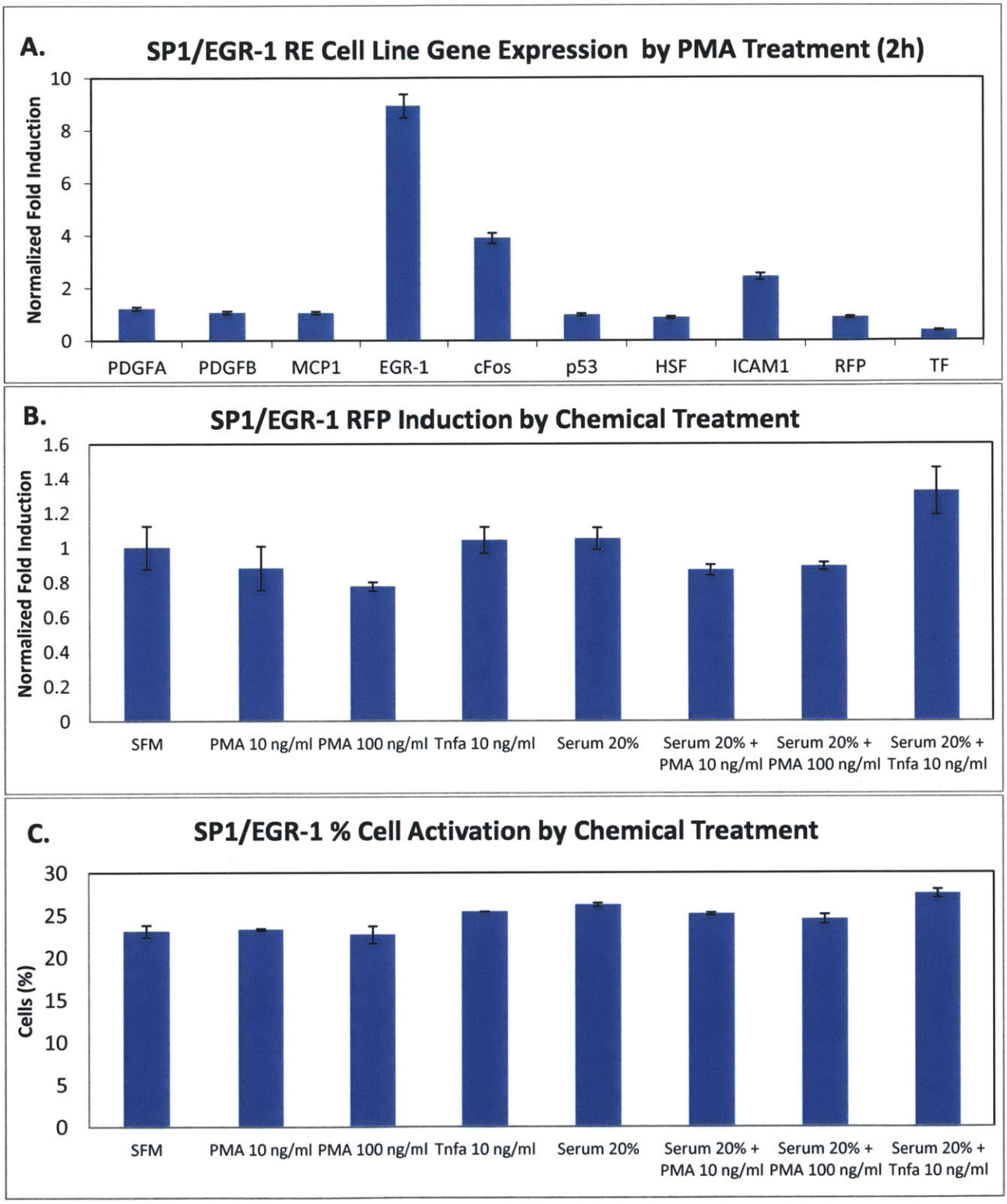

Figure 3-10 SP1/EGR-1 RE cell line chemical induction: Gene expression due to 2h of PMA exposure (A) normalized induced RFP expression (B) and fractional cell activation (C), due to a variety of chemical stimuli. N = 2, error bar: standard error of mean.

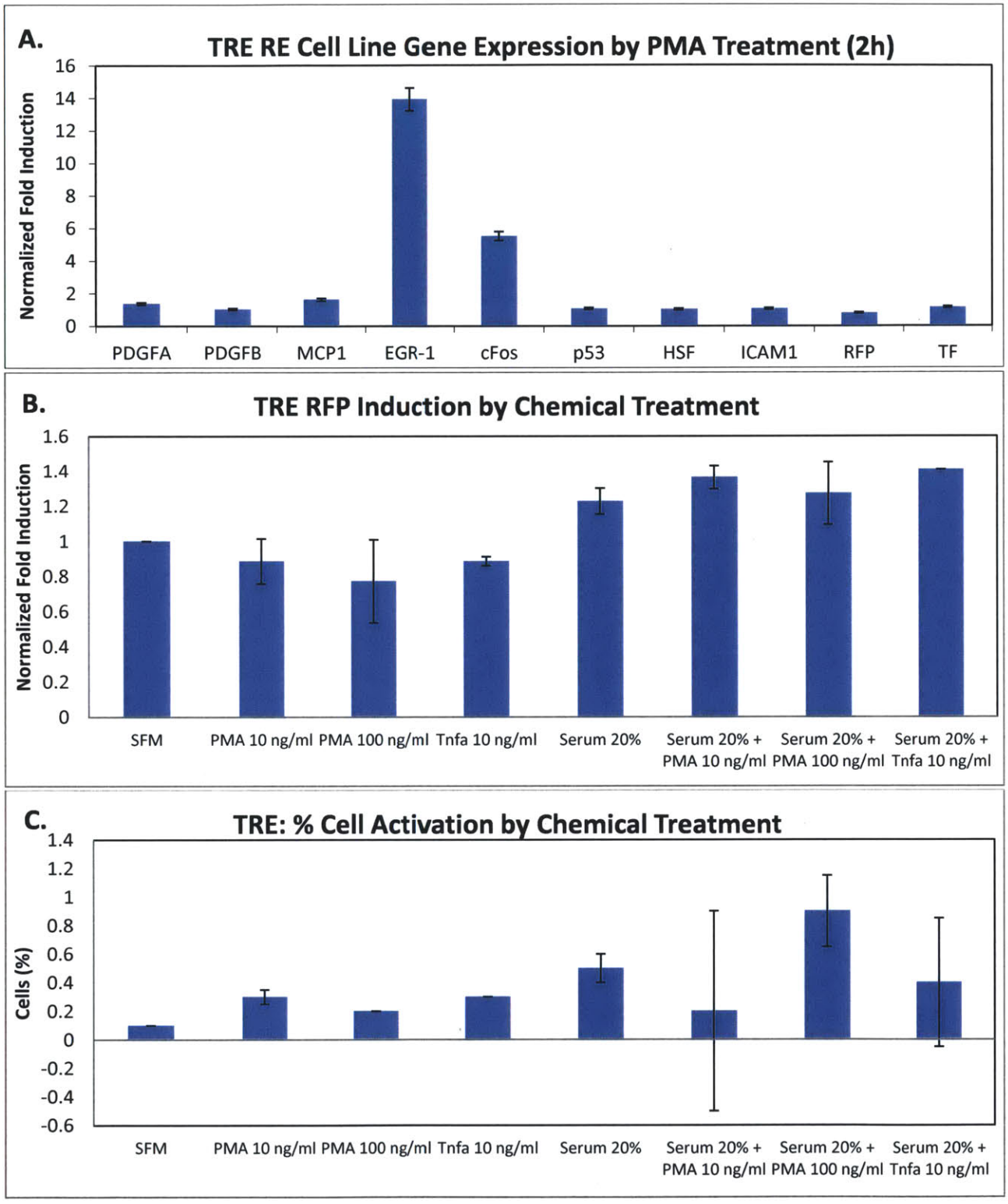

Figure 3-11 TRE RE cell line chemical induction: Gene expression due to 2h of PMA exposure (A) normalized induced RFP expression (B) and fractional cell activation (C), due to a variety of chemical stimuli. N = 2, error bar: standard error of mean.

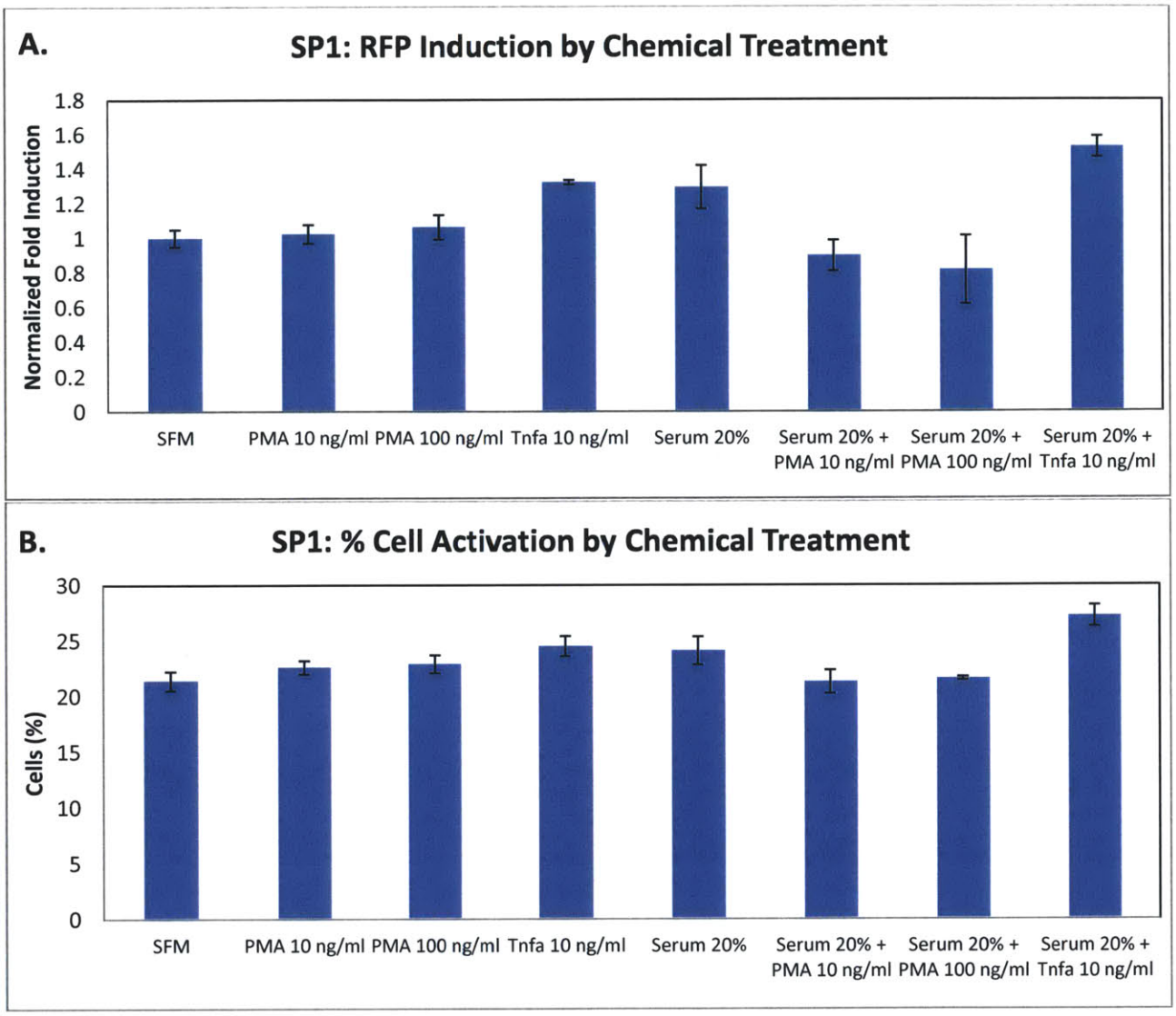

Figure 3-12 SP1 RE cell line chemical induction: normalized induced RFP expression (A) and fractional cell activation (B), due to a variety of chemical stimuli. N = 2, error bar: standard error of mean.

3.4. Conclusions

This chapter discussed the design motivation and techniques involved in constructing inducible response element reporter cell lines. Promoters containing three tandem response elements containing consensus binding sites of EGR-1, SP1, AP-1 and NF-κB transcription factors was were constructed. The reporter plasmids were transfected into NIH3T3 cells to create stable integrated reporter cell lines. Each cell line was induced with chemicals relevant to trigger the known shear pathway-transcription factor – gene mechanism. The resulting inductions were analyzed qualitatively by fluorescence microscopy, and quantitatively by RT-PCR and flow cytometry.

Cell lines carrying the TRE, EGR-1 and SSRE RE all had demonstrated expected inductions of inducible genes upon relevant chemical stimulus. However, RFP transcripts were not found to be upregulated in correlation to this stimulus for any cell line. Furthermore, these three cell lines had very few percent of cells expressing before or after induction, as seen by flow cytometry. SP1/EGR-1 and SP1 RE cell lines had significant basal fluorescence levels, as well as high number of cells expressing fluorescence without induction. It was postulated that this high basal level control may be due to constitutive binding of SP1, which was generally insensitive to applied chemical stimulus. EGR-1 and c-Fos transcripts were significantly induced due to PMA treatment; however this did not correlate to any apparent increase of transcriptional regulation through its TRE and EGR-1 RE promoters. Nevertheless, as these genes have known shear-dependent induction, it is presumable that their promoters may be shear stress sensitive as well. While promoter design optimization was beyond the scope of this chapter, it was inferred that choosing native promoters sequence to drive induced RFP expression, could have more promise than that from a synthetic promoter with tandem response elements. Finally, with comparison to results from **Section 2.3**, it was found that EGR-1 promoter would be the preferential choice to design a shear stress inducible plasmid, and therefore cell senor.

Chapter 4: EGR-1 Reporter

4.1 Introduction

This chapter discusses the motivation and development of a shear stress sensor utilizing the promoter of early growth response (EGR) transcription factor- EGR-1. The methods used to construct and select various reporter cell lines are explained. Fluorescent microscopy and flow cytometry techniques were used to characterize reporter inductions due chemical and fluid shear stress. Sensitivity and selectivity of a clonal reporter population towards shear stress are also evaluated.

4.1.1. EGR-1 Transcription and Regulation

EGR-1 is a zinc finger transcription factor known to be stimulated in many cells by extracellular signaling molecules, hormones and stress pathways [84]. It falls in the category of immediate response genes because its gene is significantly upregulated right after induction. The transcribed protein regulates many downstream signaling pathways, and therefore acts as an important signal transduction node for many aspects of cell physiology such cell growth, survival and transformation [85, 86].

EGR-1 transcription factor follows similar functionality and induction kinetics as another important early induction transcription factor c-Fos [35]. A wide range of stimuli in various physiological contexts can induce both transcription factors, however, EGR-1 mRNA is known to be induced several fold higher than c-Fos [35]. More importantly, EGR-1 is known to be stimulated with mechanical injuries and stresses in endothelial cells, as shown in **Figure 4-1**[48, 49].

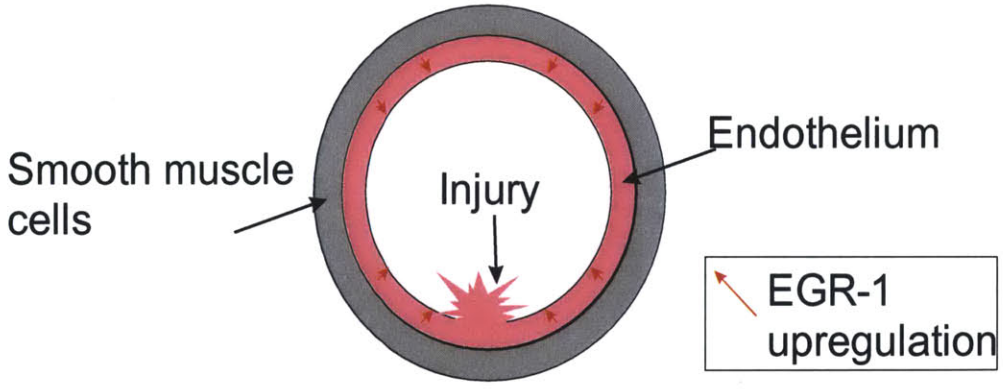

Figure 4-1 Adapted from [48, 87], illustration of EGR-1 induction upon mechanical injuries and wounds in vasculature. Mechanical streching as well as applied shear stress on the endothelium can induce such inductions in endothelial and smooth muscle cells [48, 87].

This transcription factor was found to be induced transiently due to shear stress in endothelial cells with levels proportional to the applied shear intensity [78]. At the mRNA level, EGR-1 was found to be induced up to 3 fold from control population within an hour of applied shear. Reported inductions are shown in **Figure 4-2**. Such transcription properties support EGR-1 transcription to be relevant towards developing a cell based shear stress sensor.

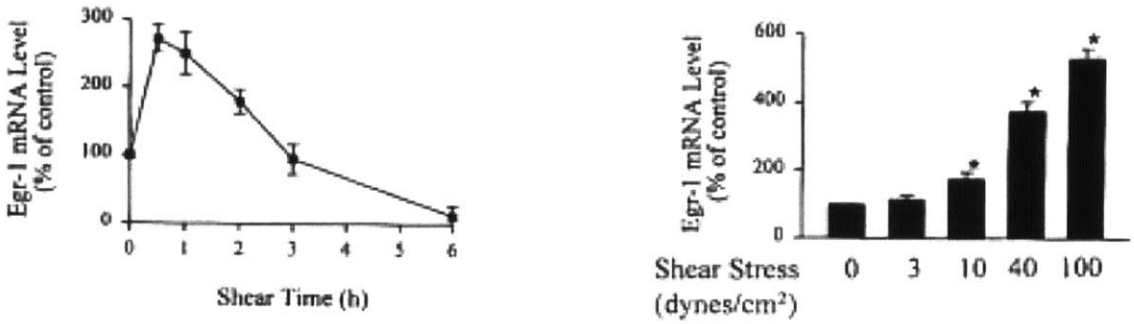

Figure 4-2 EGR-1 mRNA transcript upregulation in vascular endothelial cells exposed to shear stress showing induction maximum at an hour of applied stress of 20 dynes/cm^2 . Shear stress induced a shear intensity dependent level of mRNA as well (N= 3 experiments, error bars: standard error of mean). Obtained with permission from [78].

Furthermore, EGR-1 controls many downstream shear sensitive genes [46, 66, 88-90]. Shear stress or mechanical injuries activate the protein kinase C (PKC) pathway, upstream to mitogen activated protein kinases (MAPKs). This activation triggers the activation of extracellular signal-regulated (ERK) protein kinases which initiate the transcription of EGR-1 [42]. In the case of a well-known shear sensitive gene PDGFA, EGR-1 is known to displace transcription factor SP-1 from its native binding site within the promoter of PDGFA [50], thereby initiating PDGFA transcription. This induction and transcription process is summarized in **Figure 4-3**[51].

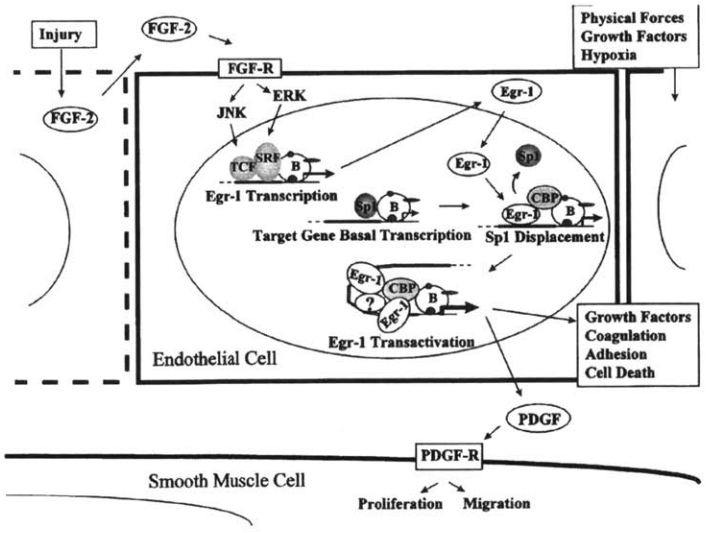

Figure 4-3 Mechanism of injury induced PDGFA transcription by EGR-1. Obtained with permission from [51].

Similarly, this ability of EGR-1 to displace SP-1 binding in order to initiate injury-driven transcription was also found to be applicable for other known shear responsive genes such as PDGF-B, u-PA, TF, and TGF-β1 [53]. The putative EGR-1 binding sites within the promoter regions of these genes, including PDGFA are shown in **Figure 4-4**.

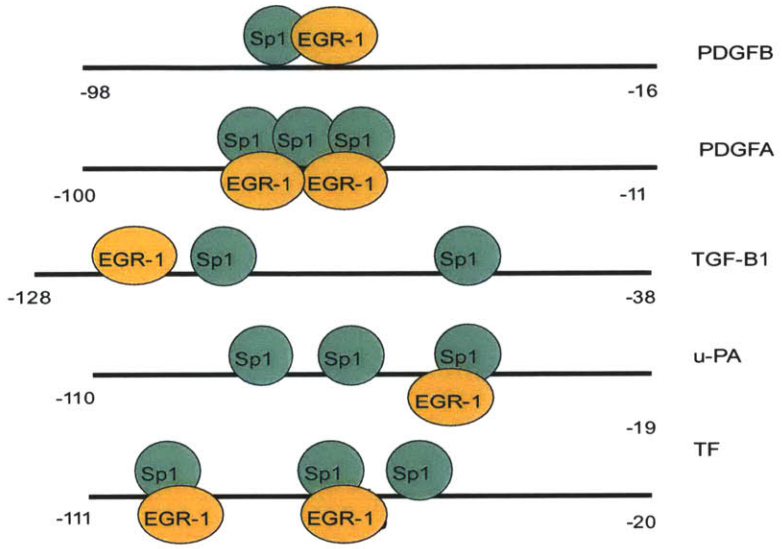

Figure 4-4 Regulatory ER-1 binding sites in the promoters of shear sensitive genes PDGF-B, PDGF-A, TGF-β1, u-PA and T, adapted from [53].

A chemical induction of the shear pathway would provide a facile handle for screening through populations in their sensitivity towards shear stress. In this case, a small molecule – PMA is commonly reported to induce EGR-1 transcription that can eventually lead to SP-1 displacement and downstream gene regulation, as shown in **Figure 4-5**[45]. While this chemical induction is an indirect method to trigger EGR-1 transcription, it provides a facile handle to investigate a variety of conditions for shear pathway inductions, akin to PDGFA upregulation mechanism.

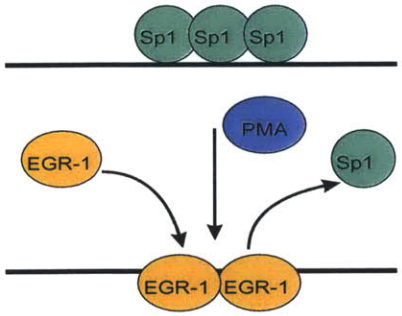

Figure 4-5 Model for EGR-1 displacing SP-1 in the promoter region of PDGFA, due to the presence of PMA. Adapted from [45].

With such motivation, the EGR-1 promoter was chosen to drive the expression of RFP in the shear stress sensor. Initial characterization and clonal selection of the sensor was based upon

population response to PMA inductions. Population fluorescence characteristics were further compared to those due to applied fluid shear stress in perfusion microfluidic devices.

4.1.2. Promoter design

In order to pick the appropriate EGR-1 promoter length, it was important to realize the role of regulatory transcription factor binding sites in the context of shear induced transcription. Specifically, it was important to investigate which binding site is crucial to include in a florescence reporter plasmid that would potentially assist in mimicking shear induction profiles of EGR-1 as fluorescence expression. This selection is also linked with the choice of appropriate promoter length. The most useful promoter region would maximize transcription sensitivity as well as sensitivity towards applied shear stress.

Sequence deletion studies are usually performed upon promoters where known transcription factor binding sites are either mutated or deleted sequentially until the stimulus-specific transcription is abolished completely. Locations of the main regulatory response elements within the EGR-1 promoter are shown in **Figure 4-6**[86]. In order to understand which of these transcription factors is relatively more responsible for shear based EGR-1 transcription, Schwachtgen [91] and others created transiently transfected chloramphenicol-acetyl transferase (CAT) reporters within HeLa cells using the EGR-1 promoter.

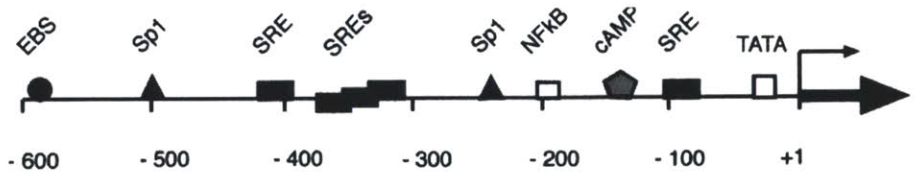

Figure 4-6 Regulatory response elements in the EGR-1 promoter. Obtained with permission from [86].

With subsequent promoter deletion assays, as shown in **Figure 4-7**, the serum response elements (SREs) were found to be imperative for shear induction of the EGR-1 promoter [91]. This result suggests that in addition to PMA, serum treatment could also enhance EGR-1 expression by induction of serum response factors acting on the shear sensitive SREs [92].

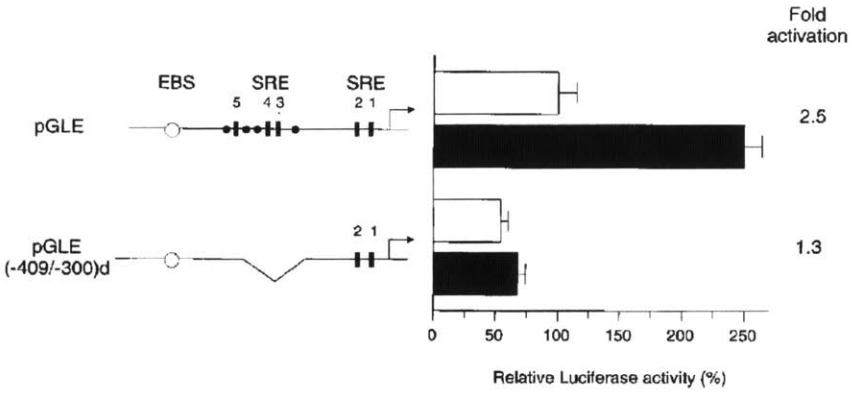

Figure 4-7 Relative luciferase activity from EGR-1 based CAT reporters shows that removing the SREs around the -400 base pair region inhibits the 2.5 fold induction due to 3 hours of applied shear (10 dyne/cm^2) in HeLa cells. White bars show luciferase levels of control while black bars represent luciferase levels after shear stress. Obtained with permission from [91].

Figure 4-8 shows results from promoter deletion studies where a minimal promoter length of 425 base pairs demonstrated the highest fold activation of luciferase activity due to shear induction [91]. Based on this result, the shear stress reporter plasmid included 527 base pairs of the native murine EGR-1 promoter upstream to its transcription start site.

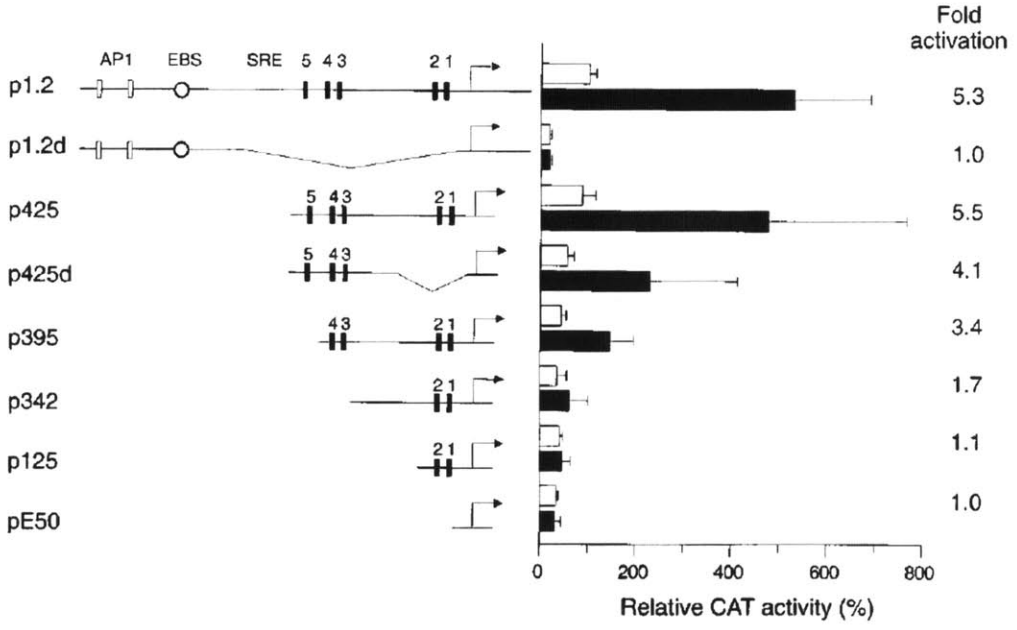

Figure 4-8 Promoter deletion assay of EGR-1 promoter with CAT activity in transiently transfected HeLa cells subject to 3 hours of shear stress at 5 dynes/cm^2. P425 plasmid had 425 base-pairs of the native promoter and showed maximal induction. Obtained with permission from [91].

4.2 Methods

4.2.1. Cell line construction: materials and methods

The promoter region was chosen as 527 base-pairs upstream of the transcription start site of the native murine EGR-1 promoter (GeneBank ID: NM_007913.5). Using this sequence, an EGR1-pTurboRFP plasmid was synthesized by Genewiz Inc. and was obtained both in lyophilized form as well as a bacterial glycerol stock. Cells were transfected and later selected in an identical process as mentioned in **Section 3.2.1**

4.2.2. PMA induction

All of the transiently transfected cells were allowed to recover overnight before initiating the chemical induction with PMA. Cells transfected with the inducible plasmid were divided into three categories depending on the culture media conditions used prior to induction. Specifically, one set of cells was exposed to media containing no serum (serum-free media, SFM) for 48 hours. The second set was exposed to SFM for 24 hours and then SFM + PMA (various doses). The last set was kept as a reference with the regular cell culture media. For the second set, PMA exposure doses were 10 ng/ml and 100 ng/ml. After 24 hours of PMA induction all cells were imaged using fluorescence microscopy for relative qualitative analysis.

PMA induction of the stable cell line was carried out in an identical manner. The dose response characterization of this population used PMA at 0.1-1000 ng/ml with ten fold increments of concentrations.

4.2.3. FACS sorting

All cell sorted were sorted using a MoFlo flow cytometer and sorter. Non-fluorescent NIH3T3 (blank) cells were used as a negative control and population expressing consitutuve RFP was used as the positive control to set the instrument gates and gains. A TRITC channel was used for the red fluorescence and a FITC channel was used for the reference fluorescence channel. When sorting at a population level as well as the clonal level, regions of interest within the fluorescent intensity histogram were marked with sorting gates. For single cell cloning, 96 well plates were filled with media containing 20% serum initially, to assist in clone survival. This media was replaced with regular culture media in two days.

4.2.4. Perfusion device fabrication and setup

The PDMS device, assembly and perfusion setup used for all of the perfusion studies is described in **Section 2.2.3** with the device shown in **Figure 2-5**. Instead of using logarthimic flows in the same experiment, each experiment consisted of running parallel perfusions at a

given flow rate (set by a peristaltic pump) for a given duration. Each perfusion consisted of three conditions - static, flow, and flow with PMA. The static condition consisted of cells in chambers experiencing no flow. This was a negative control to each experiment for addressing any effects of the seeding process, or device operation conditions. Chambers experiencing flow only and those experiencing flow with PMA were respectively connected to 20-30 mL reservoirs of cell culture media and cell culture media with PMA at 100 ng/ml. All chambers were connected by separate closed loop fluidic connections and the entire device was placed in a cell culture incubator for the perfusion duration. Following perfusion, the device was disconnected from the perfusion setup and the cells were imaged again with microscopy. The cell media within each chamber was manually replaced with Trypsin (0.25% v/v without EDTA, (at 37°C) for 5-10 minutes. The suspended cells were collected into 12 well-plates by flushing them with media. The cells were allowed to attach and recover for 24 hours prior to flow cytometry analysis.

4.2.5. Sodium Arsenite and MMS inductions

For testing of cross-talk between DNA damage and heat shock pathway, the reporter cells were induced with chemicals known to trigger the aforementioned pathways. In the case of DNA damage, Methyl methanesulfonate (MMS) was added to cell culture media at concentrations of 60, 120 and 240 µg/ml for four hours. For induction of heat shock pathway, sodium arsenite was used at concentrations of 2.5, 25 and 250 µg/ml for 30 minutes. After the incubation time, the cell cultures were rinsed twice with PBS which was then replaced with original cell culture media for 24 hours.

For preparation for flow cytometry analysis, all cells were washed with PBS buffer once and detached using 2 mL of Trypsin (0.25% v/v without EDTA) and afterwards, neutralized with 3 mL indicator-free media. The suspension was centrifuged at 1000 RPM for 5 minutes and the supernatant solution was aspirated. The cell pellet was resuspended in 1 mL of a premixed flow cytometry solution. This solution was made using PBS with 3% serum and 2% penicillin and streptomycin by volume. The cells were filtered using a cell strainer and gently vortexed to break any remaining cell pellets. In this fashion, all experimental cell conditions were prepared for flow cytometry and the same was done for control cell conditions.

4.2.6. Pathway inhibition

Cells were incubated with SFM media for 24h and then treated with SFM with 100 µM of PD98059 for 1 hour to inhibit chemical induction with PMA. This solution was then replaced with SFM and PMA containing 100 ng/ml for 24h. Additionally, sodium arsenite and MMS

inductions were also carried out as above upon cells that were pretreated with this inhibitor for 1h.

4.2.7. Flow Cytometry Setup

Flow cytometry equipment and settings were kept identical to those described in **Section 3.2.4**. For transient analysis studies, a different template was used where a four gate quadrant was set between the red and reference channel as Q1-Q4. The fluorescence cluster of the untransfected (blank) cell population was centered in the Q3 quadrant with an approximate zero mean fluorescence. The vertical gate between Q1, Q3 and Q2, Q4 was set to minimize autofluorescence bleed-through into the FITC channel. The horizontal gate was set above Q3 and Q4 to threshold the maximum background fluorescence from the control population. For all other flow cytometry experiments, the Q1-Q4 gating was replaced by a single horizontal gate to create a sub-population called P5. The distribution fluoresecence intensity was analyzed by a histogram of the red channel. The threshold set to create P5 population was identical to the threshold set to separate Q3 and Q4 in the transient analysis case. While being useful for studying future multi-color reporters, the vertical gate seperating Q1,Q3 from Q2,Q4 was not requried for subsequent studies and removed.

4.3 Results and Discussion

4.3.1. Transient Transfection

After 24 hours of transient transfection, the cells were analyzed for fluorescence expression using microscopy and the resulting images are show in Figure 4-12.

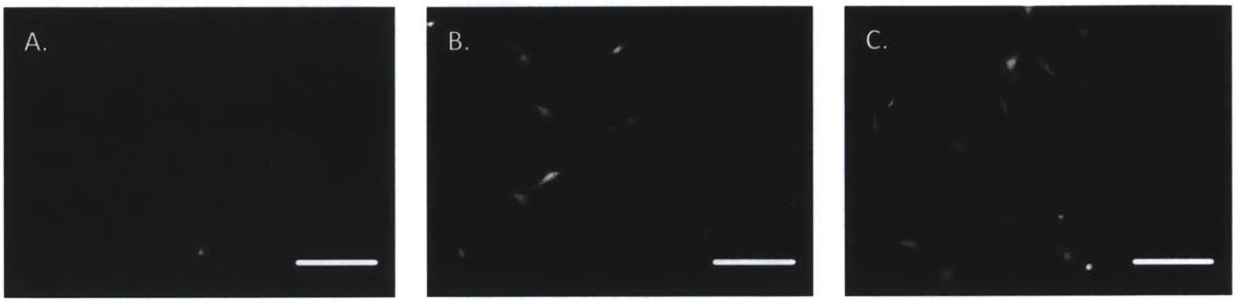

Figure 4-9 Fluorescent images of blank cells (A), inducible cells (B) and constitutive red cells taken with a 2 second exposure in the TRITC (red) channel (C). Scale bar: 100 µm.

The control population demonstrated no observable fluorescence, as expected. The population transfected with the inducible plasmid had some background fluorescence within the population of cells, suggesting in part, that the plasmid could functionally express RFP. However, such expression was not intended and could have resulted from one of many factors such as the potentially stressing transfection process itself, the cell culture process, or, simply a leaky promoter. It was seen by the microscopy images that qualitatively, the percentage of cells expressing RFP was similar with the CMV promoter when compared to those with the inducible promoter. With regards to fluorescence intensity levels, the CMV promoter population seemed to be brighter than the inducible population. With this experiment itself, the population inductions were not quantified, however it was learned that with the designed inducible and constitutively expressing plasmid, along with the transient transfection process, RFP fluorescence could be successfully observed using microscopy.

4.3.2. Transient induction

The transient transfection process was qualitatively assesed using fluorescence imaging. However, to verify promoter inducibility quantitatively, the transfected cells needed to be chemically induced and analyzed using quanitative fluorescence analysis. Here, the inducible populations were exposed to PMA and quantification of the population level induction was done using flow cytometry. Untransfected NIH3T3s were used as a negative control and those transiently transfected with the CMV-RFP plasmid were used as the positive control. Reporter population treated with SFM only was the reference to induced populations of SFM + PMA (10 ng/ml, 24 hrs) and SFM + PMA (100 ng/ml, 24 hrs). Fluorescent images and RFP intensity distribution histograms of all these populations are shown in **Figure 4-10**.

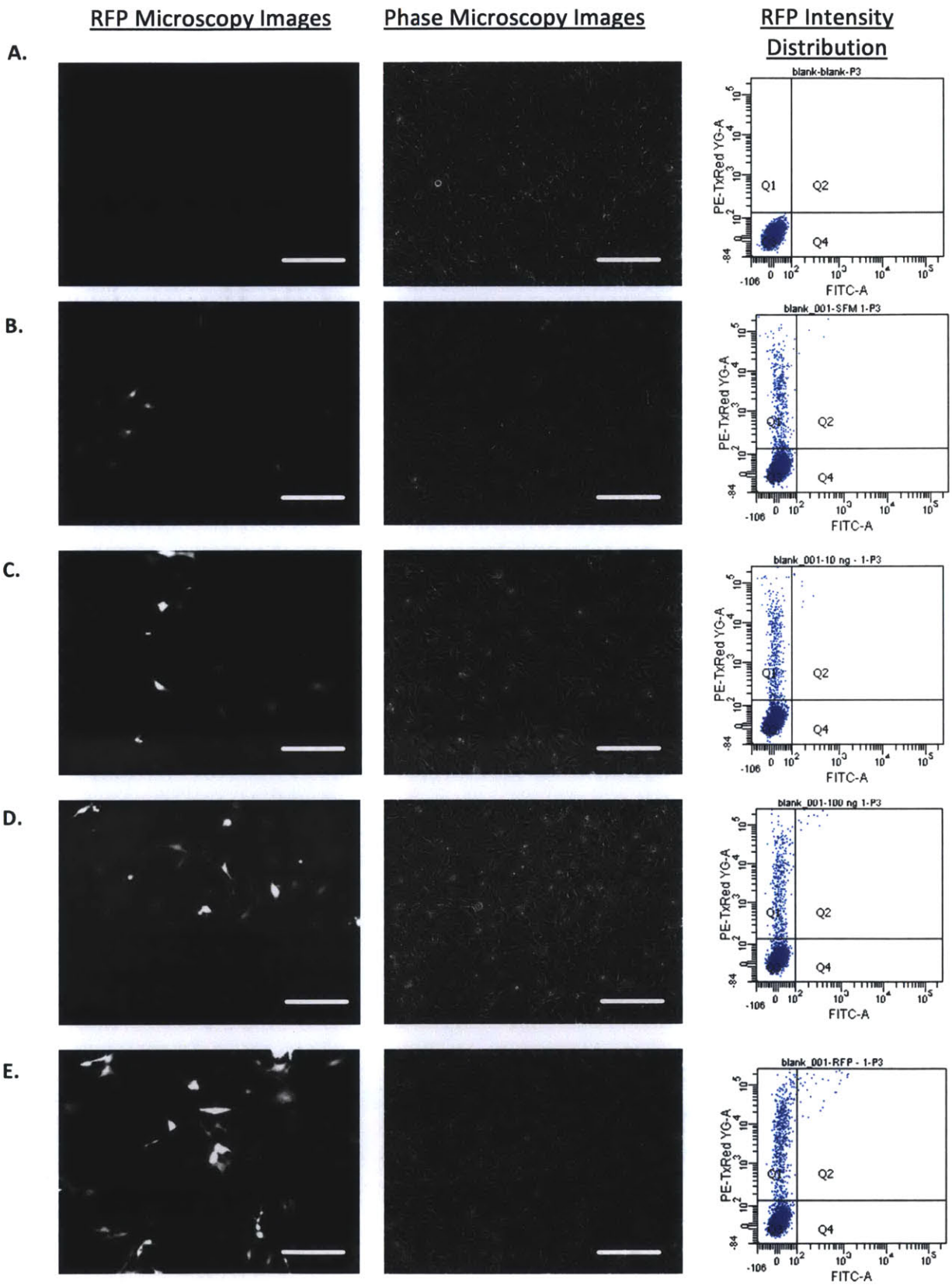

Figure 4-10 Fluorescence, phase images and RFP intensity distributions of A. Non-transfected cells B. Cells in SFM C. Cells in SFM + PMA (10 ng/ml) D. Cells in SFM + PMA (100 ng/ml) E. Cells expressing CMV-RFP. Scale bar 100 µm.

When analyzing a reporter signal-to-noise ratio, it is useful to have a low background level and high signal level. In this case, it was intended to lower the percent cells activated prior to intended induction, as well as to lower that entire population mean fluorescence level. For this purpose, cells were treated with SFM prior to PMA induction. When comparing the % activated cells (cells expressing RFP) in **Figure 4-11**, it was noted that SFM also lowered the fraction of red cells when compared to the No SFM condition. The mean RFP intensity of the entire population of all samples is plotted in **Figure 4-12**A, and the mean fluorescence level of the induced population normalized to the uninduced population is shown in Figure 4-12B. In **Figure 4-12A**, it was noticed that pretreating the cells with SFM for 24h desirably lowered the mean RFP level of the entire population from the population cultured with media containing serum (No SFM). As collectively seen from **Figure 4-11** and **Figure 4-12**, the difference between these conditions was not substantial, but was however expected and desirable.

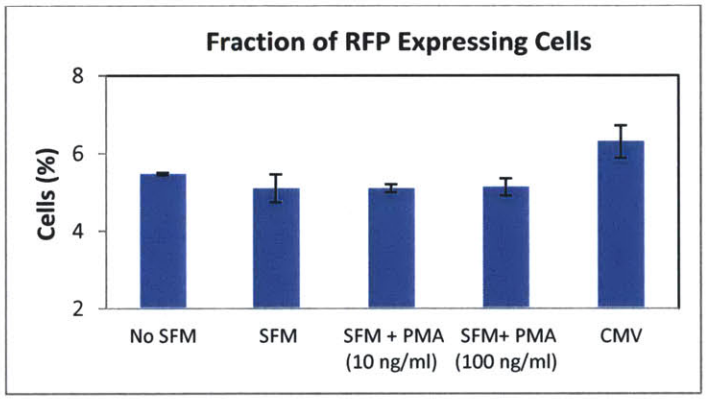

Figure 4-11 Fraction of cells expressing RFP in transient transfections and PMA inductions (N=3, error bars: standard error of mean)

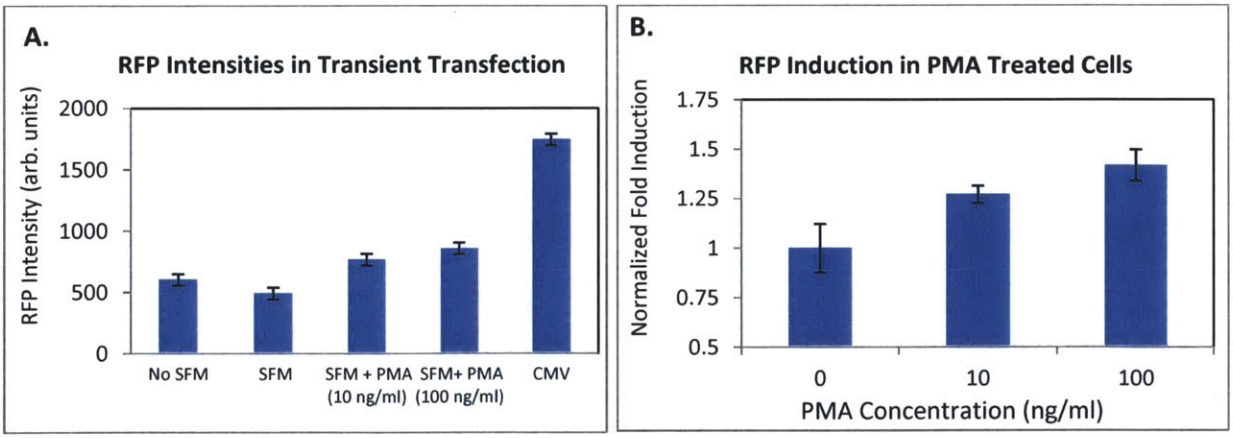

Figure 4-12 A. Absolute RFP levels for transient transfection conditions. B. Normalized fold inductions population mean fluorescence to cells treated with SFM only (N=3, error bars: standard error of mean)

Figure 4-11 also illustrates that the fraction of cells expressing RFP remains roughly the same from SFM to SFM and PMA induced conditions. It was expected that the fraction of cells turning red upon chemical induction would be higher than observed, and also sensitive to applied PMA

concentrations. However, the population of cells constitutively expressing RFP (positive control) is marginally higher than the inducible populations. This result could be more representative of this particular transfection process efficiency instead of the induction ability of the reporter itself.

This experiment illustrated an increasing fluorescence from the transiently transfected plasmid subject to increasing PMA concentrations. This successful induction of fluorescence demonstrated the functionality of the designed and transfected plasmid.

4.3.3. Induction of stable population

The transiently transfected cells were selected for G418 antibiotic resistance, a gene that was constitutively expressed in the inducible plasmid. It was presumed that the cells resistant to this antibiotic over many culture passages would have a stable integration of the inducible plasmid within their genome. Following this selection, the inducible cells were again tested for PMA induced expression of RFP in order to confirm plasmid functionality was maintained. Similar to the transient induction, the cells were treated with SFM overnight prior to induction with PMA concentrations and analyzed by flow cytometry. The fluorescence expression histograms of the reference population, control populations, and induced populations are shown in **Figure 4-13**. Compared to the negative control, the reference population (treated with SFM only) had a fraction of activated red cells in the P5 gate even before induction; however this fraction was much smaller than the majority of the population that did not express any fluorescence.

Induction with PMA at both concentrations of 10 and 100 ng/ml increased the fraction of cells expressing RFP and therefore the population mean fluorescence, shown as the 'EGR-1 Promoter' data set in **Figure 4-15**) Interestingly, for all the induced samples, the majority of the population remained under the P5 threshold set according to the blank (non-transfected) population used as a negative control. This suggested that despite the antibiotic selection process, a large portion of the potentially inducible population of the reporter was indistinguishable from the non-fluorescent background. In addition, this was also the case observed for the population selected for constitutive expression of RFP under the same antibiotic selection process. This suggested that an antibiotic selection process for stable integration may not necessarily cause homogeneity in fluorescence expression profiles. It is possible that either the promoter design and/or the stable integration of the plasmid may have caused the cells to have a heterogeneous fluorescence distribution. This hypothesis was not investigated in detail as it was assumed that a sub-population sorted by a similar fluorescence expression profile (by FACS) would have less heterogeneity in response.

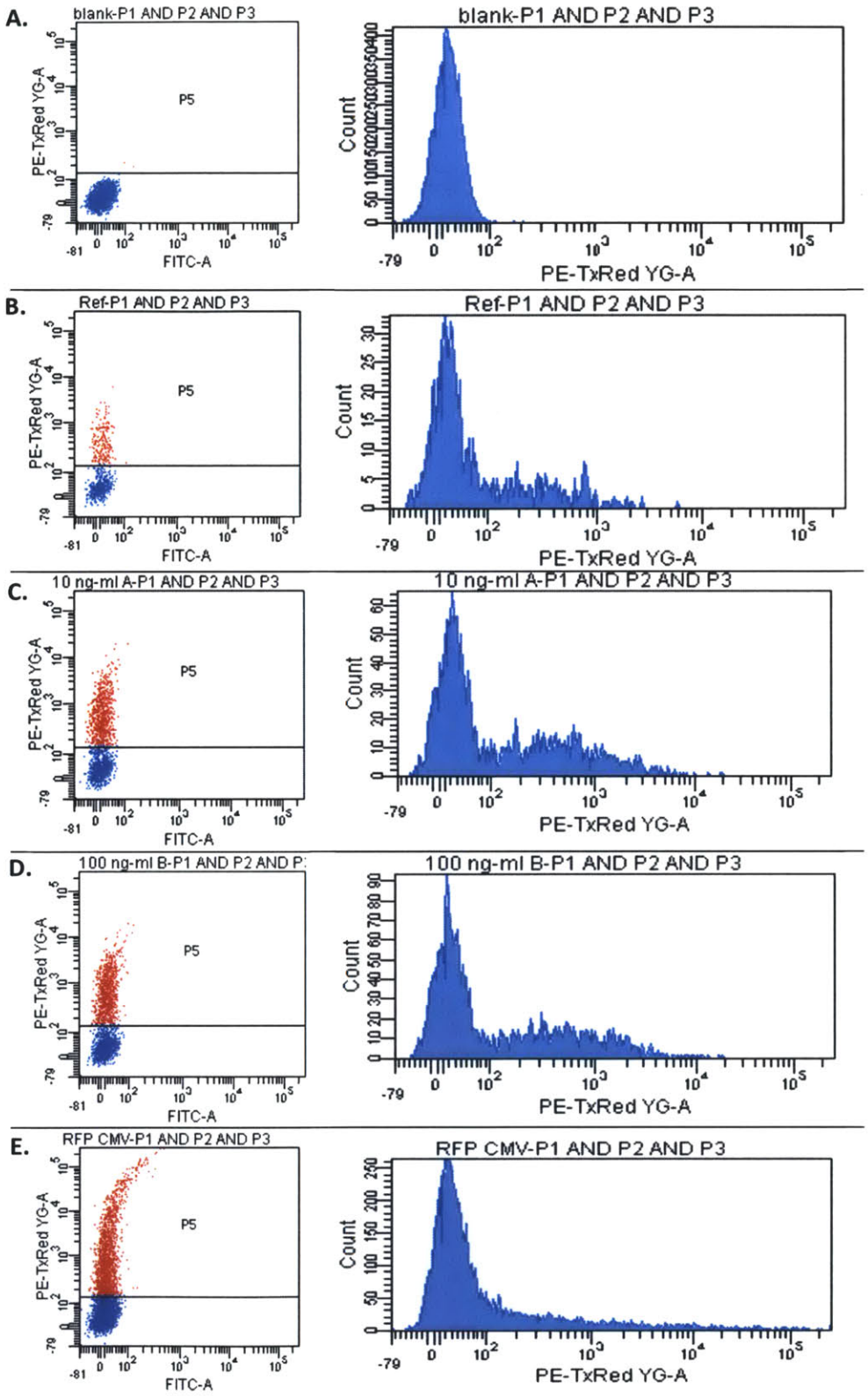

Figure 4-13 A. RFP intensity distributions of A. Non-transfected (blank) cells B. Cells in SFM C. Cells in SFM + PMA (10 ng/ml) D. Cells in SFM + PMA (100 ng/ml) E. Cells constitutively expressing CMV-RFP.

The mean fluorescence of the entire population was normalized to the reference population and compared to that observed from transiently transfected cells. As shown in **Figure 4-14**, the stable cell lines expressed similar increasing trend of RFP expression upon PMA induction, verifying that the population induction ability was retained after the stable cell line selection process.

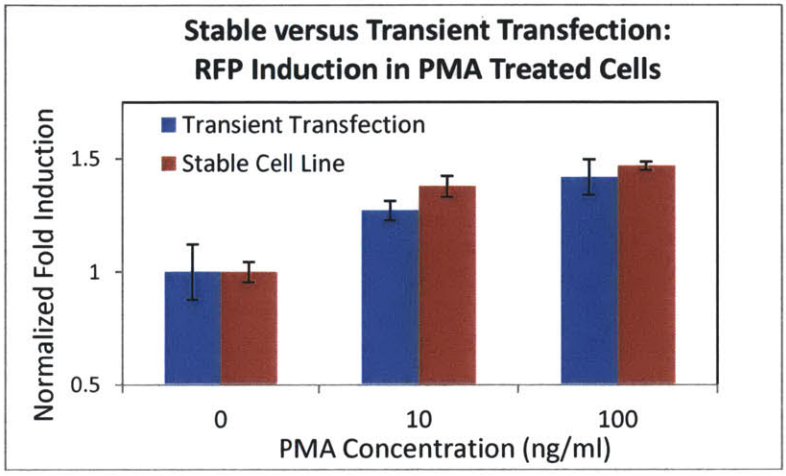

Figure 4-14 Comparison of population normalized mean RFP induction between transiently and stable transfected cells. (N=3, error bars: standard error of mean)

In addition, this population induction was compared to previously constructed inducible cell lines with identical transfection and selection processes. The main difference between these cell lines to this one is the choice of inducible promoter. In this case the cell lines chosen for comparison had three tandem response elements (RE) each in their inducible promoter. The first cell line had an overlapping binding site of SP1 and EGR-1 as found in the native promoter of PDGFA. The second and third populations had consensus response elements of transcription factors SP1 and EGR-1 respectively. The fraction of cell activation before and after PMA induction of all these populations was compared and is shown in **Figure 4-15**.

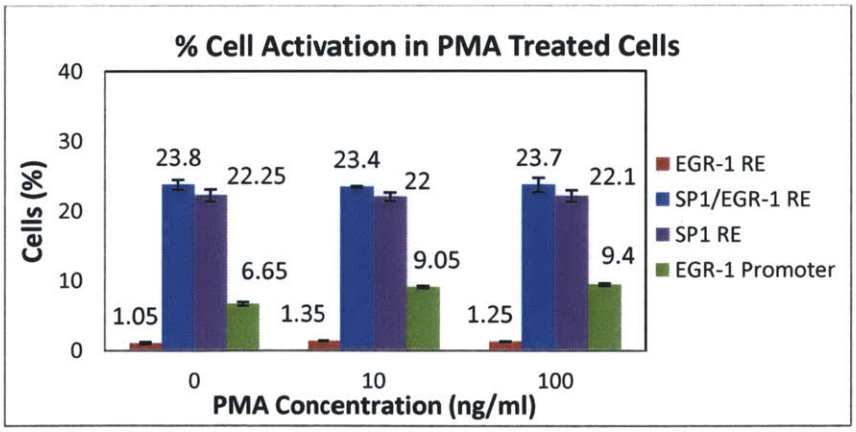

Figure 4-15 Fraction of cell activation between different reporter cells. (N=2, error bars: standard error of mean)

It was noted that for both the SP1/EGR-1 RE cell line as well as the SP1 RE cell line, the fraction initial cell activation was high and seemed unaffected by PMA induction. The proposed mechanism of EGR-1 activation and upregulation of downstream PDGFA gene was shown in **Figure 4-5**, where the transcription factor replaces bound transcription factor SP1 from its native binding site within the overlapping response element site. SP1 is a constitutively binding transcription factor which can increase activity upon phosphorylation. EGR-1 is however, more directly known to be induced by PMA through the PKC-MAPK pathway by both higher activation and upregulation [38]. Presumably the upregulation of EGR-1 transcription favors its competitive binding in the overlapping RE, and therefore upregulating downstream shear sensitive genes. In this case, the relatively similar and unaffected cell activation levels of the SP1/EGR-1 RE cell line and SP1 RE cell line suggest that the SP1 binding and regulation of fluorescence may be unaffected by PMA induction of EGR-1. The EGR-1 RE cell line demonstrated the lowest level of cell activation both before and after induction, possibly indicative of ineffective binding and therefore regulation by EGR-1 transcription factor. In contrast, the EGR-1 promoter cell line had higher background cell activation to the EGR-1 RE cell line. More importantly, among all the tested cell lines, this cell line demonstrated a PMA dose dependent induction of the population fluorescence. While the background cell activation levels suggest better binding in the SP1/EGR-1 and SP1 RE cell lines, the most useful cell line showing PMA induction was the one with the native EGR-1 promoter.

The normalized fold induction of mean RFP level of all the cell populations is shown in **Figure 4-16**. Here, the cell lines with EGR-1 RE and the EGR-1 native promoter show PMA dose sensitivity towards higher RFP expression levels. Specifically, the EGR-1 native promoter cell line demonstrated the highest induction among all compared cell lines.

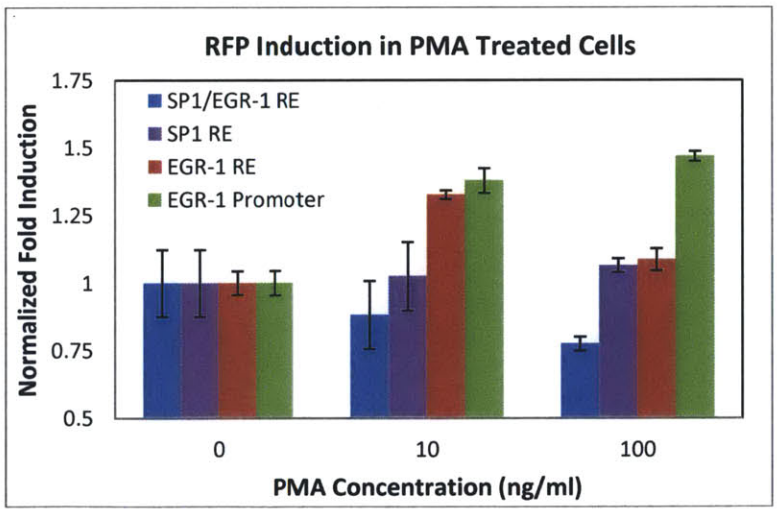

Figure 4-16 Normalized mean RFP induction in PMA treated reporter cell lines (N=2, error bars: standard error of mean)

The EGR-1 RE population demonstrated induction with PMA at 10 ng/ml. The majority of this reporter population was non fluorescent and with a RFP intensity distribution similar to the negative control population. The EGR-1 RE cell line and the EGR-1 promoter cell line mean fluorescence was normalized to the reference non fluorescent population and is plotted in **Figure 4-17**. Here, it is seen that PMA induction can effect a change in RFP expression of the EGR-1 RE population that is indistinguishable from a non-fluorescent population. On the other hand, the EGR-1 native promoter cell line is distinguishable from the negative control in both before and after PMA induction, thereby rendering it the preferable choice of reporter cell line construct for future induction studies.

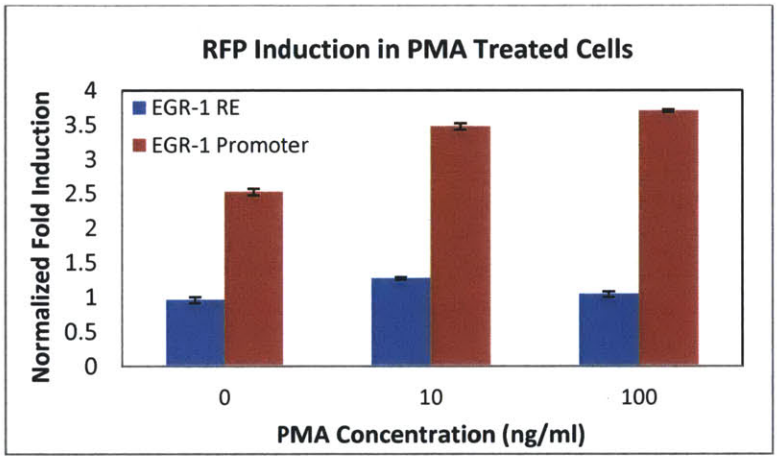

Figure 4-17 Population mean RFP level induction by PMA normalized to negative control cell fluorescence - comparison of EGR-1 response element to native promoter in context of inductions (N=2, error bars: standard error of mean)

It should be noted that the cell lines created with tandem response elements were functional in terms of some binding ability of regulating transcriptional factors. However, the promoter sequence used for these RE cell lines was not identical to any native promoter of a shear responsive gene and therefore may be lacking sequences useful for other transcription regulation functionality. Ideally, a potential cell line containing the native promoter of PDGFA (to drive RFP expression) compared within this study could have provided insight as to whether it is truly imperative to mimic a native promoter sequence for best pathway induction of fluorescence. While the exact explanations of the cell activation of all the compared cell lines was not elucidated explicitly, from this study it was evident that the cell line with the EGR-1 native promoter was relatively most sensitive to increasing PMA doses.

4.3.4. Population sub-sorting

As mentioned earlier, for a reporter population to have superior signal-to-noise ratio upon induction, it can be useful to have a lower fluorescence background. One approach to achieve

this feature was to use remove serum from culture media during chemical inductions. In **Figure 4-17**, it was observed that this change does not dramatically reduce the background fluorescence. The small but inducible activated cell fraction from the EGR-1 promoter cell line suggested the majority of the population was not showing sensitivity towards PMA induction. In fact, it was unclear if a certain background fluorescent level is required for ideal induction, or if It is possible to start with a mostly non fluorescent population that can be induced for a homogenous fluorescence induction.

To investigate this question further, the EGR-1 promoter population was sorted using FACS without any PMA induction. Non-fluorescent cells (termed blank) were used as a negative control and stable CMV driving RFP population was used as a positive control (termed CMV). Based on these controls, the fluorescence intensity distribution in the RFP channel was used to create gates R7 and R8, as shown in **Figure 4-18**.

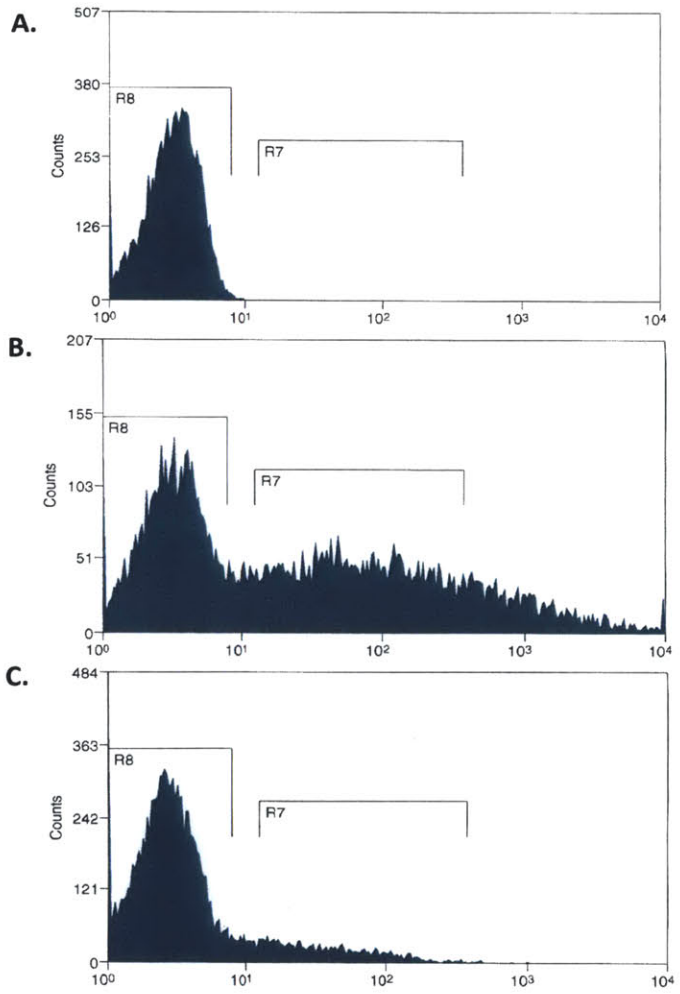

Figure 4-18 Population RFP intensity histogram and gates used for sorting cells on the RFP channel in FACS. A. Negative control population. B. Positive control population. C. Un-induced reporter population.

The sorted populations along with the unsorted original reporter population were induced by PMA again to evaluate the result of FACS sorting. The fraction of cells activated before and after PMA treatment of the three populations is shown in **Figure 4-19**. Here, it can be seen that the unsorted population had less than 10% cell activation originally that increased 2.75% after the inductions. On the other hand, the population sorted for high expression (within gate R7 in **Figure 4-18**) had a 3.55% increase in fraction of cell activated upon induction but more than 90% of the cells were expressing RFP even before induction. Interestingly, the population sorted for low expression (within gate R8 of **Figure 4-18**) had a background fluorescent level much higher than that of the unsorted population, even though it was originally sorted from the R8 region in **Figure 4-18**. This cause for this unexpected rise in background fluorescence was not investigated. Nevertheless, it was noted that this population had a 14.15% increase in percent cell activation, which was the largest change among all three populations.

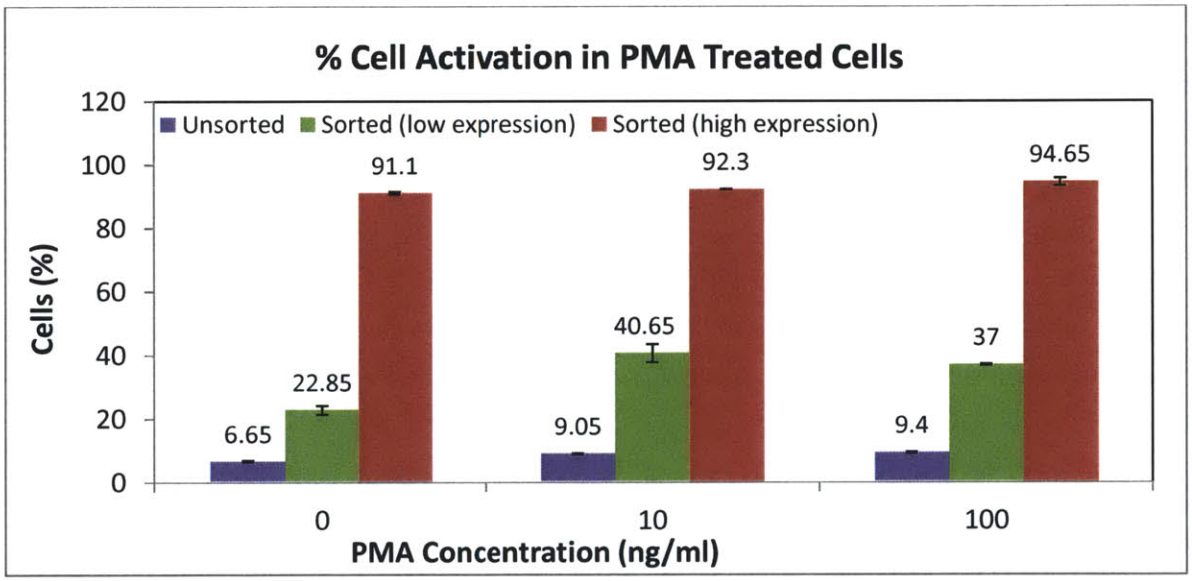

Figure 4-19 Fraction of population expressing RFP before and after PMA treatment of FACS sorted cells, compared to that of the unsorted parent population. (N =2, error bars: standard error of mean)

The normalized fold induction of the mean RFP level upon induction is plotted in Figure 4-20. Once again, it was noted that the population sorted for low background expression had highest relative dynamic range of expression.

Figure 4-19 and **Figure 4-20** indicated the FACS sorted low background expression sub-population improved the dynamic range of induction for both mean fluorescence and percent cell activation of the reporter population. With this success, the population sorted for low expression was chosen for subsequent analysis and characterization.

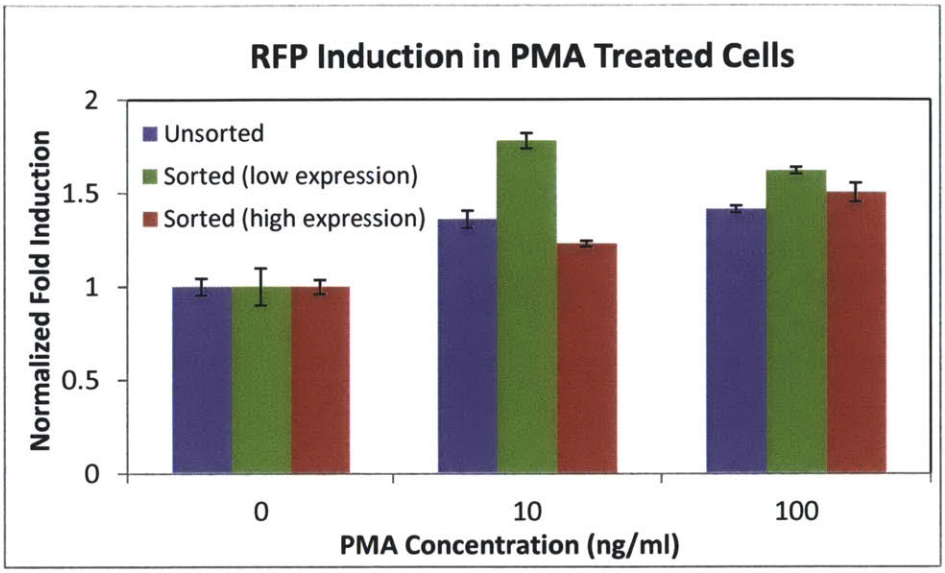

Figure 4-20 Normalized population mean RFP levels before and after PMA treatment of FACS sorted cells, compared to that of the unsorted parent population. (N =2, error bars: standard error of mean)

4.3.5. Characterization of RFP Induction Dynamics

In order to use and characterize the reporter population effectively, it is important to know its sensitivity towards a given stimulus. In addition, it is equally important to know the ideal time frame to measure the reporter response. If fluorescence expression is measured prematurely to the steady state maximum, then dose response may be an underestimate of true induction. On the other hand, a delayed measurement of fluorescence may be an inaccurate representation of induction potential as well, because the fluorescence is likely to degrade over time.

EGR-1 upregulation has been frequently reported using PMA concentrations of 10-100 ng/ml in literature, with a range of measurement delay depending on the particular assay. For the constructed reporter population, it was important to know the ideal dosage and measurement window. With this motivation, the PMA dose response was characterized using logarithmic concentrations from 0.1-1000 ng/ml over many time points. The normalized mean fluorescence for all populations is shown in **Figure 4-21** showing the time evolution and sensitivity of RFP expression.

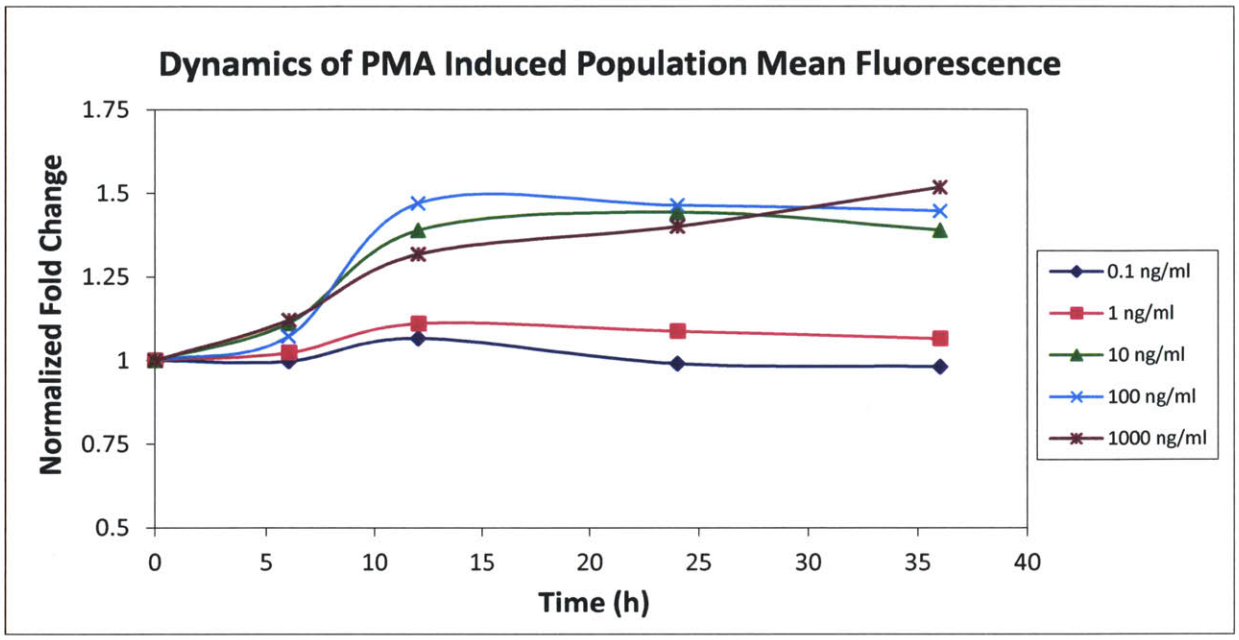

Figure 4-21 Time course evolution of normalized population mean RFP level due to increasing concentrations of PMA

Here, cells were incubated with a given concentration of PMA and analyzed using flow cytometry at 6, 12, 24 and 36 hours after initial exposure. The expression profiles demonstrated and increasing trend for all concentrations between 0-12 hours. The florescence signal appeared to be relatively saturated between 12-24 hours prior to a slight decrease around 36 hours. This trend was also observed for the normalized fold induction of the fraction of cells activated upon PMA induction, as shown in **Figure 4-22**.

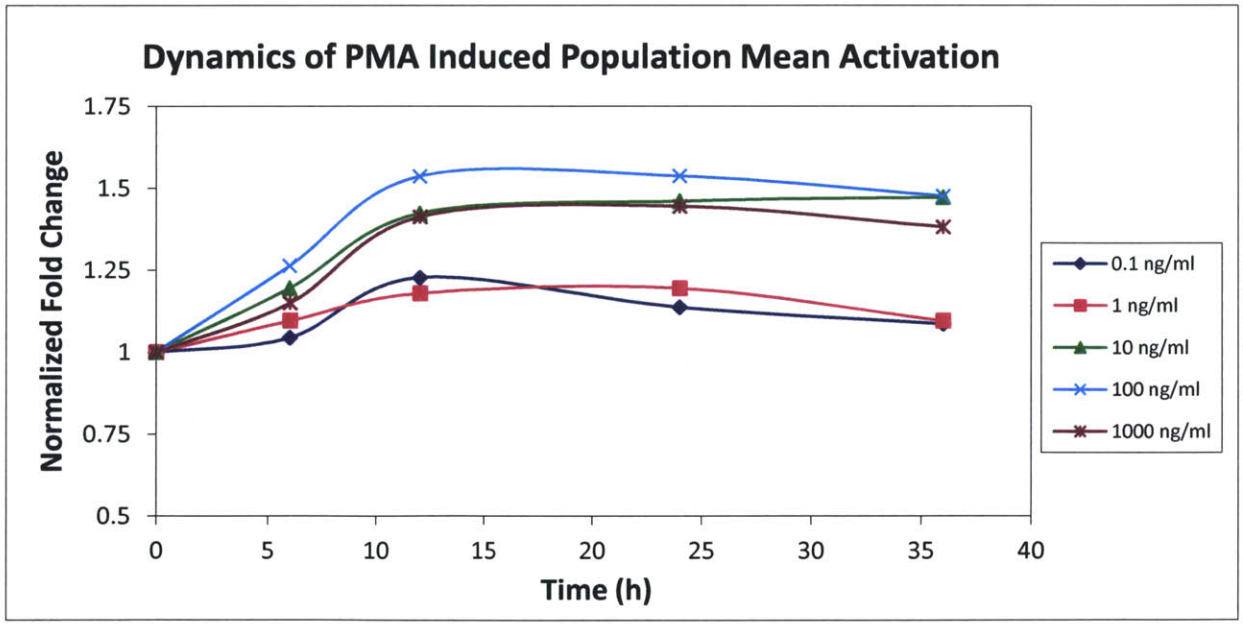

Figure 4-22 Time course evolution of normalized population activation level shifts due to increasing concentrations of PMA

From both **Figure 4-21** and **Figure 4-22**, it was observed that the reporter population demonstrated RFP expression correlating to dose concentrations from 0.1-100 ng/ml. The expression level and profile resulting from PMA concentration of 1000 ng/ml (highest dose) was similar to that from PMA at 10 ng/ml (**Figure 4-22**), but generally had relatively lower induction for up to 24 hours of exposure (**Figure 4-21**). Overall, the cells demonstrated highest response towards PMA at 100 ng/ml and the maximum induction of cell fraction and population fluorescence between 12-24 hours. This provides the dynamic range of the cells towards PMA, as well as highlights the time frame useful for measurement of fluorescence signal. Taken together, this experiment provided a map for chemical induction profile of the reporter population. In addition it was revealed that for chemical induction, the reporter could be effectively induced by PMA at 100 ng/ml and the fluorescence measurement should be made around 24 hours after induction.

4.3.6. Selection of Clonal Population

In order to investigate possible improvement in the population induction and response homogeneity, the EGR-1 population was single cell cloned after chemical induction with PMA. Using the same instrument settings and population controls as from the previous population sort, the induced EGR-1 population was gated in the RFP intensity histogram with gates of R3, R5 and R6. These three gates were embedded in the gate R4 (not shown), which marked the region of fluorescence greater than the auto-fluorescence of the negative control population. These gates are shown for all populations in **Figure 4-23**. The region of R3 selected the lower expression region, R6 with the mid-range and R5 with a highest range of expression. In this order, the percent of cells in these gates for the reference EGR-1 population were 27.08%, 27.66% and 6.76% and those for the induced population were 16%, 27.13% and 27.13% respectively.

As the induction assay and analysis happened at the population level, it was impossible to track individual reporter cell initial and final fluorescence levels. For instance, if an induced cell was to be sorted and cultured from the high expression region of R5, there was no method of predicting its eventual non-induced fluorescence level beforehand. Likewise, if a sorted cell was had a low induction fluorescence, it was not possible to predict if its signal to noise ratio would change or improve with its clonal population. Due to these reasons, it was decided to clone culture and eventually induce individual cells sorted from low, moderate and high induction level gates. Specifically, with gates of R3, R5 and R6, the induced population was sorted as a single cells into a three 96 well-plates per bin. Forty eight surviving and healthy clonal populations were chosen and cultured into three sub-population sets. The first set of cells was

induced with PMA with the methods described earlier. The second set was used as a reference in flow cytometry analysis as an un-induced population, and the last set was cultured as a back-up population that could be used for subsequent culturing.

A. Non-fluorescent negative control cells

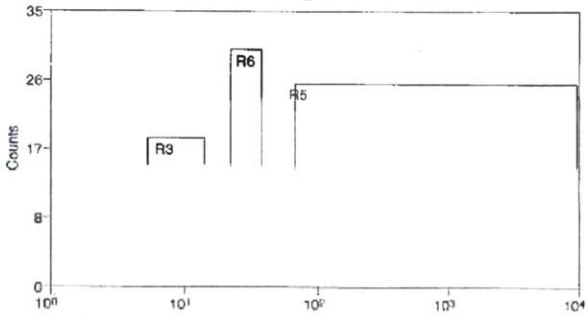

B. Constitutive RFP expressing cells

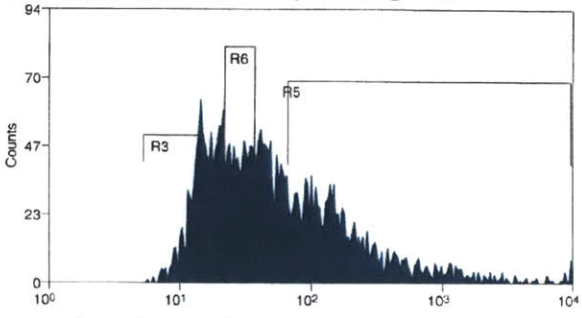

C. Reference non-induced population

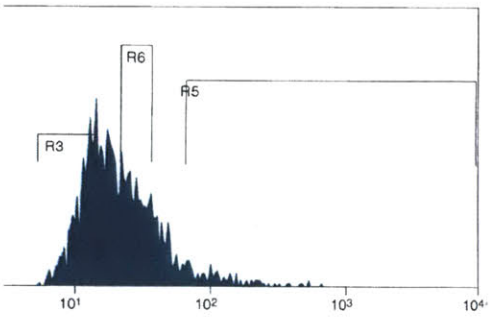

D. Induced population

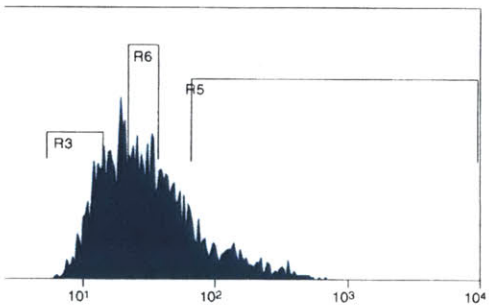

Figure 4-23 Population RFP intensity histogram and gates used for sorting single cells on the RFP channel in FACS. A. Negative control population. B. Positive control population. C. Un-induced reporter population. D. PMA induced population

Using the first two sets, all 48 clones were induced and analyzed with flow cytometry and their normalized induced cell fractions, and normalized population mean fluorescence were calculated. The distributions of these two parameters across the span of clones analyzed are depicted as histograms in **Figure 4-24** A and B.

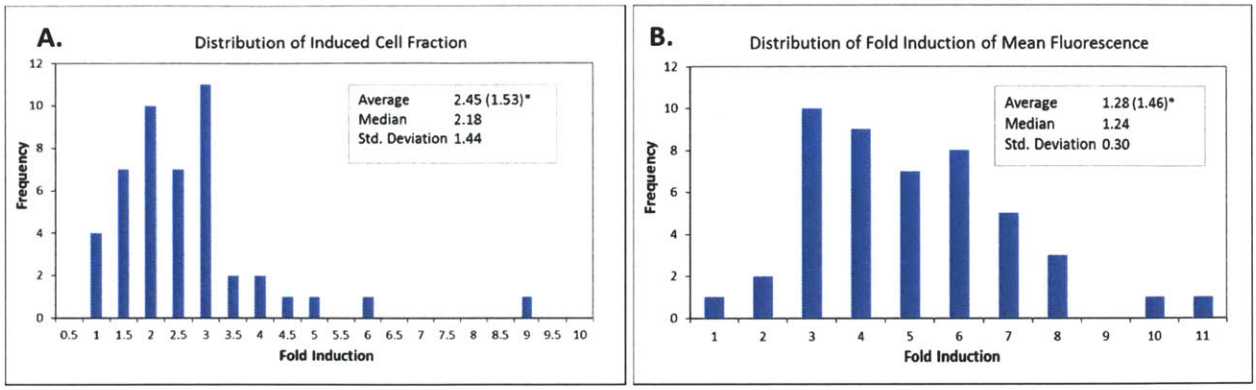

Figure 4-24 Collective results from clonal inductions: A. Distribution of normalized induced population fraction among clones. B. Distribution of normalized mean fold induction among clones. Statistics are provided in respective insets with * representing that parameter value from unsorted parent value.

The average of normalized fold induction of induced cell fraction was 2.45 fold with a median of 2.18 and standard deviation of 1.44. The same parameter calculated for an induced non-clonal population was 1.53. Likewise the average of normalized fold induction of population mean fluorescence across the clonal populations was 1.28, with a median of 1.24 and standard deviation of 0.3 fold. The average under the same conditions, the non-clonal population demonstrated a 1.46 fold induction in normalized mean RFP level.

To select an ideal clone, it was important to find a clone with superior induction compared to the non-clonal parent population. The top three chosen clones were clone #12, clone #9 and clone #47 (best). Histograms of the population fluorescence of these clones in their reference state and induced state are shown in **Figure 4-25**. The observed induction parameters for these three clones were compared to the parent population and are summarized in **Table 4-1**:

Table 4-1 Comparison of clonal populations to parent population

	Cells activated				Mean RFP
	Control (%)	Induced (%)	Range (%)	Normalized Fold Change	Normalized Fold Change
Parent population	25.9	39.8	13.9	1.53	1.46
Clone 12	10.9	14.8	3.9	1.39	1.68
Clone 9	5.9	24.9	19	1.36	1.54
Clone 47	47.9	71.9	24	1.88	2.14

Clone 47 demonstrated a higher range in the fraction of cells induced by PMA when compared to the parental population as well as a higher percentage of induced cells. The increase in the fluorescence histogram for this clone was also the highest among all induced populations. Furthermore, within the conducted experiments, the normalized fold change in the population mean fluorescence for this clone was higher than the parent population, although further

experimental repetitions and statistics may be required to evaluate consistency in results. Therefore, from this study, clone 47 was identified as the best population among the compared clones and was consequently used as the reporter candidate for subsequent studies.

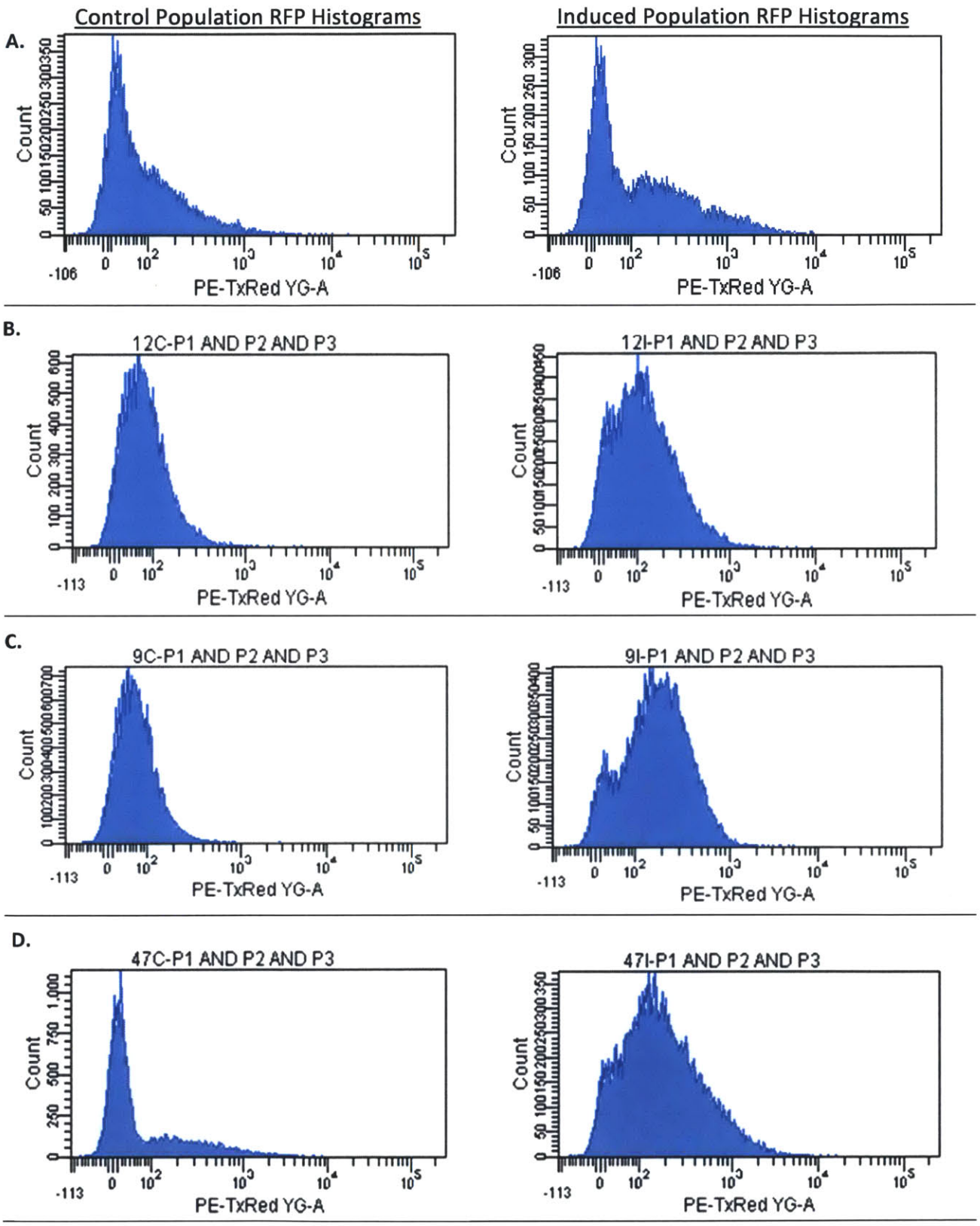

Figure 4-25 Population RFP intensity histograms for control and induced conditions for A. Parent population. B. Clone 12. C. Clone 9 and D. Clone 47.

4.3.7. Induction dynamics of Clone 47

In order to verify that clone 47 demonstrated the sensitivity to PMA and to characterize its dynamic range of induction, it was exposed to logarithmic concentrations of PMA from 0.1-1000 ng/ml, as done previously with the parent population. The fold induction of the cell activation is shown in **Figure 4-26** and the same for population mean fluorescence is shown in **Figure 4-27**. This study illustrated that the chosen clone indeed followed a similar sensitivity to PMA as the parent population. The maximum induction of the population fluorescence level as well as for percent population cell activation occurred at PMA with 100 ng/ml concentration. This confirmed that the chosen clone had better induction ability among the clonal candidates and also retained the induction characteristics of the parent population.

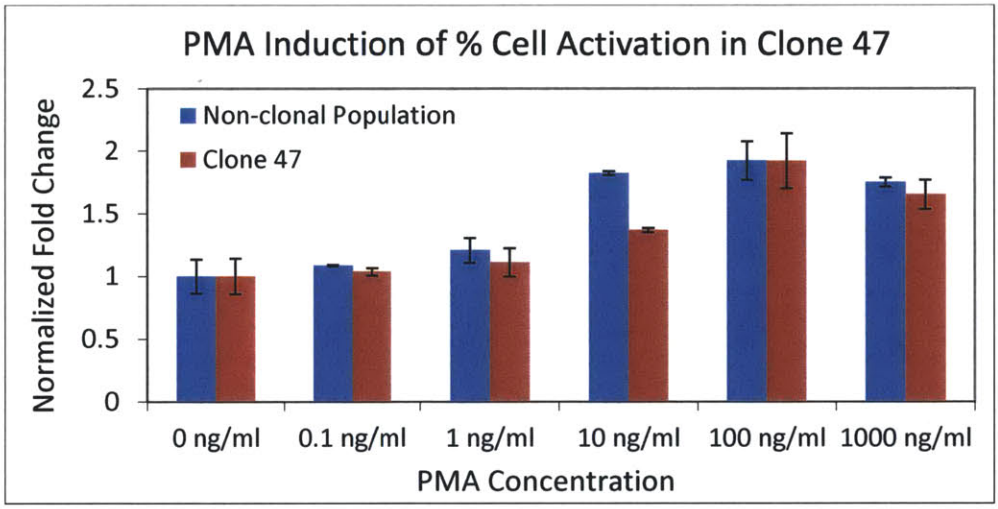

Figure 4-26 PMA dose sensitivity of Clone 47 & parental population in terms of normalized percent cell activation (N=2, error bars: standard error of mean)

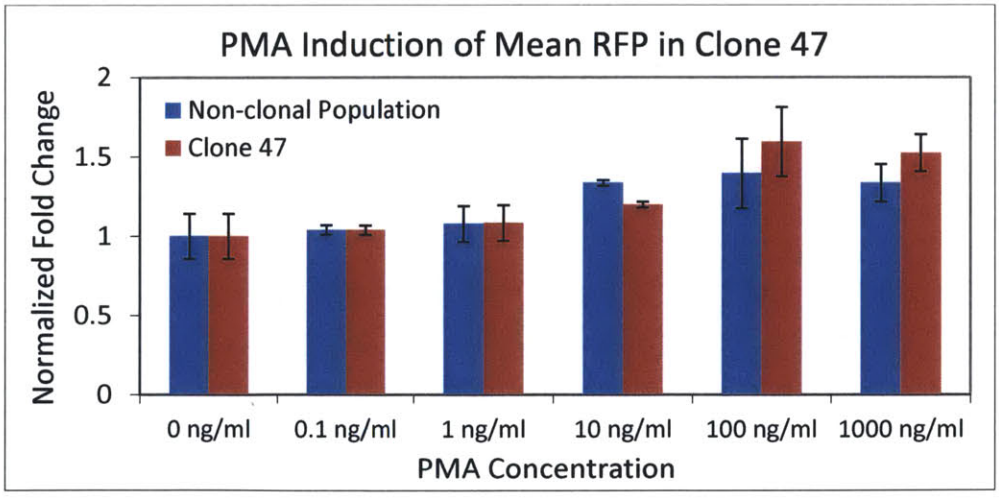

Figure 4-27 PMA dose sensitivity of Clone 47 & parental population in terms of normalized fold induction of mean population fluorescence (N=2, error bars: standard error of mean)

4.3.8. Shear sensitivity of Clone 47

In order to directly evaluate the sensitivity of clone 47 towards fluid shear stress, it was cultured in a microfluidic perfusion device. Cells were seeded and cultured overnight in 8 individual chambers simultaneously. Cells seeded in the device experiencing no flow were taken as the reference negative control. Cells experiencing shear stress set by a culture media perfusion, with a flow rate through a peristaltic pump, were used to evaluate the shear induction ability of the reporter. Additionally, reporter cells perfused similarly with culture media with added PMA (100 ng/ml) were used as the reference positive control to each experiment. All cells were imaged by microscopy before and after perfusion. To illustrate, cells seeded in a perfusion device that were imaged before and after perfusion are shown in **Figure 4-28** along cells used a static control.

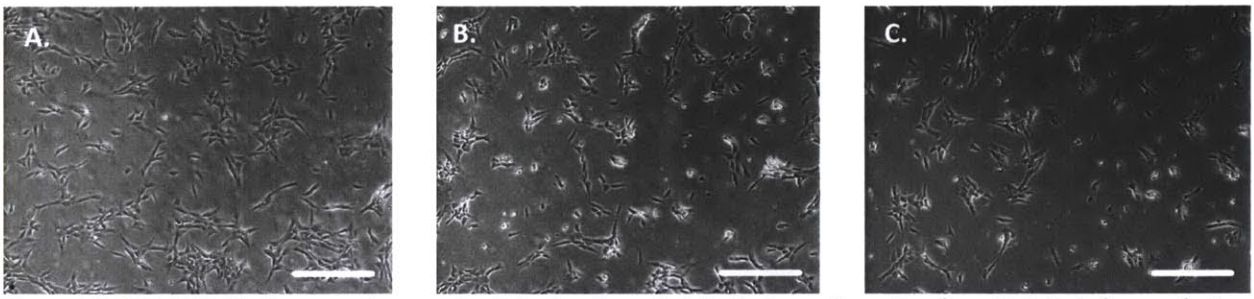

Figure 4-28 Bright field microscopy images of cells in chambers. A. Cells that experienced no flow. B. Cells before perfusion. C. Cells after perfusion at 16 dyne/cm^2. Scale bar: 100 µm

While not directly quantified, occasionally in perfusion experiments there was a small fraction of cells which detached, presumable due to the shear stress. This effect may in part be because the cells were cultured on a glass surface as opposed to more preferable polystyrene surfaces used in typical cell culture dishes. To strengthen cell adhesion during perfusion, the surfaces were pretreated with a 0.1% gelatin solution prior to cell seeding. Doing so helped the cell morphology resemble that seen from cells grown in a culture dish. Regardless of any cell detachment losses however, there were sufficient cells recovered from the perfusion chambers that could be cultured for 24 hours and used for flow cytometry analysis. Fluorescence intensity histograms of a sample population experiencing flow, flow with PMA, and cells experiencing now flow conditions are all shown in **Figure 4-29**. From here it was seen that perfusion could indeed change the florescence distribution profile of the reporter cells, thereby indicating a shear based induction.

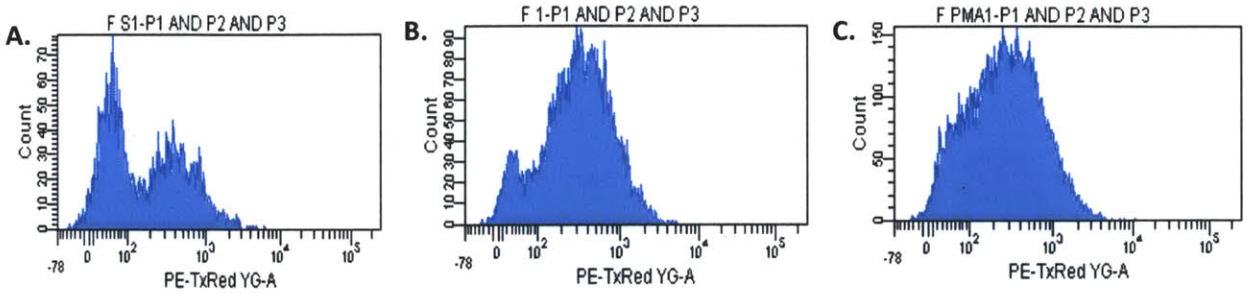

Figure 4-29 Population RFP intensity histogram for A. Static cells (negative control) B. Cells perfused with media perfusion. C. Cells perfused with media containing PMA (positive control). Shear intensity of 16 dynes/cm^2 for a duration of 3 hours.

To quantify this shear induction, the population mean fluorescence of cells experiencing flow, as well as that of the cells experiencing flow with PMA, was normalized to that of the static control for each shear intensity experiment. The normalized shear induced RFP expression for 1, 4 and 16 dynes/cm^2 applied for 3 hours of perfusion experiments is shown in **Figure 4-30** Figure 33.

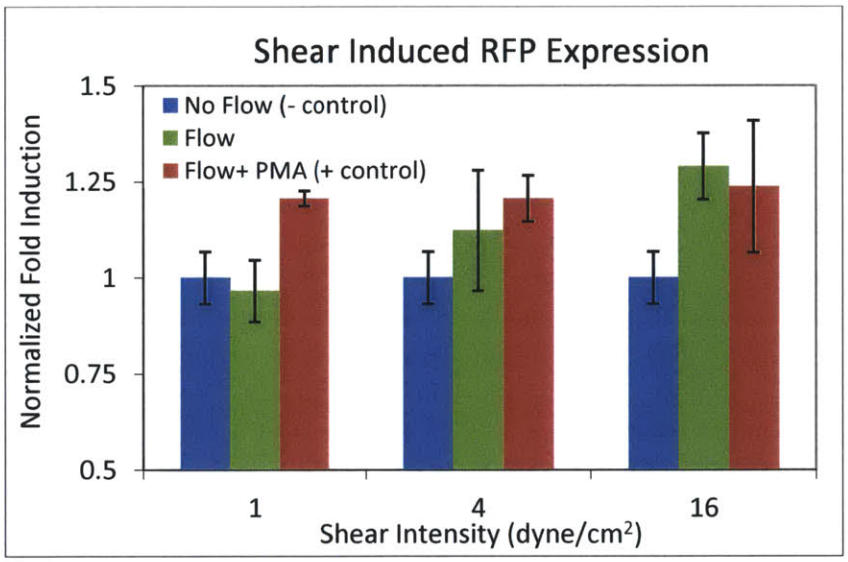

Figure 4-30 Shear induced mean RFP expression normalized to the device static control, across increasing shear intensities. (N = 2, error bars: standard error of mean)

From this result, it was observed that the positive control condition of flow with PMA resulted in similar expression across all shear intensities. It can be postulated that this condition caused RFP expression due to the presence of PMA in the perfusion media, at a concentration (100 ng/ml) kept constant between shear intensities. More importantly, it was observed that the population mean fluorescence demonstrated a monotonic increasing trend from 1 to 16 dynes/cm^2. This suggests that the reporter was indeed sensitive to shear stress intensities as expected. The population begins to show a response to shear stress of 4 dynes/cm^2 which may be the lower limit of detection in the given experiments. The shear-induced cell activation was also calculated and is show in **Figure 4-31**. Here, it was observed that for 4 dynes/cm^2 intensity

did not significantly induce any change in the fraction of cell activated upon induction for either the flow only condition or the flow with PMA (positive control) condition. A significant change in this parameter was only observed for the highest tested shear intensity of 16 dynes/cm^2.

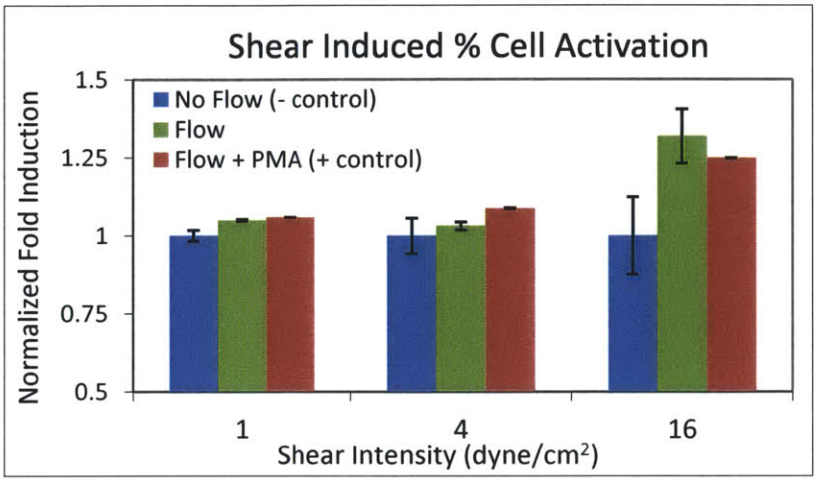

Figure 4-31 Shear induced fraction of population activation normalized to device static control, across increasing shear intensities (N = 2, error bars: standard error of mean)

The upper limit of shear induction tested was 16 dynes/cm^2, however this intensity may not be the absolute upper limit of detection for the reporter. To establish such a limit further studies would be required to investigate if the fluorescence signal saturates at a regime of shear stress intensities. Additionally, it was of interest to evaluate how quickly the reporter could be induced due to shear stress. For this experiment, cells in the microfluidic device were perfused at 16 dynes/cm^2 from ten minutes to 3 hours. The normalized population median fluorescence is shown in **Figure 4-32** where it is compared to the same from cells exposed to the same duration of PMA in a static (no flow) condition. These results suggest that the reporter cells started to show induction upon exposure to either shear stress or PMA for one hour and onwards.

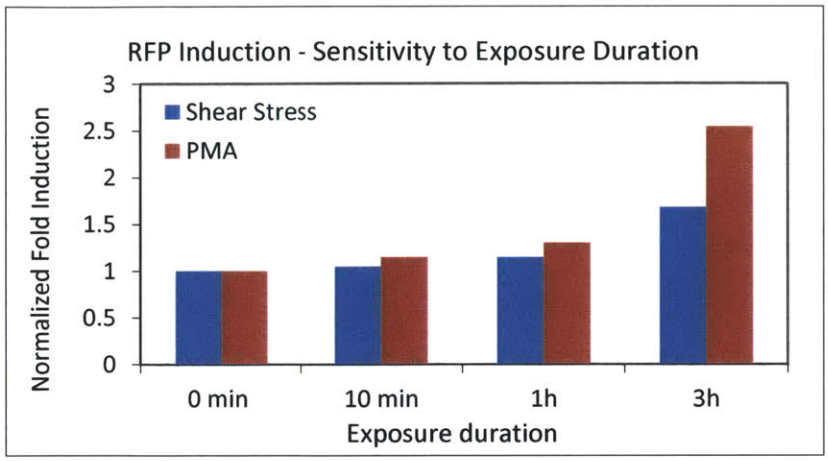

Figure 4-32 Shear induced median RFP expression normalized to the device static control, across increasing durations of applied shear stress of 16 dynes/cm^2.

Taken together, the clonal population chosen from chemical induction experiments demonstrated sensitivity towards shear stress and proved its functionality as a shear stress reporter. This population could be induced as quickly as an hour of applied chronic shear stress at 16 dynes/cm^2 and showed an increasing florescence response with shear intensities from 4 dynes/cm^2. In the context of EGR-1 based shear inductions, prior efforts have been made on constructing transiently transfected HeLa cells which increase luciferase activity upon shear. Specifically, Schwachtgen and others reported normalized luciferase inductions of 4.5-6 fold due to a comparable range and duration of shear stress [91]. Similar to the reporter presented here, their results may depend on a choice of factors such as the chosen cell type, transfection method, shear stress apparatus and measurement assay parameters. Comparatively, the induced signal to background ratio of the sensor presented here is lower than that reported in the aforementioned case. Nevertheless, the reporter presented here is still advantageous as the sensing ability is embedded to the genome of the clonal population. This allows for cell line propagation and therefore, ability to maintain shear stress sensitivity.

This work presented the first version of a fluorescence based shear stress reporter within NIH3T3 cells where the sensor demonstrated promising potential to evaluate the physiological impact of shear stress in long term perfusion platforms where cells may experience chronic shear stress.

4.3.9. Selectivity of sensor induction towards shear stress

While the reporter demonstrated fluorescence induction due to shear stress, it was important to investigate the specificity of the chosen reporter induction pathway towards the shear pathway. Many cell stress pathways are interconnected with common induction nodes,

transcription factors and inducible genes. To first ensure that the PMA induction of the reporter was indeed transduced through the PKC-MAPK pathway, its pathway inhibitor was used to check if the reporter response could be abolished due to its pretreatment [39, 93]. This molecule is also reported to abolish a shear-dependent induction of EGR-1 (**Figure 4-5**) by blocking MEK1 activation of ERK1/2 needed for EGR-1 transcription. [91]. Here, the reporter was incubated with 100 µM of PD98059 for 1 hour prior to induction with PMA at 100 ng/ml. In addition to this condition, the same reporter was identically induced with PMA without the presence of the inhibitor. The normalized fold induction of the population mean fluorescence and the percent cell activation for these conditions is shown in **Figure 4-33**.

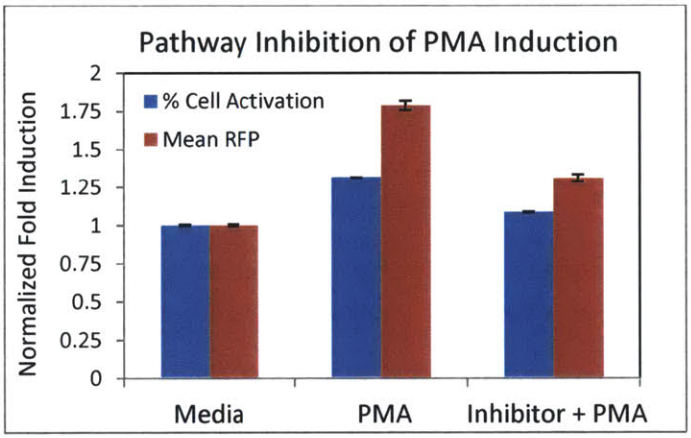

Figure 4-33 Inhibition of PMA induction of population mean fluorescence with PD98059, (N = 2, error bars: standard error of mean)

The inhibitor indeed reduced both the fraction of induced cells in the reporter as well as the induced fluorescence response. While the levels were marginally higher than the no-inhibitor and no-PMA reference control, it was concluded that the PKC-MAPK pathway was likely to be responsible for the PMA induced upregulation of RFP though its EGR-1 promoter. Even though this inhibitor is commonly used to inhibit EGR-1 transcription, in this case it did not completely knock down the induction. While this molecule was still effective, possible further studies using siRNA could be used to test further induction inhibition. Such experiments may reveal if there could be any cross-regulatory control due to another PMA induced stress pathway.

EGR-1 can be also be induced by cell stress caused by ionizing radiation, hypoxia or heat shock pathways [87,93, 94]. To evaluate if the sensor could be induced by other cell stress pathways such as DNA damage pathway or heat shock pathway, the reporter population was incubated with small molecules known to trigger those pathways. Specifically, the population was incubated with 60-240 µg/ml of MMS for 4 hours for DNA damage pathway induction[95]. Seperately, the reporters were also incubated with 2.5-250 µg/ml of sodium aresenite for 30 min in order to trigger the heat shock pathway in the population[96]. These cross-pathway inductions were performed on both the clone 47 reporter chosen for the shear stress studies,

as well as on its parent non-clonal population. The response of the populations to the triggered DNA damage pathway is shown as normalized fold inductions in the population mean fluorescence and fraction of cell activation, and are shown in **Figure 4-34**A and B respectively.

It was seen that the sensor could be indued by the tested concentrations of MMS. The clonal popuation showed highest sensitivty to 240 µg/ml while the parental population showed the same for 60 µg/ml. In both populations, there was a high amount cell death observed from the 240 µg/ml dose (data not shown). As this was the lethal dose for the population, data from 60 and 120 µg/ml would be more reliable and representative of sensor response, as apoptosis at the lethal dosage could lead to other cell death pathways to affect RFP expression.

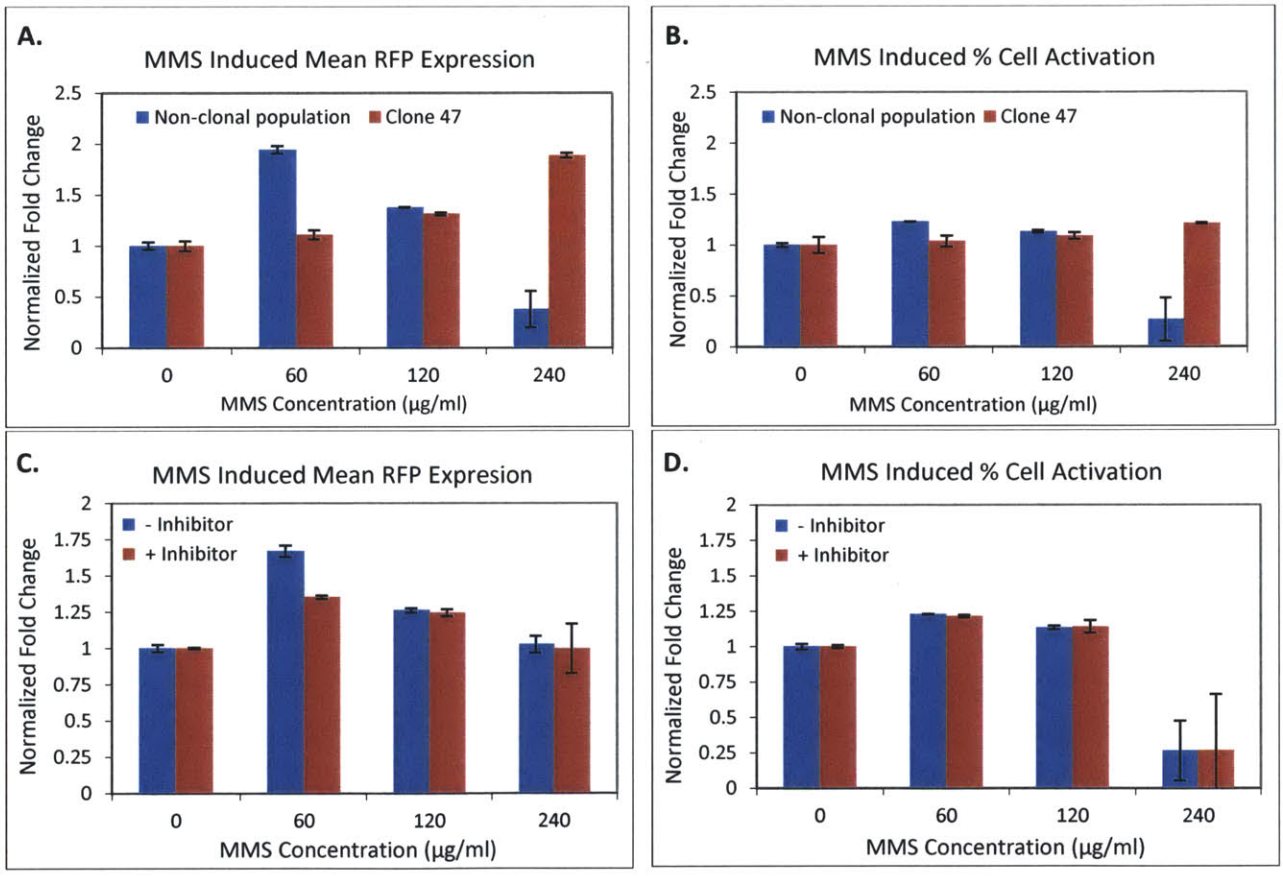

Figure 4-34 MMS induction of DNA damage pathway in EGR-1 reporter. Normalized population mean RFP levels due to MMS treatment of A. Clone 47 and parent population. C. Parental population with or without PD98059 (100 µM). Normalized population fraction activation due to MMS treatment of B. Clone 47 and parent population. D. Parental population with or without PD98059 (100 µM). (N =2, error bars: standard error of mean)

Furthermore, to test if the inhibitor that abolished the PMA sensitivty could also abolish the MMS induced response, the non-clonal population was incubated with the inhibitor and

induced with MMS. The changes in the population activation and fluorescence are shown in **Figure 4-34** C and D, where it is observed that the inhibitor was ineffective in changing the MMS induction. Elk-1, a transciption factor known to upregulate EGR-1, transcription has also been reported to regulate DNA damage induced transcription of p21 and BAX genes in a p53 independent manner [95, 97]. This implies that the MMS induction of EGR-1 could have occurred due to common upstream regulatory events that triggering the EGR-1 reporter response through a divergent pathway from PMA induction.

Similarly, the sensor also showed cross-sensitivity to the heat shock pathway in its normalized mean fold induction of population RFP levels and normalized induced population fractions due to sodium arsenite doses, shown in **Figure 4-35** A and B.

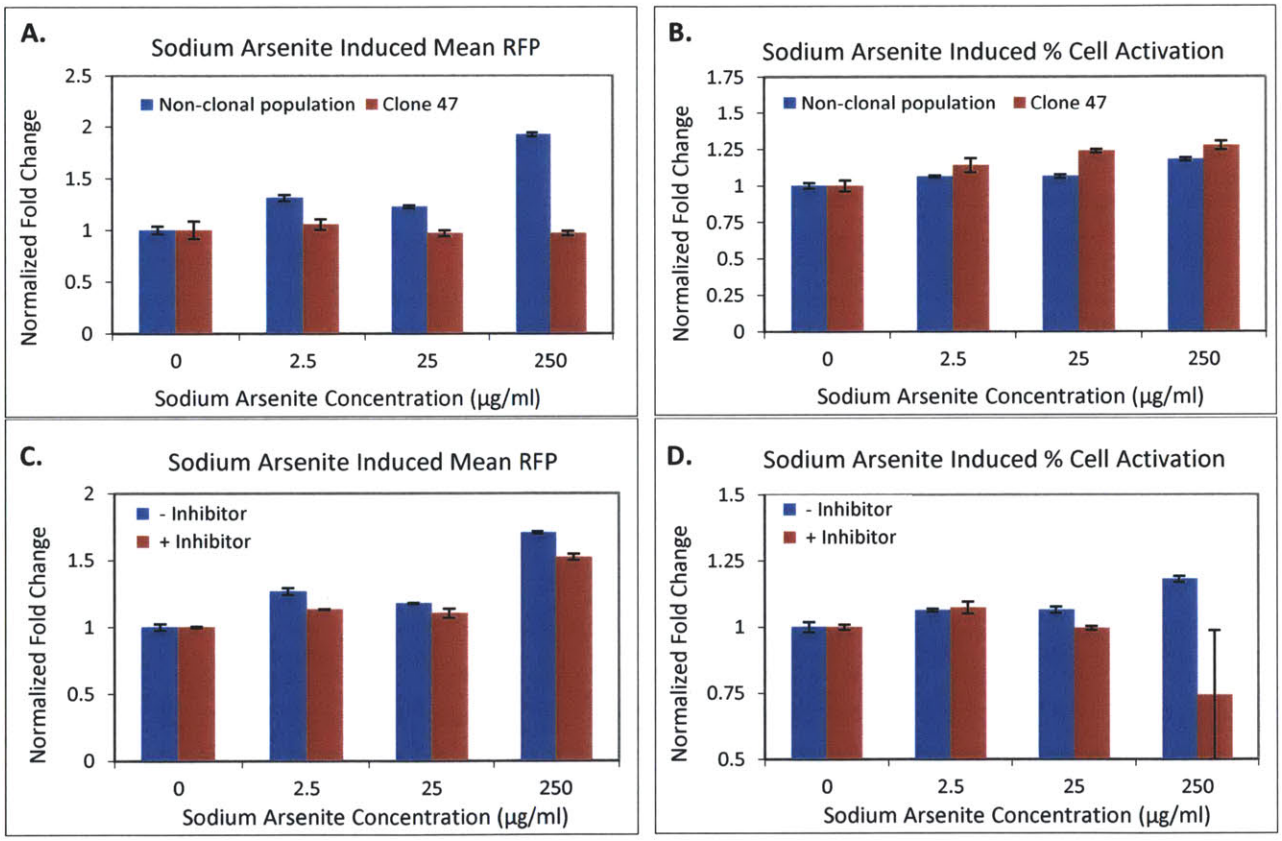

Figure 4-35 Sodium Arsenite induction of heat shock pathway in EGR-1 reporter. Normalized population mean RFP levels due to arsenite treatment of A. Clone 47 and parent population. C. Parental population with or without PD98059 (100 µM). Normalized population fraction activation due to arsenite treatment of B. Clone 47 and parent population. D. Parental population with or without PD98059 (100 µM). (N =2, error bars: standard error of mean)

In this case, the highest dose tested was the apparent lethal dose causing the majority of cells to die due to the chemical treatment. It is likely, as postulated with the DNA damage inductions, that the lethal dose may cause population fluorescence behavior to change in a complex and unreliable manner. Therefore, the doses of interest were chosen to be 2.5 and 25

μg/ml, which have been reported to successfully induce the pathway [96]. With these, there was no apparent rise in the mean of population RFP levels upon arsenite treatment of Clone 47 relative to that observed for the parent population. However the clonal population showed marginally higher fractions of induced cells relatively compared to the non-clonal parental population, which were also monotonically increasing due to arsenite dosage. While not entirely conclusive, it was learned that indeed, the EGR-1 reporter population could be induced due to triggering of the heat shock pathway with sodium arsenite. Again, in order to test if such cross-sensitivity of the reporter to heat shock could be removed by the inhibitor used earlier; the parental non-clonal population was treated with sodium arsenite, but in the presence of the shear pathway inhibitor. The comparison of the parental population inductions with or without the inhibitor, in terms of their normalized mean RFP levels as well as their normalized induced population fractions, is show in Figure 38 C and D respectively. Overall, the shear pathway inhibitor was unable to drastically reduce the effect of heat shock pathway stimulation and consequent activation of RFP. It was therefore postulated that such inductions may not be occurring through the same pathway induction nodes as for that for shear stress.

Taken together, it can be said that the shear stress sensor could be induced by alternative stress pathways by virtue of its native promoter design. These results are not entirely surprising as cross-talk of stress pathways induced by UV, arsenite and heat shock has been reported to induce EGR-1 transcription in NIH3T3 cells [98]. While such cross-sensitivity may not be ideal for designing a sensor specifically for shear stress, the characterization results provided insight into reporter stress pathway induction characteristics that could be used to design the next generation of shear stress sensors.

4.4 Conclusions

This chapter discussed the motivation and approaches to construct a cell based sensor that fluoresces upon applied shear stress. The native promoter of EGR-1 was chosen to drive this fluorescence due to known shear upregulation sensitivity and quick induction properties. NIH3T3 cells transfected with the designed plasmid could be chemically induced to express RFP in a dose dependent manner, thereby validating the approach and functionality of the reporter plasmid.

A cell population with stable integration of this plasmid into its genome was selected using antibiotics and then using FACS sorting methods. It was learned that population response heterogeneity could be marginally reduced by pretreatment of cells with serum free media, as well as FACS sorting of sub-populations based on basal expression homogeneity in a given florescence intensity window. The reporter plasmid induction was better than that seen from

previously constructed reporter candidate cell lines based on only the shear stress response elements. This improvement was attributed to using the native promoter sequence as opposed to a synthetically designed promoter with tandem response elements. The parental population of EGR-1 reporter cells was induced by PMA and sorted into single cell clonal populations which were then individually induced and compared, in order to find the best clonal candidate as a potential shear sensor. Clone 47 provided the best signal to noise ratio (in its normalized fold induction of mean fluorescence and fractional cell activation) when compared to all the clones, as well as its parental population. With this motivation, it was chosen for subsequent shear stress characterizations.

The PMA dose response and sensitivity of this population and its parental population were investigated to ensure that the clonal population indeed had similar induction profiles as the parental population. Furthermore, fluorescence induction of Clone 47 due to PMA could also be blocked by known pathway inhibitor, supporting validity of the model envisions for the shear based inductions of the population.

More directly, clone 47 was used for characterizing potential shear stress experienced during long-term perfusions. It was cultured in a microfluidic device and its induction was compared to a control population within the device that did not experience any flow. When normalized to this condition, Clone 47 indeed demonstrated sensitivity to 4 and 16 dyne/cm2 with a dose dependent increase in expression. Furthermore, it was seen that the population could be induced within an hour of applied shear stress. The reporter did not respond to PMA inductions for shorter durations than 1 hour (among tested experiments), suggesting that this minimum time was required to induce EGR-1 upregulation pathway at the protein level either by chemical induction, or by fluid shear stress.

Finally the cross sensitivity of this sensor induction was tested against other cell stress pathways such as DNA damage and heat shock. These pathways were triggered by known chemical inducers MMS and Sodium Arsenite (respectively). The sensor showed fluorescence response to non-lethal inductions of both pathways which could not be successfully inhibited by the shear pathway inhibitor tested earlier. These results provided insight into the induction characteristics of the sensor that may be indicative of known cross-talk among cell stress pathways. This knowledge could be utilized to create newer versions of the shear stress sensor, with added design elements and approaches to further enhance the shear stress sensitivity and selectivity.

Chapter 5: Contributions and Future Work

This chapter discusses the conclusions and contributions from each section of this thesis as well as opportunities for future work.

5.1. Conclusions and Contributions

5.1.1. The first cell-based fluorescent shear stress sensor

One of the main contributions of this report is the successful development of the first cell-based shear stress sensor. The EGR-1 reporter based sensor could be induced at the population level to demonstrate increased both the fraction activated cells, as well as the population mean fluorescence levels up to 1.3 fold within tested conditions. Under adherent conditions in a perfusion device, the sensors could be activated within an hour of shear stress of 16 dynes/cm^2. This was also the minimum exposure duration required to induce the sensor by PMA induction. The lower limit of shear stress sensitivity was found to be 4 dynes/cm^2 with the upper limit tested being 16 dynes/cm^2. The sensor induction was characterized using various dosages and durations of different chemical stressors. Such inductions can be used to generate a map of sensor sensitivity and selectivity towards any stressing stimuli. Within this context, this sensor could be distributed to the microsystems community where it could be used to evaluate physiological implications of device design and operations upon cell health. The chosen EGR-1 pathway is conserved among several cell phenotypes, making it more applicable to a variety of cell based devices. NIH3T3 cells themselves are easy to culture and propagate, and therefore pose promise in easy adaptation in microsystems community. As the reporter is embedded within the genome, no transfections are required to evaluate shear stress inductions, as done historically. Conveniently, the assay requires no added chemicals or protocols (such as staining or labeling cells). The cells can be calibrated from passage to passage with a subset of the population used as a reference control against applied experimental conditions. Sensor response can be measured either at the single cell level, or at a population level using quantitative fluorescence tools that are commonly accessible. Parallel to previous work done for a heat-shock sensor [96], the benefits of this shear sensor allow it to be used as a 'standard' to evaluate case studies of different microfluidic systems and platforms.

To this end, preliminary work has been done in using these cell-sensors to evaluate fluid shear stress environment of an inertial microfluidic device, as a case study. To investigate sensitivity towards short-but-intense shears, the cell sensors were tested in a microfluidic margination device used for sorting cells [8]. Here, cells experience extremely high shear (>1000 dynes/cm^2) for small durations (10's ms). Applying typical operating parameters, these cells demonstrated 1.9-2.9-fold normalized mean induced fluorescence (**Figure 5-1**).

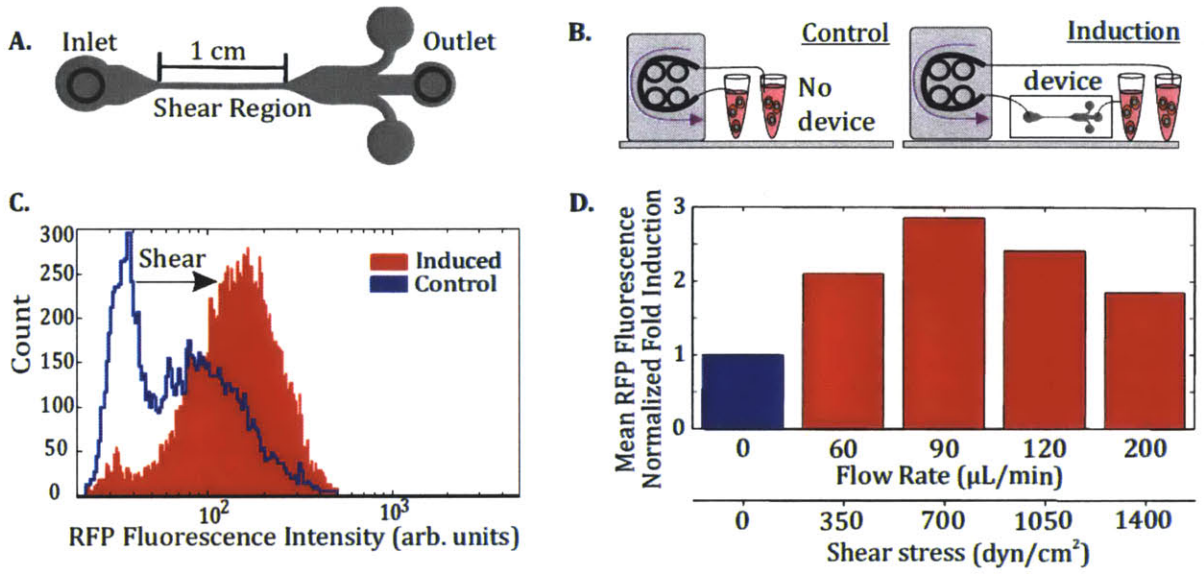

Figure 5-1 A. High-shear region within the margination device. B. Experimental setup: cells flowing through the setup without the device (controls) and with the device (induced) C. Flow cytometry analysis of control and induced population. D. Normalized fold inductions of mean fluorescence at various flow rates.

While experimental repetitions would provide statistics and error margins, this initial experiment suggests that the developed adherent-cell sensors could characterize FSS by their induction, while being used in a non-adherent 'flow-through' fashion. It can be anticipated that these cell sensors will have wide application in the microsystems community, allowing the device designer to engineer systems with acceptable fluid shear stress, and allowing the end-user to evaluate impact of fluid shear stress upon their assay of interest.

5.1.2. Characterization and comparison of response element promoters

In **Chapter 3**: , a number of reporter cell lines were constructed using inducible promoters designed with tandem response elements of shear stress activated transcription factors. In the field of fluid shear stress biology, it is typical to find promoter deletion assays where promoter sequences were mutated or deleted in order identify critical transcription factor binding sites needed to elicit a response from a given stimulus. Luciferase or CAT based reporters utilizing these response elements or native promoters of inducible genes have commonly been transfected into cells for transient stimulus-driven induction of a non-native (or regulated) gene. Such reporters are usually employed to verify stimulus-driven expression through a specific transcription factor binding site. Only one study has reported construction of hybrid promoters using multiple shear stress response elements identified from different genes [83]. The significance of response element sequences and precise positioning within the promoter was highlighted as one of the main factors influencing expression regulation.

In this context, many commercially available reporter plasmids utilize tandem response elements of various transcription factors within their inducible promoter region. The work presented in Chapter 3 signifies the first comparative study of tandem shear stress response element driven fluorescent reporters. Chemical pathway stimulation was used to evaluate mRNA transcript levels of inducible genes and the induction of population level fluorescence as a measure of promoter induction. The correlation of these two techniques was useful to debug promoter design to gain insight in possible underlying regulatory mechanisms. While the response element based plasmids or cell lines showed limited inductions upon chemical stimulation, it is possible that the plasmids or stable NIH3T3 reporters could be tested in another pathway induction context, such as within a shear stress platform to further evaluate promoter design. Furthermore, the comparison of response element cell lines to the EGR-1 promoter generated new insight in understanding the importance of using a native promoter sequence over tandem response elements for designing an inducible reporter plasmid. While optimization of promoter design in this context was beyond the scope of this thesis, the studies performed in the context of promoter analysis provide new perspectives and insight useful for understanding inducible promoter design for reporting shear stress.

5.1.3. Microfluidic device for analysis of shear pathway inductions

In this thesis microfluidic perfusion experiments were used to investigate shear induced gene expression profiles of NIH3T3s. Such an approach has been previously reported, where logarithmic shear flows were used to study induced gene profiles in the context of embryonic stem cell biology [12]. It was shown that such approach is also possible for elucidating shear induced gene expression in NIH3T3 cells. However, certain design features and operations created challenges for effective experimentation. Specifically, the small size footprint of the device chambers limited the number of cells used for seeding, and therefore post-perfusion analysis. At most a few thousand cells could be cultured in each chamber. The process of collecting RNA from such small cell numbers using a typical assay can be possible. However, the application of such assays to this device operation was certainly challenging. According to the assay, maintaining a liquid environment around the cells prior to lysis was required for high integrity of the genetic content. However, addressing such a requirement hindered proper sealing and fluidic isolation of perfused cells by the vacuum manifold used in the reported protocol [12]. Frequent leaks and cross-contamination from other chambers made this device cumbersome to use for the intended application.

Such challenges were overcome by the development of a new microfluidic platform with larger chamber footprint and a cell recovery protocol that resulted in minimal loss of cellular genetic material, as described in **Chapter 2**: . Eliminating the need for a vacuum manifold by virtue of a plasma bonded device made the device performance insensitive to clamping pressures and

recovery losses. This improvement made the process of genetic analysis after microfluidic perfusions much more convenient and repeatable. Furthermore, the platform was also utilized in **Chapter 4**: , where fluid shear stress was applied to the EGR-1 reporter cells. Here it was important to maintain cell integrity as well as cell quantity after perfusions. Due its larger footprint and convenience in cell recovery processes, this device was able to provide adequate cells required for flow cytometry analysis. Such a feat was not demonstrated by the previous work. Despite the simplicity of the overall device design, it could be easily adapted for a variety of 'single-condition' microfluidic screening assays. Similar to previous work, this device allowed for successful long and short term cell culture, which could be used to study dynamics of shear stress biology over a range of shear stress intensities and exposure upon adherent cells.

5.2. Future Work

5.2.1. Development of a screening platform for multiplexed perfusions

While beneficial, the device used to evaluate shear stress inductions at the genetic and fluorescence levels has potential to be improved for future applications. It is possible to conceive the next generation of this device where fluidic control is provided by on-chip valve control, as opposed to external fluidic connectivity. Furthermore, with added control systems and algorithms, pneumatic valves could be programed to induce various flow profiles (chronic, acute, pulsed flow etc.). The new design could have fluidic control elements of the previous device [12], with the chamber area footprint of the current one. With an ability to recover cells using on-chip valves and fluidic control, the system could potentially be automated for multiplexed shear stress experiments and subsequent flow cytometry or PCR. Such ability would allow for multiplexing in terms of shear stress dosages, as well as combining shear stress with multiplexed chemical stressor dosages to investigate sensor shear pathways further.

5.2.2. Enhancing sensitivity and selectivity of shear stress reporter

The current cell sensor sensitivity towards shear stress could potentially be maximized by investigating promoter design in detail. The results from **Chapter 2:** indicated shear sensitivity of PDGFA gene. While PDGFA may not be an immediate-early response gene it could still be useful in increasing the induced RFP signal with reference to the background non-induced signal. Further work could investigate promoters and response element combinations which may lead to enhanced selectivity of induction upon shear stress with minimal cross-induction from other stress pathways.

5.2.3. Investigating new avenues of shear stress biology

Finally, it is conceivable that new avenues of shear stress biology could be explored using many of the methodologies mentioned in this thesis. It may be of interest to evaluate chemical induced pathway inductions to understand the correlation at the translational level for a more direct comparison to RFP. It may also be worthwhile evaluating effects of population background level florescence and its sensitivity to culture passages and well as to culture techniques. Another avenue of interest could be to multiplex this shear sensor with other cell health sensors in order to assess the physiological effects of microsystems on cell health at a broader level.

References

1. Bhatia, S.N., M.L. Yarmush, and M. Toner, *Controlling cell interactions by micropatterning in co-cultures: hepatocytes and 3T3 fibroblasts.* J Biomed Mater Res, 1997. **34**(2): p. 189-99.
2. Huh, D., et al., *Reconstituting organ-level lung functions on a chip.* Science, 2010. **328**(5986): p. 1662-8.
3. Wang, M.M., et al., *Microfluidic sorting of mammalian cells by optical force switching.* Nat Biotechnol, 2005. **23**(1): p. 83-7.
4. Gascoyne, P.R., et al., *Dielectrophoretic Separation of Cancer Cells from Blood.* IEEE Trans Ind Appl, 1997. **33**(3): p. 670-678.
5. Xia, N., et al., *Combined microfluidic-micromagnetic separation of living cells in continuous flow.* Biomed Microdevices, 2006. **8**(4): p. 299-308.
6. Di Carlo, D., L.Y. Wu, and L.P. Lee, *Dynamic single cell culture array.* Lab Chip, 2006. **6**(11): p. 1445-9.
7. Kim, L., et al., *A practical guide to microfluidic perfusion culture of adherent mammalian cells.* Lab Chip, 2007. **7**(6): p. 681-94.
8. Wei Hou, H., et al., *A microfluidics approach towards high-throughput pathogen removal from blood using margination.* Biomicrofluidics, 2012. **6**(2): p. 24115-2411513.
9. Wu, L., et al., *Encapsulation of single cells on a microfluidic device integrating droplet generation with fluorescence-activated droplet sorting.* Biomed Microdevices, 2013. **15**(3): p. 553-60.
10. Baret, J.C., et al., *Fluorescence-activated droplet sorting (FADS): efficient microfluidic cell sorting based on enzymatic activity.* Lab Chip, 2009. **9**(13): p. 1850-8.
11. Honegger, T., et al., *Electrokinetic confinement of axonal growth for dynamically configurable neural networks.* Lab Chip, 2013. **13**(4): p. 589-98.
12. Toh, Y.C. and J. Voldman, *Fluid shear stress primes mouse embryonic stem cells for differentiation in a self-renewing environment via heparan sulfate proteoglycans transduction.* FASEB J, 2011. **25**(4): p. 1208-17.
13. Przybyla, L.M. and J. Voldman, *Attenuation of extrinsic signaling reveals the importance of matrix remodeling on maintenance of embryonic stem cell self-renewal.* Proc Natl Acad Sci U S A, 2012. **109**(3): p. 835-40.
14. Jang, K.J., et al., *Fluid-shear-stress-induced translocation of aquaporin-2 and reorganization of actin cytoskeleton in renal tubular epithelial cells.* Integr Biol (Camb), 2011. **3**(2): p. 134-41.
15. Jang, K., et al., *Development of an osteoblast-based 3D continuous-perfusion microfluidic system for drug screening.* Anal Bioanal Chem, 2008. **390**(3): p. 825-32.
16. Topper, J.N. and M.A. Gimbrone, Jr., *Blood flow and vascular gene expression: fluid shear stress as a modulator of endothelial phenotype.* Mol Med Today, 1999. **5**(1): p. 40-6.
17. Shin, H.Y., S.I. Simon, and G.W. Schmid-Schonbein, *Fluid shear-induced activation and cleavage of CD18 during pseudopod retraction by human neutrophils.* J Cell Physiol, 2008. **214**(2): p. 528-36.
18. Davies, P.F., *Flow-mediated endothelial mechanotransduction.* Physiol Rev, 1995. **75**(3): p. 519-60.
19. Fink, S.L. and B.T. Cookson, *Apoptosis, pyroptosis, and necrosis: mechanistic description of dead and dying eukaryotic cells.* Infect Immun, 2005. **73**(4): p. 1907-16.
20. Fulda, S., et al., *Cellular stress responses: cell survival and cell death.* Int J Cell Biol, 2010. **2010**: p. 214074.
21. Minami, T. and W.C. Aird, *Endothelial cell gene regulation.* Trends Cardiovasc Med, 2005. **15**(5): p. 174-84.

22. Nevill, J.T., et al., *Integrated microfluidic cell culture and lysis on a chip.* Lab Chip, 2007. **7**(12): p. 1689-95.
23. Lecault, V., et al., *High-throughput analysis of single hematopoietic stem cell proliferation in microfluidic cell culture arrays.* Nat Methods, 2011. **8**(7): p. 581-6.
24. Ji, J.Y., H. Jing, and S.L. Diamond, *Shear stress causes nuclear localization of endothelial glucocorticoid receptor and expression from the GRE promoter.* Circ Res, 2003. **92**(3): p. 279-85.
25. Malek, A.M., S.L. Alper, and S. Izumo, *Hemodynamic shear stress and its role in atherosclerosis.* JAMA, 1999. **282**(21): p. 2035-42.
26. Davies, P.F. and S.C. Tripathi, *Mechanical stress mechanisms and the cell. An endothelial paradigm.* Circ Res, 1993. **72**(2): p. 239-45.
27. Barakat, A. and D. Lieu, *Differential responsiveness of vascular endothelial cells to different types of fluid mechanical shear stress.* Cell Biochem Biophys, 2003. **38**(3): p. 323-43.
28. Resnick, N., et al., *Endothelial gene regulation by laminar shear stress.* Adv Exp Med Biol, 1997. **430**: p. 155-64.
29. Wasserman, S.M., et al., *Gene expression profile of human endothelial cells exposed to sustained fluid shear stress.* Physiol Genomics, 2002. **12**(1): p. 13-23.
30. Braddock, M., et al., *Fluid Shear Stress Modulation of Gene Expression in Endothelial Cells.* News Physiol Sci, 1998. **13**: p. 241-246.
31. Malek, A.M. and S. Izumo, *Control of endothelial cell gene expression by flow.* J Biomech, 1995. **28**(12): p. 1515-28.
32. Shyy, J.Y., et al., *The cis-acting phorbol ester "12-O-tetradecanoylphorbol 13-acetate"-responsive element is involved in shear stress-induced monocyte chemotactic protein 1 gene expression.* Proc Natl Acad Sci U S A, 1995. **92**(17): p. 8069-73.
33. Kurulgan Demirci, E., et al., *Genome-Wide Gene Expression Analysis of NIH 3T3 Cell Line Under Mechanical Stimulation.* Cellular and Molecular Bioengineering, 2011. **4**(1): p. 46-55.
34. Treisman, R., *The serum response element.* Trends Biochem Sci, 1992. **17**(10): p. 423-6.
35. Sukhatme, V.P., et al., *A zinc finger-encoding gene coregulated with c-fos during growth and differentiation, and after cellular depolarization.* Cell, 1988. **53**(1): p. 37-43.
36. Spencer, J.A. and R.P. Misra, *Expression of the serum response factor gene is regulated by serum response factor binding sites.* J Biol Chem, 1996. **271**(28): p. 16535-43.
37. McMahon, S.B. and J.G. Monroe, *Role of primary response genes in generating cellular responses to growth factors.* FASEB J, 1992. **6**(9): p. 2707-15.
38. Dieckgraefe, B.K. and D.M. Weems, *Epithelial injury induces egr-1 and fos expression by a pathway involving protein kinase C and ERK.* Am J Physiol, 1999. **276**(2 Pt 1): p. G322-30.
39. Hodge, C., et al., *Growth hormone stimulates phosphorylation and activation of elk-1 and expression of c-fos, egr-1, and junB through activation of extracellular signal-regulated kinases 1 and 2.* J Biol Chem, 1998. **273**(47): p. 31327-36.
40. Chai, J. and A.S. Tarnawski, *Serum response factor: discovery, biochemistry, biological roles and implications for tissue injury healing.* J Physiol Pharmacol, 2002. **53**(2): p. 147-57.
41. Janknecht, R., M.A. Cahill, and A. Nordheim, *Signal integration at the c-fos promoter.* Carcinogenesis, 1995. **16**(3): p. 443-50.
42. Cheng, J.J., et al., *Sequential activation of protein kinase C (PKC)-alpha and PKC-epsilon contributes to sustained Raf/ERK1/2 activation in endothelial cells under mechanical strain.* J Biol Chem, 2001. **276**(33): p. 31368-75.
43. Korenaga, R., et al., *Negative transcriptional regulation of the VCAM-1 gene by fluid shear stress in murine endothelial cells.* Am J Physiol, 1997. **273**(5 Pt 1): p. C1506-15.
44. Shyy, J.Y., et al., *Multiple cis-elements mediate shear stress-induced gene expression.* J Biomech, 1995. **28**(12): p. 1451-7.

45. Khachigian, L.M., A.J. Williams, and T. Collins, *Interplay of Sp1 and Egr-1 in the proximal platelet-derived growth factor A-chain promoter in cultured vascular endothelial cells.* J Biol Chem, 1995. **270**(46): p. 27679-86.
46. Lin, M.C., et al., *Shear stress induction of the tissue factor gene.* J Clin Invest, 1997. **99**(4): p. 737-44.
47. Hsieh, H.J., N.Q. Li, and J.A. Frangos, *Shear stress increases endothelial platelet-derived growth factor mRNA levels.* Am J Physiol, 1991. **260**(2 Pt 2): p. H642-6.
48. Yan, S.F., et al., *Egr-1: is it always immediate and early?* J Clin Invest, 2000. **105**(5): p. 553-4.
49. McCaffrey, T.A., et al., *High-level expression of Egr-1 and Egr-1-inducible genes in mouse and human atherosclerosis.* J Clin Invest, 2000. **105**(5): p. 653-62.
50. Silverman, E.S., et al., *Inducible PDGF A-chain transcription in smooth muscle cells is mediated by Egr-1 displacement of Sp1 and Sp3.* Am J Physiol, 1997. **273**(3 Pt 2): p. H1415-26.
51. Silverman, E.S. and T. Collins, *Pathways of Egr-1-mediated gene transcription in vascular biology.* Am J Pathol, 1999. **154**(3): p. 665-70.
52. Resnick, N., et al., *Signalling pathways in vascular endothelium activated by shear stress: relevance to atherosclerosis.* Curr Opin Lipidol, 2000. **11**(2): p. 167-77.
53. Khachigian, L.M., et al., *Egr-1-induced endothelial gene expression: a common theme in vascular injury.* Science, 1996. **271**(5254): p. 1427-31.
54. Rorsman, F. and C. Betsholtz, *Characterization of the mouse PDGF A-chain gene. Evolutionary conservation of gene structure, nucleotide sequence and alternative splicing.* Growth Factors, 1992. **6**(4): p. 303-13.
55. Bonthron, D.T., et al., *Platelet-derived growth factor A chain: gene structure, chromosomal location, and basis for alternative mRNA splicing.* Proc Natl Acad Sci U S A, 1988. **85**(5): p. 1492-6.
56. Lin, X., et al., *Functional analysis of the human platelet-derived growth factor A-chain promoter region.* J Biol Chem, 1992. **267**(35): p. 25614-9.
57. Kaetzel, D.M., Jr., et al., *Platelet-derived growth factor A-chain gene transcription is mediated by positive and negative regulatory regions in the promoter.* Biochem J, 1994. **301 (Pt 2)**: p. 321-7.
58. Angel, P. and M. Karin, *The role of Jun, Fos and the AP-1 complex in cell-proliferation and transformation.* Biochim Biophys Acta, 1991. **1072**(2-3): p. 129-57.
59. Hsieh, H.J., N.Q. Li, and J.A. Frangos, *Pulsatile and steady flow induces c-fos expression in human endothelial cells.* J Cell Physiol, 1993. **154**(1): p. 143-51.
60. Resnick, N., et al., *Platelet-derived growth factor B chain promoter contains a cis-acting fluid shear-stress-responsive element.* Proc Natl Acad Sci U S A, 1993. **90**(10): p. 4591-5.
61. Shaner, N.C., P.A. Steinbach, and R.Y. Tsien, *A guide to choosing fluorescent proteins.* Nat Methods, 2005. **2**(12): p. 905-9.
62. Shaner, N.C., et al., *Improved monomeric red, orange and yellow fluorescent proteins derived from Discosoma sp. red fluorescent protein.* Nat Biotechnol, 2004. **22**(12): p. 1567-72.
63. Shcherbo, D., et al., *Bright far-red fluorescent protein for whole-body imaging.* Nat Methods, 2007. **4**(9): p. 741-6.
64. Merzlyak, E.M., et al., *Bright monomeric red fluorescent protein with an extended fluorescence lifetime.* Nat Methods, 2007. **4**(7): p. 555-7.
65. Cao, X., et al., *Detection and characterization of cellular EGR-1 binding to its recognition site.* J Biol Chem, 1993. **268**(23): p. 16949-57.
66. Khachigian, L.M., et al., *Egr-1 is activated in endothelial cells exposed to fluid shear stress and interacts with a novel shear-stress-response element in the PDGF A-chain promoter.* Arterioscler Thromb Vasc Biol, 1997. **17**(10): p. 2280-6.

67. Barnett, S.C., et al., *Differential regulation of AP-1 and novel TRE-specific DNA-binding complexes during differentiation of oligodendrocyte-type-2-astrocyte (O-2A) progenitor cells.* Development, 1995. **121**(12): p. 3969-77.
68. Nguyen, T., P.J. Sherratt, and C.B. Pickett, *Regulatory mechanisms controlling gene expression mediated by the antioxidant response element.* Annu Rev Pharmacol Toxicol, 2003. **43**: p. 233-60.
69. Shyy, Y.J., Y.S. Li, and P.E. Kolattukudy, *Structure of human monocyte chemotactic protein gene and its regulation by TPA.* Biochem Biophys Res Commun, 1990. **169**(2): p. 346-51.
70. Risse, G., et al., *Asymmetrical recognition of the palindromic AP1 binding site (TRE) by Fos protein complexes.* EMBO J, 1989. **8**(12): p. 3825-32.
71. Gutman, A. and B. Wasylyk, *Nuclear targets for transcription regulation by oncogenes.* Trends Genet, 1991. **7**(2): p. 49-54.
72. Karin, M., Z. Liu, and E. Zandi, *AP-1 function and regulation.* Curr Opin Cell Biol, 1997. **9**(2): p. 240-6.
73. Khachigian, L.M., et al., *Nuclear factor-kappa B interacts functionally with the platelet-derived growth factor B-chain shear-stress response element in vascular endothelial cells exposed to fluid shear stress.* J Clin Invest, 1995. **96**(2): p. 1169-75.
74. Davis, M.E., et al., *Shear stress regulates endothelial nitric oxide synthase expression through c-Src by divergent signaling pathways.* Circ Res, 2001. **89**(11): p. 1073-80.
75. Nagel, T., et al., *Shear stress selectively upregulates intercellular adhesion molecule-1 expression in cultured human vascular endothelial cells.* J Clin Invest, 1994. **94**(2): p. 885-91.
76. Misra, R.P., et al., *The serum response factor is extensively modified by phosphorylation following its synthesis in serum-stimulated fibroblasts.* Mol Cell Biol, 1991. **11**(9): p. 4545-54.
77. Taylor, S.J. and D. Shalloway, *Cell cycle-dependent activation of Ras.* Curr Biol, 1996. **6**(12): p. 1621-7.
78. Chiu, J.J., et al., *Nitric oxide regulates shear stress-induced early growth response-1. Expression via the extracellular signal-regulated kinase pathway in endothelial cells.* Circ Res, 1999. **85**(3): p. 238-46.
79. Goetze, S., et al., *TNFalpha induces expression of transcription factors c-fos, Egr-1, and Ets-1 in vascular lesions through extracellular signal-regulated kinases 1/2.* Atherosclerosis, 2001. **159**(1): p. 93-101.
80. Young, S.R., et al., *Activation of NF-kappaB by fluid shear stress, but not TNF-alpha, requires focal adhesion kinase in osteoblasts.* Bone, 2010. **47**(1): p. 74-82.
81. Khachigian, L.M. and T. Collins, *Early growth response factor 1: a pleiotropic mediator of inducible gene expression.* J Mol Med (Berl), 1998. **76**(9): p. 613-6.
82. Khachigian, L.M. and T. Collins, *Inducible expression of Egr-1-dependent genes. A paradigm of transcriptional activation in vascular endothelium.* Circ Res, 1997. **81**(4): p. 457-61.
83. Silberman, M., et al., *Shear stress-induced transcriptional regulation via hybrid promoters as a potential tool for promoting angiogenesis.* Angiogenesis, 2009. **12**(3): p. 231-42.
84. Jamieson, G.A., Jr., et al., *Multiple intracellular pathways induce expression of a zinc-finger encoding gene (EGR1): relationship to activation of the Na/H exchanger.* J Cell Physiol, 1989. **139**(2): p. 262-8.
85. Thiel, G., et al., *Egr-1-A Ca(2+)-regulated transcription factor.* Cell Calcium, 2010. **47**(5): p. 397-403.
86. Thiel, G. and G. Cibelli, *Regulation of life and death by the zinc finger transcription factor Egr-1.* J Cell Physiol, 2002. **193**(3): p. 287-92.
87. Yan, S.F., et al., *Egr-1, a master switch coordinating upregulation of divergent gene families underlying ischemic stress.* Nat Med, 2000. **6**(12): p. 1355-61.

88. Chien, S., S. Li, and Y.J. Shyy, *Effects of mechanical forces on signal transduction and gene expression in endothelial cells.* Hypertension, 1998. **31**(1 Pt 2): p. 162-9.
89. Houston, P., et al., *Fluid shear stress induction of the tissue factor promoter in vitro and in vivo is mediated by Egr-1.* Arterioscler Thromb Vasc Biol, 1999. **19**(2): p. 281-9.
90. Yun, S., et al., *Transcription factor Sp1 phosphorylation induced by shear stress inhibits membrane type 1-matrix metalloproteinase expression in endothelium.* J Biol Chem, 2002. **277**(38): p. 34808-14.
91. Schwachtgen, J.L., et al., *Fluid shear stress activation of egr-1 transcription in cultured human endothelial and epithelial cells is mediated via the extracellular signal-related kinase 1/2 mitogen-activated protein kinase pathway.* J Clin Invest, 1998. **101**(11): p. 2540-9.
92. Shin, S.Y., et al., *Suppression of Egr-1 transcription through targeting of the serum response factor by oncogenic H-Ras.* EMBO J, 2006. **25**(5): p. 1093-103.
93. Datta, R., et al., *Ionizing radiation activates transcription of the EGR1 gene via CArG elements.* Proc Natl Acad Sci U S A, 1992. **89**(21): p. 10149-53.
94. Yan, S.F., et al., *Hypoxia-associated induction of early growth response-1 gene expression.* J Biol Chem, 1999. **274**(21): p. 15030-40.
95. Zhan, Q., et al., *Tumor suppressor p53 can participate in transcriptional induction of the GADD45 promoter in the absence of direct DNA binding.* Mol Cell Biol, 1998. **18**(5): p. 2768-78.
96. Desai, S.P. and J. Voldman, *Cell-based sensors for quantifying the physiological impact of microsystems.* Integr Biol (Camb), 2011. **3**(1): p. 48-56.
97. Shin, S.Y., et al., *The ETS family transcription factor ELK-1 regulates induction of the cell cycle-regulatory gene p21(Waf1/Cip1) and the BAX gene in sodium arsenite-exposed human keratinocyte HaCaT cells.* J Biol Chem, 2011. **286**(30): p. 26860-72.
98. Lim, C.P., N. Jain, and X. Cao, *Stress-induced immediate-early gene, egr-1, involves activation of p38/JNK1.* Oncogene, 1998. **16**(22): p. 2915-26.